DISSERTATION

WESTERN EQUINE ENCEPHALITIS VIRUS: DEVELOPMENT AND APPLICATION OF A NEW WORLD ALPHAVIRUS TRANSDUCING SYSTEM

Submitted by

Charles Brandon Stauft

Department of Microbiology, Immunology, and Pathology

In partial fulfillment of the requirements

For the Degree of Doctor of Philosophy

Colorado State University

Fort Collins, Colorado

Spring 2012

Doctoral Committee:

Advisor: Kenneth Olson

Carol Brennan
Brian Foy
Richard Bowen

ABSTRACT

WESTERN EQUINE ENCEPHALITIS VIRUS: DEVELOPMENT AND APPLICATION OF A NEW WORLD ALPHAVIRUS TRANSDUCING SYSTEM

A recombinant western equine encephalitis virus (WEEV) was generated that expressed firefly luciferase (FLUC) as a marker of infection. *In vivo* imaging technology was used to visualize bioluminescence in the context of WEEV infection of outbred (CD-1) and inbred (C57/BL6) strains of mice as well as *Culex tarsalis* mosquitoes. Bioluminescent imaging permitted us to follow a neurovirulent strain of WEEV in the living tissue of a single animal over time. The recombinant virus also permitted detection by bioluminescence of WEEV in the mosquito vector, *Culex tarsalis*. *In vivo* imaging was used to test the hypothesis that an alphavirus transducing system could be used to predict efficacy of a cationic lipid RNA complex (CLRC) immunomodulator in the suppression of WEEV infection. Bioluminescent imaging in screening potential antivirals for activity against WEEV *in vivo* was confirmed to be consistent, clear, and in agreement with traditional survival curve analysis.

WEEV is maintained in an enzootic cycle through transmission by *Culex tarsalis* to passerine bird species. Tangential transmission to equine or human hosts has been associated with severe outbreaks of disease in the past. These hosts are considered to be dead-end hosts as they may become infected during epizootics but do not generate sufficient viremia titers to infect a bloodfeeding mosquito. Understanding the determinants of transmission to the vector from the host, dissemination within the vector, and secretion in saliva of WEEV are crucial to understanding the overall cycle. The recent development of a WEEV transducing system

facilitated the study of WEEV interaction with the midgut, ovary, and salivary gland tissue of *C. tarsalis*. The expression by a recombinant alphavirus of monomeric cherry fluorescent protein allowed an overall picture of infection, dissemination, and transmission with both enzootic (IMP181) and epidemic (McMillan) strains of WEEV. Salivary gland infection rate was hypothesized to be greater for IMP181 than McMillan. IMP181 was hypothesized to be transmitted at a higher rate compared to McMillan and present in higher viral titers in saliva. The barriers to McMillan infection of salivary glands or transmission were hypothesized to be dose dependent. Increased viral titer of injected McMillan was expected to result in a higher salivary gland infection rate, transmission rate, and amount of virus detected in the saliva.

A midgut barrier to infection was circumvented by injection of each virus strain into mosquitoes. There was no significant difference in McMillan and IMP181's ability to infect salivary glands or transmit at 7 and 14 days post infection. IMP181 infection resulted in higher viral titers found in expectorated saliva. The use of chimeric recombinant WEEV also revealed WEEV sequence determinants in the structural coding regions and 3'UTR of IMP181 that enhanced virus titers in expectorated *C. tarsalis* saliva. The transmission rate and not the salivary gland infection rate were found to be dose dependent after intrathoracic injection with both strains of WEEV.

TABLE OF CONTENTS

LIST OF FIGURES

LIST OF TABLES

Chapter I: Literature Review

Introduction

Arthropod borne viruses (arboviruses) replicate in a vector, are then transmitted to a vertebrate host through the bite of the infected vector, and are transmitted to an arthropod host. This life cycle is unusual among animal viruses in that arboviruses must contend with both vertebrate and invertebrate hosts. Arboviruses bring together the fields of virology, molecular biology, ecology, entomology, and epidemiology. The involvement of a vertebrate host and invertebrate vector strongly influence viral evolution. Vector-borne viruses are capable of causing severe and widespread disease. The families of arboviruses most involved in causing human and veterinary disease are *Togaviridae, Flaviviridae,* and *Bunyaviridae*. One example is the outbreak of chikungunya virus (CHIKV; Family: *Togaviridae,* Genus: *Alphavirus*) that occurred in 2005-2006 affecting a number of regions bordering the Indian Ocean and spread to the Mediterranean basin. CHIKV is normally found in Africa and Asia; however, an African strain spread to La Reunion Island and India (Sudeep and Parashar, 2008). This outbreak caused over 200,000 cases of CHIK on La Reunion Island and 1.4 million cases in India in part due to adaptation of CHIKV to *Aedes albopictus* (Pialoux et al, 2007; Renault et al, 2007). Venezuelan equine encephalitis virus (VEEV; Family: *Togaviridae,* Genus: *Alphavirus*) was responsible for an outbreak in Venezuela in 1995. There were between 75,000 and 100,000 human cases of VEEV with a case fatality rate of 0.5% (Zacks and Paessler, 2010).

The major vector-borne flaviviruses are yellow fever virus (YFV), dengue virus (DENV), Japanese encephalitis virus (JEV), and West Nile virus (WNV). These arboviruses are classified in the genus *Flavivirus*. YFV may cause as many as 200,000 cases of human disease and 30,000

deaths each year. Transmission is endemic throughout the Amazon basin in South America and sub-Saharan Africa. Six hundred million people in Africa are at risk for exposure to YFV and incidence of infection continues to rise despite the existence of a safe and effective vaccine (Barrett and Higgs, 2007). The prevalence of dengue fever (caused by four serotypes of DENV) has increased dramatically in the last 50 years. More than fifty million human cases of dengue fever are recorded each year, with a fraction of this number developing dengue hemorrhagic fever which is potentially lethal. Over 2.5 billion people living in regions of endemic transmission by competent vectors including Africa, South America, and South-East Asia are at risk for infection. JEV is the leading cause of epidemic encephalitis and is endemic throughout India, East Asia, and South-East Asia. JEV causes 50,000 cases and 15,000 fatalities each year throughout these regions. JEV is thought to be spread from region to region through the migration of infected bird species (Weaver and Barrett, 2004). Another member of the JEV complex, WNV, has been responsible for several recent outbreaks in Romania and Russia before spreading to the continental United States. WNV spread westward in the US after its introduction to New York in 1999. WNV caused illness in tens of thousands of horses and approximately 30,000 people, with a human case fatality rate of nearly 10 % (Gerhardt, 2006; Murray et al, 2011).

Rift Valley fever virus (RVFV) is an important emerging virus within the family *Bunyaviridae*, genus *Phlebovirus*. RVFV is transmitted by a variety of *Culex* and *Aedes* mosquitoes and is associated with outbreaks after dramatic increases in vector populations. RVF is an acute and severe disease in livestock that commonly results in fetal abortion and hepatitis. RVF in humans presents with a variety of symptoms including hepatitis, encephalitis, and hemorrhagic fever. RVFV was responsible for an outbreak of RVF in late 1997 following a

period of heavy rainfall that resulted in the infection of 27,500 people and 170 deaths in Kenya. In 2000, cases of RVF were reported on the Arabian Peninsula, highlighting RVFV's potential of spreading from Africa due to the trafficking of RVFV infected animals (Soldan and Gonzalez-Scarano, 2005; Hollidge et al, 2010).

Human involvement in zoonotic arboviral disease occurs as a result of three distinct transmission cycles; epidemic, enzootic, and epizootic. Arboviruses such as CHIKV, YFV, and DENV are capable of infecting humans during urban epidemic cycles due to dense populations of *Aedes* mosquitoes as vectors. With an enzootic cycle, humans are incidental hosts that are bitten by infected mosquitoes normally involved in transmission between animals. This cycle predominates with WNV transmission to humans and horses. In contrast, rural epizootic cycles can use domestic animals as amplification hosts and involve human beings as dead-end hosts. Massive VEEV outbreaks have occurred in Central America that exemplify this cycle. However, people are frequently incapable of sustaining viremia sufficient for transmission in enzootic or rural epizootic cycles and so are referred to as dead-end hosts (Weaver et al, 2006).

A number of factors are responsible for the resurgence and prevalence of arthropod-borne viral diseases. Among these is the lack of effective vaccines for susceptible populations. DENV requires a vaccine that is effective against all four serotypes in order to preclude the phenomenon of increased pathology as a result of pre-existing non-neutralizing antibodies (antibody-dependent enhancement). A safe and effective vaccine is available for YFV. However, current stocks of this vaccine are insufficient to stop a severe urban epidemic such as the ones that have occurred in the past. The live attenuated YFV vaccine requires refridgeration which poses a problem in tropical, third-world countries. Poor pesticide management and efficacy are another alarming trend that has led to an increase in arboviral disease. Populations of *Aedes aegypti*

mosquitoes as well as a number of *Culex* mosquito species are increasingly resistant to some pesticides. *Aedes* and *Culex* genera of vectors are responsible for the transmission of numerous arboviruses and their resistance to chemical control is alarming. A reduction in pesticide usage due to public concern over harm to non-target species has also occurred. Dichloro-diphenyl-trichloroethane (DDT) was highly effective in limiting vector populations and was responsible for a reduction in vector-borne disease (Hemingway et al, 2002). DDT was banned due to use in agricultural applications and concerns over effects on off-target species. Consequently, pathogens that were previously controlled through DDT use were once again able to exist in numbers sufficient for the spread of vector-borne diseases (Beaty, 2005). The threat of re-emergence makes continued research into the treatment and ecology of arboviruses important for world public health. Long quiescent viruses such as western equine encephalitis could cause severe epizootics or epidemics if and when favorable conditions occur in the absence of effective vaccination.

Alphaviruses

Togaviridae contains two genera, *Alphavirus* and *Rubivirus*. Other than rubella virus, the only member of the genus *Rubivirus*, the majority of alphaviruses are mosquito-borne (Weaver et al, 2006). Approximately thirty species of alphavirus have been identified and differentiated into seven groups through antigen similarity as determined by serum neutralization of live virus. These antigenic groups are the Barmah Forest complex, the Ndumu complex, the Middelburg complex, Semliki Forest complex, WEE complex (which includes SINV, WEEV, and Highlands J virus), EEE complex, and VEE complex. (Powers et al, 2001). Common vertebrate hosts include birds (WEEV, EEEV), small mammals (VEEV), and humans (RRV). Generally, humans and domestic animals are incidental hosts and show clinical symptoms of disease (Weaver et al,

2006). Alphaviruses are usually transmitted by culicine mosquitoes between hosts. CHIKV can cause serious epidemic disease in humans (Chevillon et al. 2008). VEEV and EEEV are associated with severe epizootics and epidemics involving horses and people (Calisher et al. 1994).

Replication cycle

Alphaviruses have an ~11kb positive-sense single stranded RNA genome with a 5' methyl G cap and a 3' poly A tail. The 5' 2/3rds of the genome encodes the alphaviral replication complex and the remaining 3' 1/3 of the genome encodes the structural proteins. The alphaviral replication cycle begins with attachment of the virus to a host cell receptor and uptake through receptor mediated endocytosis. Fusion of host and viral membranes occurs following acidification of the late endosome. The genome is translated to form a non-structural poly-protein which is cleaved during replication by nsP3. The non-structural proteins then form a replicative complex that transcribes genomic RNA into template negative-sense antigenomic RNA. Cleavage of the non-structural polyprotein results in a shift to production of positive-sense genomic mRNA and subgenomic mRNA that is translated into the structural polyprotein. The capsid protein cleaves itself from the poly-protein and associates with genomic RNA in the cytoplasm while the envelope proteins are processed by the host secretory pathway (endoplasmic reticulum and Golgi) before insertion into the host plasma membrane. Assembly of the virion and genomic RNA occurs at the plasma membrane and is followed by budding from the cell (Simmons and Strauss, 1972b; Strauss and Strauss, 1994).

Molecular biology

The 5' end of the alphavirus genomic RNA begins with a 40-80 nucleotide untranslated region (UTR) composed of a conserved secondary structure having a small stem-loop followed

by a larger stem-loop. A 51 nucleotide conserved sequence element (CSE) is also found downstream of the UTR that forms a pair of small stem-loop structures. The 5' terminal elements of the genomic RNA act *in cis* to initiate translation and in the antisense strand the 5' 200-250 nucleotides mediate the transcription of genomic RNA from intermediate anti-sense strands (Ou et al, 1983; Frolov et al, 2001).

Logue et al (2008) described the role of the 5'UTR in determining the virulence of SFV strains in mice. There was no difference in the rates of RNA synthesis between a virulent and avirulent strain. Substitution of the 5' UTR of the virulent strain with that of the avirulent strain significantly decreased mortality and neural pathology in intranasally infected mice. The reciprocal cross of 5' terminal sequence did not result in an alteration of virulence, indicating that other virulence factors are involved. The sequence of the 5' UTR was highly sensitive to alteration, as the two strains differed by only three nucleotides (Logue et al, 2008).

The 5' two-thirds of the alphavirus genome codes for the non-structural proteins, of which there are four. Non-structural protein 1 (nsP1) is membrane-associated and mediates viral RNA synthesis. It is also responsible for installing the 5'mG cap structure on alphavirus messenger RNA. Four steps are necessary to complete this reaction. Initially, nsP2 catalyzes removal of the 5' phosphate group from the mRNA. A methyl group is then transferred from S-adenosyl methionine to GTP by nsP1. Cleavage of pyrophosphate from 7-methyl GTP provides the energy for a covalent bond between nsP1 and 7mGMP. Finally, the 7-methyl-guanylyl group is transferred to the nascent mRNA. This process differs from cellular mRNA capping in that GTP is bound to the methyl group prior to its addition to the 5' end of the viral mRNA (Kaariainen and Ahola, 2002; Strauss and Strauss, 1994). Kiiver et al (2008) described how overexpression of nsP1 reduced the multiplication of SFV by up to ten-fold. Interference did not

occur at the level of viral entry or replication initiation. Instead, the level of genomic RNA synthesis was reduced and the production of structural proteins was delayed. Non-structural protein 1 was also found to be stable in infected cell culture, with a half-life of 5 hours (Kiiver et al, 2008). Minus-strand synthesis may also be affected through the action of nsP1. A temperature sensitive mutation in the amino acid sequence results in a specific loss of minus-strand RNA transcription while allowing the production of positive-strand RNA (Kaariainen and Ahola, 2002).

Non-structural protein 2 (nsP2) is an approximately 800 amino acid protein with a carboxy terminal helicase domain and an amino-terminal protease domain. The helicase domain comprises the N-terminal 470 amino acids of the protein and possesses nucleotriphosphatase and RNA helicase activities. The RNA helicase activity is likely responsible for the separation of double-stranded viral RNA species or clearance of template secondary structure. The RNA triphosphatase activity possessed by the N-terminal end of this protein is also essential for the capping of viral mRNAs. The papain-like cysteine protease domain at the C-terminal end of nsP2 serves to cleave the non-structural polyprotein at the 1:2, 2:3, and 3:4 junctions. The protease activity is temporally regulated, with 1:2 being cleaved first to yield either P234 or P23 (Kaariainen and Ahola, 2002; Strauss and Strauss, 1994). These cleavage events are necessary in order for positive RNA synthesis to occur. Inactivation of nsP2 results in the accumulation of anti-sense RNA species and a paucity of genomic and subgenomic RNAs. Enhanced proteolytic activity resulted in a cessation of viral RNA synthesis (Lemm et al, 1994). Unique among alphaviral non-structural proteins, nsP2 is transported into the nucleus of mammalian cells during infection (Kaariainen and Ahola, 2002; Strauss and Strauss, 1994). SINV nsP2 in its free form is also toxic to cells by shutting down cellular transcription. The ability to inhibit host cell

transcription is localized outside of the helicase or protease domains in the N-terminus. Cytopathic effects were shown to be induced by nsP2 independent of SINV infection (Garmashova et al, 2006).

Non-structural protein 3 (nsP3) is a protein of variable length with two distinct domains. The N-terminal domain is conserved among different alphavirus species. The C-terminal domain is highly variable in terms of both length and sequence. It is also capable of suffering lengthy amino acid deletions without significant consequence to the alphavirus (Kaariainen and Ahola, 2002; Strauss and Strauss, 1994). An alternative stop codon (opal stop codon) lies immediately downstream of the nsP3 coding sequence in some alphaviruses (Strauss et al, 1983). Consequently, two forms of nsP3 are produced depending upon whether the ribosome terminates at the opal codon or reads through, resulting in a 7 amino acid addition to the end of the protein. Despite the lack of a known specific function for nsP3, it is important for viral RNA synthesis. This is shown by the presence of a temperature sensitive mutation in nsP3 that halts viral RNA transcription at 40°C. Non-structural protein 3 is also essential for minus-strand RNA synthesis, subgenomic RNA synthesis, and nsP2 cleavage specificity (LaStarza et al, 1994; Strauss and Strauss, 1994; Wang et al, 1994; de Groot et al, 1990).

The alphavirus RNA dependent RNA polymerase is known as non-structural protein 4 (nsP4). It is an unstable protein present in limited amounts due to the presence of the opal stop codon between nsP3 and nsP4 in most alphaviruses. Read-through of the stop codon by the host translational complex is necessary to produce the P1234 non-structural polyprotein. The nsP2 protease cleaves nsP4 prior to viral replication. In addition, nsP4 is degraded rapidly in the cytoplasm of host cells. Thus, the concentration of nsP4 is regulated at both the genetic and metabolic level. Transcription of viral RNA is mediated by a membrane associated complex of

alphaviral nonstructural proteins. This complex is localized to large cytoplasmic vacuoles descended from lysosomes and endosomes. The transcription complex interacts with the 5' and 3' CSEs on the genomic RNA and initiates production of a complementary, negative-sense RNA with an apocryphal unpaired guanine at the 3' end. Proteolytic processing of P123 by nsP2 into its component proteins triggers a conformational change that shifts RNA production over to make genomic and subgenomic mRNAs. Alternation between genomic (42S) and subgenomic (26S) RNA is assisted by an nsP2 transcription factor (Strauss and Strauss 1994; Lemm et al, 1994; Kaariainen and Ahola, 2002). Polymerization of full length minus-strand and plus-strand RNA can be accomplished through the action of nsP4 alone. However, transcription of subgenomic RNA requires the action of other non-structural proteins. Minus-strand RNA production is mediated by a 3' CSE and the polyA tail of the positive-strand template. Transcription of genomic RNA depends upon a 3' CSE in the negative-strand. The RNA-dependent RNA polymerase uses these features in order to identify template RNA and commence transcription (Thal et al, 2007). During the process of alphaviral transcription, three double-stranded RNA replicative intermediates are formed. One of these replicative forms is complementary to the alphaviral genomic RNA and another is complementary to 26S RNA (Simmons and Strauss, 1972a). The 3' polyadenylate tail on the end of alphaviral genomic and subgenomic mRNA is added by nsP4. The terminal adenylyltransferase activity of nsP4 was observed in purified recombinant protein that acted on a 45 nucleotide RNA substrate corresponding to a sequence 5' of the poly A tract of SINV RNA (Tomar et al, 2006).

The alphavirus structural polyprotein is encoded by a 26S RNA species whose transcription is initiated by a subgenomic promoter. The core unit of the SINV promoter consists of the 18 or 19 nucleotides upstream and 5 nucleotides downstream of the nsP4:capsid junction.

This sequence is conserved across a number of different alphaviruses (Levis et al, 1990). Raju and Huang (1991) used a plasmid with two SINV subgenomic promoters driving expression of chloramphenicol acetyl transferase (CAT) to evaluate the contextual and sequence-based factors influencing promoter activity. They showed that the full length promoter (-98 to +14) is 6-7 times more potent than the minimal promoter. Transcription of genes driven by the promoter proximal to the 3' end of the genome was more active than the 5' promoter. Their research also demonstrated that there is competition between the 5' and 3' promoters. Utilization of the minimal promoter placed at the 5' end was diminished with the insertion of progressively more powerful 3' promoters (Raju and Huang, 1991).

The alphavirus subgenomic RNA transcribed and then translated into a structural polyprotein. The structural proteins make up the matrix that is responsible for the containment and delivery of the alphaviral genetic information into a host cell. Structurally, the alphavirus virion is composed of a full-length genomic RNA surrounded by a nucleocapsid that is associated with a host-derived lipid bilayer membrane containing two viral glycoproteins. Two-hundred-fourty copies of the capsid protein make up a 400 angstrom diameter nucleocapsid that is arranged with T=4 symmetry. The alphaviral capsid protein mediates assembly and morphology of mature virions. Envelope glycoproteins are responsible for attaching to cell receptors and undergoing pH mediated conformational changes during fusion with the late endosome and subsequent uncoating (Li et al, 2010). Mutation of the capsid amino acid sequence by Ferreira et al, (2003) resulted in incorporation of greater numbers of capsid, E1, and E2 into the virion in a mathematically progressive series of T numbers (4, 9, 16, 25, 36; Ferreira et al, 2003).

The alphaviral membrane contains E2-E1 heterodimers organized in trimeric spikes projecting outward (Li et al, 2010). The carboxy terminus of E2 crosses into the interior side of the lipid membrane and interacts with the nucleocapsid to stabilize the lattice of membrane proteins. The net result of this interaction wraps the membrane and its constituent proteins in a T=4 icosahedral lattice around the virion. The E2-E1 heterodimers form a spike structure that protrudes from the surface of the virion and is responsible for host-cell receptor binding (Paredes et al, 2005). New and Old World viruses typified by VEEV and SINV seem to use the same receptor to enter cells (Strauss and Strauss, 1994). The envelope glycoproteins have frequently been associated with alterations of host specificity and virulence. Differences in the virulence of strains of WEEV following intranasal inoculation in mice have been associated with genetic variability in structural gene sequence (Nagata et al, 2006). A number of mutations in the structural gene sequence have been associated with strains of VEEV associated with major outbreaks. Phenotypes of epizootic VEEV include an increase in equine virulence and/or an altered vector preference. Hypotheses for enhanced transmission include the ability to induce sufficient viremia in horses for transmission to *Aedes taeniorhynchus* or an increased ability to infect *A. taeniorhynchus.* A threonine to arginine mutation at position 213 altered the immunological profile (serotype) of an enzootic strain of VEEV to that of an epizootic strain. A combination of mutations converted the plaque phenotype in Vero cells for VEEV from large (enzootic) to small (epizootic). A mutation in E2 at site 117 from a glucine to a lysine also resulted in a small plaque phenotype typical of epizootic VEEV strains in another enzootic strain (Anischenko et al, 2006; Brault et al, 2004b; Brault et al, 2001). From 2005 to 2007, CHIKV caused major epidemics in Italy and on islands east of Madagascar including La Reunion Island. CHIKV is normally transmitted by *Aedes* spp. mosquitoes and urban outbreaks have been

associated with *Aedes aegypti*. CHIKV transmission during recent outbreaks was attributed to *Aedes albopictus,* the Asian tiger mosquito. A change from an alanine to a valine residue at site 226 of the E1 protein allowed CHIKV to infect *A. albopictus*. As the E proteins are important for attachment to host-cell receptors and viral fusion, it is possible that this mutation allowed CHIKV to more easily penetrate a midgut entry barrier in *A. albopictus*. Transmission by this new vector allowed CHIKV to dramatically increase its geographic range into areas formerly clear of infection (Tsetsarkin et al, 2007).

A small protein encoded by a sequence immediately 5' of the E1 sequence, 6K is a ~6kD protein that was found to be incorporated into the alphaviral virion in small amounts. The 6K protein is characterized by a significant degree of acylation, hydrophobicity, and a cysteine-rich amino acid sequence. Interestingly, 6K appears to undergo a -1 ribosomal frameshift, resulting in the production of a tenth alphaviral protein TransFrame protein (TF) that migrates at around 8kD (Strauss and Strauss, 1994; Firth, 2008).

Modulation of host cell transcription

In addition to serving a structural function, capsid protein is transported to the nucleus of mammalian cells and is used by New World alphaviruses to inhibit host cell transcription (Atasheva et al 2008). The capsid protein does not appear to enact transcriptional shut-off for Old World viruses. Instead, nsP2 serves this purpose for SINV and SFV. Similar to evidence pointing towards an alternative function of capsid protein in VEEV, the non-structural protein 2 of SFV was shown to be localized to the nucleolus in BHK-21 cells. The development of cytopathic effects in cell culture is linked to the activity of VEEV capsid protein. Interestingly, both groups of alphaviruses have developed seemingly independent means of altering the

intracellular milieu to favor viral transcription (Aguilar et al, 2007; Garmashova et al, 2007a; Garmashova et al, 2007b; Peranen et al, 1990).

Defective-interfering genomes

Defective-interfering (DI) genomes of SINV occur naturally and are characterized by an ability to inhibit the replication of closely related viruses. DI segments can result from the repeated passage of virus at a high multiplicity of infection through cell culture. Common elements include the initial 50 nucleotides of the 3' sequence, one of three different termini at the 5' end, and a signal sequence allowing packaging of the RNA into virions (Monroe et al, 1982; Monroe and Schlesinger, 1983; Tsiang et al, 1985; Tsiang et al, 1988). Of note, three independent cases demonstrated the presence of cellular asparagine transfer RNA at the 5' terminus of DI genomes. This suggests that fully effective transcription of negative sense RNA from the SINV genome is mediated by conserved secondary structure (Monroe and Schlesinger, 1983). DI genomes are truncated, predominantly occurring in lengths between 2.0 and 2.5 kilobases and are capable of replication and packaging into virions in the presence of a helper virus. The sequence is malleable enough for a substantial portion to be deleted and replaced with a foreign genetic sequence (Frolov et al, 1996; Levis et al, 1987).

Alphavirus expression systems

Levis et al (1987) deleted a substantial portion of a SINV defective-interfering (DI) genome and replaced it with the coding sequence of chloramphenicol acetyl transferase. Transfection of eukaryotic cell culture resulted in the production of active CAT enzyme (Levis et al, 1987; Frolov et al, 1996). Similar systems have been used to study multiple aspects of alphaviral biology. The insertion of subgenomic promoter sequences at varying locations in a DI genome was used to elucidate the role of promoter sequence and relative location in efficiency of

expression (Raju and Huang, 1991). Levis et al (1986) used cDNA clones of DI genomes to illustrate the sequences necessary for the replication and packaging of SINV. Deletion of sections of the cDNA clone demonstrated the necessity of certain sequences for the replication of the DI RNA produced following transfection into cell culture. Their experiments showed that a 162 nucleotide region in the 5' region of the DI genome and a 19 nucleotide region in the 3' end were essential for replication (Levis et al, 1986).

Replicon SINV expression systems consist of the non-structural coding region of the genome with a gene of interest under the direction of the subgenomic promoter. These constructs were replication-competent but incapable of packaging without the structural proteins being supplied *in trans* by a helper virus (Frolov et al, 1996). Xiong et al (1989) replaced the structural genes of SINV with a gene encoding CAT. This system rapidly expressed large copy numbers of CAT *in vitro*. The use of this expression system in avian, mammalian, and insect cells with seven passages underscored its use as a broad-spectrum expression system of notable stability (Xiong et al, 1989). Replicons expressing GFP under the subgenomic promoter identified Langerhans' cells as the primary cell type infected by VEEV. The replicons are capable of replication but cannot exit the host cell. GFP expression was therefore localized only to cells infected immediately after injection. Replicons possessing packaging signals were produced in cell culture with truncated helper viruses expressing the VEEV capsid and envelope proteins. The helper viruses lacked packaging signals and so were not present in the released virions. Cell types showing expression of GFP represent the initial target of the packaged replicon (MacDonald and Johnston, 2000). The use of SINV alphavirus replicons has demonstrated bone and muscle tissue as targets for viral replication. Replicons are only capable of a single round of

replication. Therefore, the expression of GFP in tissue following inoculation represents the initial targets of viral infection (Heise et al, 2000)

Replicons capable of both replication and packaging have been constructed with the use of a defective helper RNA. These RNAs are composed of the structural genes of SINV under the control of a subgenomic promoter and also contain sequences essential for packaging. The net result is a bipartite genome that is capable of efficient replication and packaging into an infectious virion. This was first done with SINV and resulted in the expression of CAT in chicken embryo fibroplasts through multiple passages. Medium from these cells yielded up to 1 x 10^6 PFU/mL (Geigenmuller-Gnirke et al, 1991). A SINV replicon system was used to express CAT in *C. pipiens pipiens* salivary gland tissue and saliva. These experiments highlighted the possibility of using this system to study the role of salivary gland proteins in mosquitoes (Kamrud et al, 1997).

Western equine encephalitis virus

WEEV was first isolated by Meyer et al in 1931. Equine brain homogenates from animals sacrificed during an epizootic yielded an infection clinically identical to cases described during the epizootic. WEEV was passed from animal to animal through infected central nervous system (CNS) material and was proven to retain infectivity after filtration, identifying the etiologic agent as a virus (Meyer et al, 1931). WEEV was found to be present in the blood of infected subjects and was transmitted to guinea pigs, horses, mules, rabbits, monkeys, mice, and rats (Howitt, 1932) as well as pigeons (Giltner and Shahan, 1933a). WEEV was distinguished from EEEV by exhibiting a less acute course of illness in combination with a lesser mortality. Histological examination also revealed a similarity in neural pathology. The two viruses were distinguished immunologically and separated into eastern and western equine encephalomyelitides (Giltner and

Shahan, 1933b). The principal vector for WEEV was established as *C. tarsalis* Coquillet (Hammon et al, 1942) and WEEV is maintained in a bird-mosquito transmission cycle (Hardy, 1987). WEEV has been isolated from sparrows, a mourning dove, and a Swainson's Hawk. In addition, evidence of infection of ducks (Burton et al, 1961), turkeys (Burton and McLintock, 1970), chickens (Hoff et al, 1970), and a number of other birds was described. The squirrel species, *Spermophilus richardsonii*, has yielded WEEV isolates on several occasions and may serve as an additional reservoir species (Burton et al, 1966; Leung et al, 1975). Leung et al (1975) provided further evidence supporting this hypothesis by describing a higher seroprevalence rate of WEEV in *S. richardsonii* during an epidemic year compared to years absent of epidemic transmission (Leung et al, 1975). *Aedes dorsalis* was implicated as the vector responsible for WEEV transmission between small mammals (Burton et al, 1966).

Taxonomy

WEEV is the result of a recombination event between a SINV-like and EEEV-like ancestor (Hahn et al, 1988). This idea is supported by sequence data confirming significant homology of the WEEV non-structural genes and part of the capsid gene with EEEV. The structural genes coding for envelope glycoproteins E1 and E2 bear substantial similarity with SINV. Thus, it seems likely that WEEV acquired its nonstructural and capsid genes from the EEEV-like ancestor and the genes encoding structural glycoproteins from its SINV-like ancestor. The recombination event is hypothesized to have occurred 1,300 to 1,900 years ago according to estimates of nucleotide mutation rates in the envelope glycoproteins of WEE viruses (Hahn et al, 1988; Weaver et al, 1993b; Weaver et al, 1997). Resolution of the structure of the WEEV virion by cryoEM (Figure 1.1) was completed by Sherman and Weaver. Purification of WEEV and electron microscopy revealed a viral population with diverse morphology in terms of size and

membrane configuration. The archetypal WEEV virion, however, exhibits the same T=4 symmetry and is largely similar to the structure seen in solved structures of other alphaviruses, with some differences. Capsomer rotation was found to be similar to SINV (Old-World) but significantly different from VEEV and AURAV (New World) which is remarkable considering the degree of homology between WEEV and new-world capsid proteins (Sherman and Weaver, 2010).

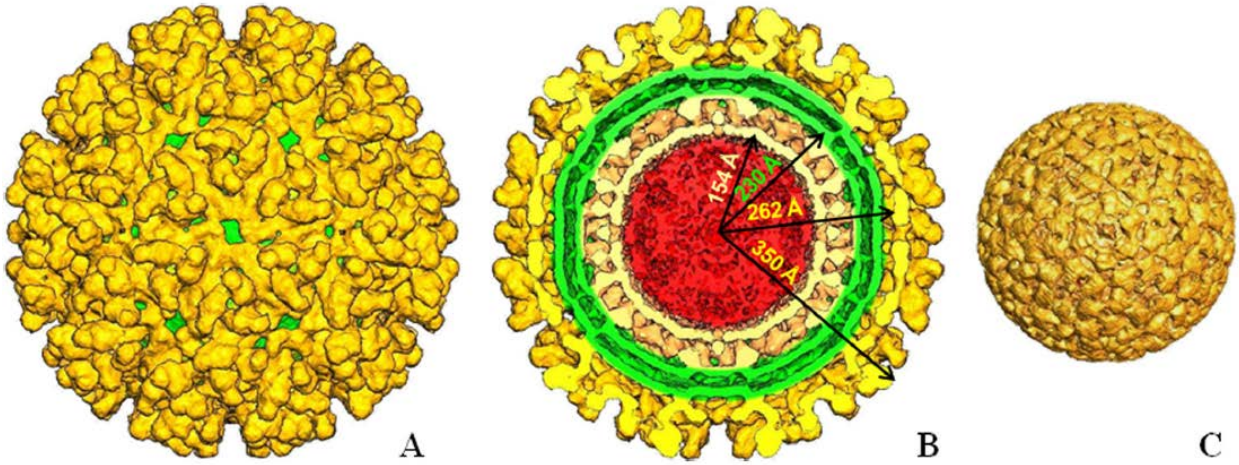

Figure 1.1 WEEV virion (A), sectioning of virion showing nucleocapsid and packaged RNA (B), and nucleocapsid (C) structures as determined by cryoEM (Sherman and Weaver, 2010).

The WEE antigenic complex includes SINV, Ft. Morgan virus (FMV), Highlands J virus (HJV), WEEV, Buggy Creek virus (BCRV), and Aura virus (AURAV). The WEE antigenic complex was identified and separated from other alphaviruses using serology and nucleic acid sequence analysis (Calisher et al, 1988; Weaver et al, 1993; Weaver et al, 1997). HJV is located throughout the eastern United States and exhibits a transmission cycle involving *C. melanura* mosquitoes and passerine birds in mimicry of EEEV transmission (Hayes et al, 1977a). HJV is closely related antigenically and genetically to WEEV but was determined to be a separate virus (Calisher et al, 1988; Allison and Stallknecht, 2009). SINV was first isolated in Egypt from *Culex* mosquitoes (Taylor and Hurlbut, 1953; Taylor and Hurlbut, 1955). SINV is transmitted

between avians by ornithophilic mosquitoes in the Old World (Niklasson, 1988). FMV and BCRV are transmitted by a hemipteran vector, *Oeciacus vicarious,* in the Cimicidae family between nesting cliff swallows (Hayes et al, 1977b, Moore et al, 2007). AURAV, unlike other viruses in the WEE complex, is not a recombinant virus and appears to be a New World Sindbis-like virus. AURAV was isolated from *A. serratus* in northern Argentina and Brazil and is pathogenic in mice (Causey et al, 1963; Rumenapf et al, 1995).

In the United States, WEEV was isolated from mosquitoes in the upper Mississippi Valley in Minnesota (Burroughs and Burroughs, 1954), locations throughout California (Kramer and Fallah, 1999), Texas (Ayers et al, 1994; Hayes et al, 1967) Washington (Hammond and Hewitt, 1942), and Colorado (Cockburn et al, 1957). WEEV was isolated as far south in the Americas as Argentina (Calisher et al, 1985). Populations of WEEV show a significant degree of genetic homogeneity between strains isolated in locations spread throughout the Americas. Despite the similarities between structural genetic and amino acid sequences, strong differences in virulence have been observed between strains with over 96% homology. WEEV isolates may be broadly divided into high and low virulence phenotypes in mice (Nagata et al, 2006). Kramer and Fallah (1999) examined viruses isolated over 60 years in California and demonstrated a division into four phylogenetic clades. The same group included viruses separated temporally by up to 30 years and spatially by the mountain ranges separating the major valleys in California (Kramer and Fallah, 1999).

WEEV was shown to induce significant pathology in both mosquitoes and mammals. WEEV infection of *C. tarsalis* via blood meal resulted in sloughing of the midgut epithelium and necrosis of epithelial cells (Weaver et al, 1992). *C. tarsalis* demonstrated a reduction in flight

activity by 27.5% and engaged in 26.1% fewer spontaneous flights during a 6-11 day period following infection by WEEV (Lee et al, 2000).

Epidemics

The first case of WEE diagnosed in a human occurred when a patient was admitted to Tulare County Hospital in the San Joaquin Valley of California. He presented initially with a severe headache, malaise, and a stiff neck. He progressed into a coma and developed a fever of 108°F, dying four days later. Howitt, using serum from the patient, was able to diagnose the infection as the western type of equine encephalitis (Howitt, 1939). WEEV infection in humans commonly results in an asymptomatic illness, with the proportion of cases showing symptoms from infection reduced demographically as the age of the person increases. The proportion of symptomatic:asymptomatic cases in children less than one year of age is 1:1. The fraction of cases lacking symptoms increases to a ratio of 58:1 in children between the ages of 1 and 4. The vast majority of cases in people over 14 years old exhibit no clinical symptoms. Those infections that go on to present clinically do so with fever, headache, nausea, vomiting, malaise, and anorexia. A subset of cases progress to encephalitis or encephalomyelitis with neck-stiffness, somnolence, coma, and death. Other neurological signs such as seizures, confusion, and altered mental capacity may be present. Of those who progressed to convalescence from encephalitis, 15-30% developed neurological sequelae. Sequelae were most prevalent in children less than one year of age. Basal ganglia supporting vasculitis and focal hemorrhages have been observed in the brains of those who have succumbed to WEE. Other common pathological signs include accumulation of lymphocytes around blood vessels (perivascular cuffing) and foci of necrotic or inflamed tissue in the CNS (Adamson and Dubo, 1942; Rozdilsky et al, 1968; Anderson, 1984; Zacks and Paessler, 2010). Neurological signs severe enough for the patient to seek

hospitalization oftentimes do not present until a year or more has passed since the initial infection. In one study surveying persons with documented cases of WEEV from 1940 to 1952, 15 out of 101 patients developed neurological problems (Fulton and Burton, 1953). Neurological repercussions of WEE following an outbreak in Texas included mental retardation, brain dysfunction, spastic weakness, speech and hearing deficits, and convulsions. Poor prognoses were more likely if the patient was under one year of age when infected (Earnest et al, 1971).

Table 1.1 Symptoms exhibited by human patients during an outbreak of WEEV in 1941 (Adamson and Dubo, 1942).

Symptom	*Percentage occurrence*
Headache	96.3
Frontal	81.8
Frontal alone	34.2
Temporal alone	7.5
Occipital alone	4.8
Sleep disturbance	92.2
Somnolence alone	71.3
Insomnia alone	6.2
Both (insomnia followed by somnolence)	14.7
Cerebral symptoms	73.7
Muscle pains	62.5
Neck	42.0
Back	46.6
Limbs	20.0
Chills and sweats	75.5
Vomiting	46.8
Visual disturbances	14.7

WEE epidemics are favored by an increase in surface water, increased numbers of *C. tarsalis*, availability of virus to the vectors, large numbers of susceptible avian hosts, and a decrease in the extrinsic incubation period of the virus due to higher ambient temperatures. Preference by mosquitoes for unprotected hosts left outside (such as chickens and horses) supports the abortion of epidemics despite increased rates of vector infection and transmission.

Effective mosquito control programs also contribute to the prevention of WEE epidemics (Reeves et al, 1964). Vaccination has been shown to be highly effective in abrogating the effects of WEE epizootics by protecting susceptible animals from infection (Potter et al, 1977). Increased numbers of *C. tarsalis* captured in light traps were correlated with a higher incidence of WEEV cases in humans from 1953-1973 in California. However, the highest levels of *C. tarsalis* population were associated with a zero incidence of WEEV in humans (Olson et al, 1979). In Alberta, Canada it was noted that outbreaks of WEEV in humans were coincident with epizootics in horses during August and September (Morgante et al, 1968). A shift in feeding preferences on the part of the vector could also explain outbreaks in humans and equines as *C. tarsalis* is largely ornithophilic. Changes in feeding preferences have been observed in conjunction with outbreaks (Sellers and Maarouf, 1988).

Southerly winds have been hypothesized to transport infected *C. tarsalis* from outbreaks in the United States north to Canada, thereby instigating outbreaks among horses and man. Sequential transport of these mosquitoes by southerly winds would carry infected mosquitoes north from Texas and deposit them in Oklahoma. Infected *C. tarsalis* populations would then spread to Kansas and Nebraska followed by Minnesota, Wisconsin, and Manitoba. Breaks in weather would allow bloodfeeding and reproduction of infected females (Sellers and Maarouf, 1988; Sellers and Maarouf, 1993).

Low rates of natural transmission in some regions may also partially explain the lack of major WEE outbreaks. Hardy et al (1979) caught *C. tarsalis* from regions of California that had yielded WEEV isolates from mosquitoes. The *C. tarsalis* from these regions was assayed for transmission competence with chicks. Wild-caught mosquitoes exhibited a lower (20-30%)

transmission rate compared to a laboratory strain of *C. tarsalis* which transmitted WEEV 100% of the time (Hardy et al, 1979).

During the summer of 1941; North Dakota, Minnesota, and the neighboring Canadian provinces experienced an unusually severe outbreak of WEEV that affected over 3,000 people. The mortality rate ranged from 8-15% in those affected (Burroughs and Burroughs, 1954). At the same time there was a series of epidemics in the plains provinces of Canada. Saskatchewan had 543 cases of human WEE, Alberta had 42, and 509 cases were reported in Manitoba. In Manitoba, the case fatality rate was 15.3%. Most cases occurred in males or in persons over 20 years of age (Artsob and Spence, 1979; Davidson, 1942; Jackson, 1942; McGugan, 1942, Donovan and Bowman, 1942). A series of epidemic years in the Yakima Valley of Washington from 1939-1941 affected 115 people and killed at least 13 from encephalitis. The outbreak was determined to be from a combination of WEEV and St. Louis encephalitis (Hammon and Howitt, 1942; Hammon et al, 1945). Kern County, California suffered an outbreak in the summer of 1943 involving 203 patients with viral infection of the CNS, 19 were laboratory confirmed to be infected with WEEV (Hammon et al, 1945). A concurrent outbreak of echovirus 9 and WEEV was identified in Alberta, Canada in 1963 followed by an outbreak of WEEV in 1965. Researchers diagnosed WEEV in 6 (1963) and 7 (1965) patients from blood and CSF samples (Morgante et al, 1968). Between July and August of 1975, 39 cases of WEE were laboratory confirmed through serology in eastern North Dakota and western Minnesota in the Red River Valley. The onset of the human outbreak occurred 5 weeks after the first equine case of WEE was diagnosed in the same area (Potter et al, 1977). In 1987, the Centers for Disease Control and Prevention (CDC) received reports of 37 cases of WEEV with 29 reported from Colorado, 3 from Nebraska, 2 each from North Dakota and Texas, and 1 from Montana (CDC, 1987).

Epizootics

WEEV has been associated with a number of epizootics involving domesticated animals. During the summer of 1930, almost 6,000 horses exhibited symptoms of encephalomyelitis in the San Joaquin Valley of California. Approximately 3,000 horses either succumbed to infection or were sacrificed after the onset of severe symptoms (Meyer et al, 1931). A series of epizootics throughout the plains provinces of Canada from 1935-1938 affected over 60,000 horses. Southern and northwestern Manitoba bore witness to 52,500 cases of equine encephalitis with 15,000 succumbing to infection or sacrificed due to illness (Artsob and Spence, 1979; Savage, 1942; Davidson et al, 1942). From June to September of 1975, 281 cases of WEE in horses were reported in the Red River Valley of eastern North Dakota and western Minnesota (Potter et al, 1977). In 1987, 132 equine cases of WEEV were reported to the CDC from 11 states and Manitoba Province, Canada. In April and June of that year, most of the cases were confined to the Southwest portion of the United States. Cases were reported later in the year until August as widely distributed north as Manitoba, east to Wisconsin, and west across the continental divide (CDC, 1987). The year 1992 bore witness to an outbreak among a population of domesticated emus in western Texas that affected over 100 birds (Ayers et al, 1994).

Vertebrate models

Epizootic strains of WEEV have been associated with neurovirulent and neuroinvasive phenotypes. Enzootic strains of WEEV have frequently been found to have neither phenotype. Greater virus replication was found in mouse tissues infected by strains of WEEV isolated from equine epizootics compared to enzootic strains, leading to a dramatic difference in viremia and viral titers in the brain. All strains of WEEV were found to be lethal in suckling mice following intraperitoneal (IP) inoculation (Bianchi et al, 1993).

Vertebrate animals used in the study of WEEV have included rodents, birds, horses, and primates. WEEV is infectious in hamsters through intracranial, interperitoneal, and intranasal routes at a dose of 10 LD_{50}. A virulent strain of WEEV exhibited a lethal phenotype in the hamsters through these routes. Time to death was different depending upon the route of infection. WEEV infection by intranasal inoculation and intracranial injection resulted in clinical signs by three days post-infection. Following a clear presentation of illness, hamsters infected by the intranasal route succumbed in a matter of hours while intracranially injected animals survived for a further 1-2 days. Interperitoneal and intradermal WEEV inoculations of hamsters resulted in illness after 4 and 5 days, respectively. Death occurred at 6 days post infection with both routes of infection. WEEV infection was associated with prominent lesions in the brain. Common to the interperitoneal and intracranial routes of infection was hemorrhage located around the olfactory bulb 24 and 48 hours post-infection. All routes of infection exhibited astrocyte proliferation soon after infection. Symptoms of WEEV infection consisted of a loss of coordination, rapid breathing, and shivering (Zlotnik et al, 1972).

Monkeys have been used as a model for human WEEV and EEEV infection. Both *Macaca mulatta (*Rhesus macaques; Wyckoff and Tesar, 1939; Hurst, 1936; Syverton et al, 1933) as well as *Macaca fascicularis* (cynomolgus macaques; Reed et al 2009; Hurst, 1936; Syverton et al, 1933) have been used to demonstrate infection by WEEV and EEEV through various routes. Rhesus macaques are susceptible to intracerebral inoculation with both EEEV and WEEV. In addition, Wyckoff and Tesar used young Rhesus macaques to demonstrate infection by the subcutaneous (groin), intravenous (saphenous vein), intranasal, and intralingual routes. Intranasal and intralingual inoculations were found to be similarly lethal to intracerebral injection with similar rates seen for both EEEV and WEEV, though progression to death with

WEEV was slower. Paralysis with EEEV infection occurred after a temperature decrease subsequent to the febrile period of illness. Also observed was a period of paroxysms punctuated with a period of inactivity correlated with reducing temperature. Coma developed gradually, and persisted until the death of the animals. WEEV differed from EEEV in that the peak day of fever occurred on day 5-6 as opposed to day 3-4. Peak body temperature was lower for WEEV and the rise and fall of the febrile period did not occur as rapidly compared to EEEV. The comatose period at the end of the infection for WEEV also lasted longer than was typical for EEEV in these monkeys. WEEV was introduced into the stomach of Rhesus macaques by Wyckoff and Tesar (1939) using a stomach tube but was not shown to conclusively cause disease by this route. WEEV infection by subcutaneous and intravenous injection was difficult to induce, as none of their animals showed symptoms. The macaques developed a protective antibody response (measured through intranasal challenge and serology). The macaque model was also used to test ocular delivery as a means of EEEV infection. Neither of the animals inoculated became ill or developed a measurable immune response. Age-dependent mortality with fatal illness developed in most young monkeys but older macaques (albeit ones used in previous experiments) demonstrated resistance with only a few developing minor neurological signs (Wyckoff and Tesar, 1939).

Cynomolgus macaques were used to test an aerosol model of WEEV infection. Onset of fever, duration, and peak temperature were similar to what was shown previously with intranasal inoculation of cynomolgus macaques. It was found that a higher dose ($1 \times 10^{7.3}$ PFU) triggered a significant increase in white blood cell, lymphocyte, neutrophil, and monocyte populations over the course of WEEV infection. The ID_{50} for aerosol infection of cynomolgus macaques with WEEV was found to be $1 \times 10^{6.25}$ PFU. The first symptom after WEEV infection was fever with

the more severe manifestations of disease occurring after the fever had reached its zenith. Neurological manifestations of encephalitis after aerosol exposure were found to be more likely with WEEV than VEEV. The duration and severity of tremors were more pronounced following WEEV infection compared to VEEV (Reed et al, 2005). WEEV infected macaques were examined for virus in the blood and peripheral organs without evidence being found of pathology or live virus, indicating a CNS specific infection. Similar to aerosol exposure to VEEV, WEEV has been postuled to enter the CNS through the olfactory nerves. Olfactory entry into the CNS is supported by WEEV infection by both aerosol and intranasal inoculation in laboratory animals (Logue et al, 2009; Reed et al, 2005, Wyckoff and Tesar, 1939; Hurst, 1936).

In 1936, Hurst infected guinea pigs intramuscularly and was able to recover virus from blood-free nasal washings with WEEV infected animals but not EEEV infected animals. He also noticed that following intranasal inoculation, both WEEV and EEEV were isolated first from the anterior frontal region and olfactory bulbs. Guinea pigs with surgically excised olfactory bulbs had delayed neurological symptoms after intranasal inoculation as did animals inoculated intramuscularly (Hurst, 1936). Examination of pathology demonstrated lesions in the olfactory nervous system of intranasally inoculated guinea pigs and fewer lesions in intramuscularly inoculated animals. The guinea pig model differed from the macaque model in that Rhesus macaques demonstrated virus in the cerebral spinal fluid initially and did not have virus present in the nasal washes. Macaques that recovered from systemic infection were not always immune to intracerebral challenge (Hurst, 1936). Sacrificed cynomolgous macaques were examined for pathologic changes after aerosol exposure to WEEV. Lesions were confined to the CNS and consisted of nonsuppurative meningocephalitis and demyelination of white matter in the brain and spinal cord. Pathologic investigation of the CNS revealed multifocal necrosis and

inflammation of microglia and lymphocytes. Neutrophils, glial nodules, apoptotic and necrotic cells, and extravasated erythrocytes were also spotted in smaller quantities in the grey matter. Pathology was greater in the brain than the spinal cord, and in the spinal cord the cervical region demonstrated a greater degree of pathology than the lumbar region (Reed et al, 2005).

Horses experimentally infected intranasally and subcutaneously demonstrated significant pathology in the olfactory bulbs, brain stem, optic thalamus, and hypothalamic region. Histological presentation of horses experimentally infected with WEEV revealed lesions similar to horses infected naturally during an outbreak (Hurst, 1934). WEEV has caused a variety of neurological symptoms in horses including loss of motor coordination, fatigue, and differing paralyses depending upon the location of lesions in the CNS (Meyer et al, 1931; Sponseller et al, 1966).

The Swiss mouse (Rockefeller strain) model of WEEV infection was used to identify tissues and pathologies associated with WEEV not passaged in mouse brains. Non-neuroadapted WEEV caused mortality and lesions in s.c. inoculated mice. In 1-2 day old mice, pathologies were mostly due to necrosis and inflammation in connective tissues such as skeletal and smooth muscle, cartilage, and bone marrow. The CNS of older mice was largely absent of lesions. However, 21 day old mice generally exhibited diffuse necrotizing encephalitis, pathologies not seen in younger animals (Aguilar, 1970).

Logue et al (2009) initiated a study that aimed to characterize the differences in virulence between strains of WEEV in CD-1 mice. The McMillan strain, isolated from a human case from Canada in 1942, is characterized by a neurovirulent (mean time to death of 1.9 days following intracerebral inoculation of 10^3 PFU) phenotype in outbred mice following direct introduction into the brain. The McMillan strain of WEEV has a lacuna in passage history documentation

between 1941 and 1973. The IMP181 strain was isolated in 2005 from a *C. tarsalis* mosquito captured in Imperial County, California and caused no mortality after intracerebral inoculation of 10^3 PFU. Both viruses, however, were shown to be neuroinvasive in this study with the McMillan strain exhibiting significantly higher titers in the brain (Logue et al, 2009). The virulence of each respective strain was measured using panoply of techniques addressing cell culture growth kinetics, neuropathology, morbidity, mortality, viremia, course of infection *in vivo,* and time to death following inoculation. Logue et al (2009) examined these characteristics in response to viral challenge after aerosol, intranasal, intravenous, and subcutaneous infection of CD-1 mice. The six strains examined in this study were sorted into three groups based on this characteristic with IMP181, 71V-1658, BFS-2005, and 85-452-NM showing 0-20% mortality with a MTD of 7-9 days. The intermediate group was composed of Montana-64 with a MTD of 6-7 days and a 70% mortality rate. Highest mortality was assigned to McMillan with a 100% mortality rate and a mean time to death (MTD) of 4 days. Of the strains examined, only IMP181 was associated with a consistent 0% mortality. Logue et al (2009) examined in detail the course of infection for the low virulence (IMP181) and high virulence (McMillan) isolates after subcutaneous inoculation. Of 17 organs examined by plaque titration, 8 were shown to exhibit a significant difference in viral titers between IMP181 and McMillan. By 24 hours, McMillan exhibited a 10^3 higher titer in the popliteal and inguinal lymph nodes compared to IMP181. McMillan demonstrated a 10^3-10^5 –fold greater virus titer in the brains of infected mice compared to IMP181. In both isolates the brain contained the highest viral titers with a 10^2-10^3 more PFUs compared to other organs. The spleen at 24 hours post infection with IMP181 demonstrated a $\log_{10}$ higher titer. IMP181 also showed a higher titer in the knees of infected mice by a magnitude of 1-2 $\log_{10}$. Route dependent course of infection was evident with aerosol

transmission showing a reduction in the viral titers of all organs except for the brain, spleen, lung, and salivary gland which were shown to be significantly greater. IMP181 killed 1 of 10 mice examined for mortality following aerosol inoculation. The amount of detectable virus varied according to each organ and strain of WEEV without correlation to virulence. In mice, viremia resulting from subcutaneous inoculation of WEEV was transient and not related to virulence. Logue et al (2009) evaluated six strains for virulence in out-bred CD-1 Swiss mice. WEEV was undetectable in the blood of any of the infected mice 6 hours post infection and only a few members of each study group had viremia several days after infection. Detectable viremia was not present in any of the mice that demonstrated morbidity following infection. Logue et al (2009) examined the brains of mice infected with the McMillan or IMP181 strain of WEEV. McMillan exhibited neural lesions in all infected mice examined that were progressively more severe closer to the MTD. Neural necrosis and edema were mostly localized to the fore-brain. Pathology was laminar and multifocal in nature and distributed in a seemingly random pattern. Apoptotic nuclei and perivascular edema were associated with small blood vessels in infected brains. Two-thirds of the mice infected with IMP181 yielded brains consistent with a normal appearance. The remaining third exhibited a pattern similar to but much less severe than McMillan infected animals (Logue et al, 2009).

Avian species have been used to study WEEV as early as 1945, with experiments describing the transmission of WEEV by peripheral inoculation and bite of *C. tarsalis* in chickens performed in the laboratory. Subcutaneous inoculation resulted in viremia 24 hours post inoculation that was largely undetectable at 48 hours and later post infection (Reeves and Hammond, 1945). WEEV isolated from mosquitoes taken from the Central and Coachella Valleys were compared in their ability to induce viremia and antibody responses in captured

house finches. Age, sex, malaria infection, and location of viral isolation were unrelated to viremia response. Age was related to antibody titers, with younger birds having more WEEV antibodies as determined by indirect enzyme immunoassay (Reisen et al, 2000). A study conducted by Reisen et al in 2006 suggested that young Gambel's and California quail (*Callipepla gambelii* and *Callipepla californica*) were involved in amplification of WEEV as older animals failed to sustain a sufficient viremia for transmission to mosquitoes (Reisen et al, 2006). Further studies with chicks and house finches were used to determine that there was not a significant difference in viremia titer following infection by the BFS 1703 strain of WEEV introduced via mosquito inoculation and syringe injection (Reisen et al, 2000). Serum viremia titer and the probability of chronic infection in house finches were also shown to be independent of concentration of WEEV used in syringe inoculation. Researchers found no difference between injection with 100 PFU (approximately that introduced with a mosquito bite) and 100,000 PFU in terms of viremia or antibody response (Reisen et al, 2004). Reisen et al inoculated 27 bird species from the Coachella and San Joaquin Valleys of California with sympatric isolates of WEEV in order to determine what avian species were competent hosts. It was found that eleven species of this cohort were competent for potential transmission of WEEV. These experiments were used to reach the conclusion that the species range of WEEV during epizootics becomes greatly expanded (Reisen et al, 2003). Translation between avian and mammalian models may be difficult because virulence in baby chicks for mosquito derived strains of WEEV does not translate to virulence in mice. Strains of WEEV were found to be lethal in recently hatched chicks but varied in terms of virulence in neonatal and adult mice (Hardy et al, 1997). Chicks have been promoted as a more sensitive means of detection for encephalitic alphaviruses than mice and are capable of passing virus in feces after subcutaneous inoculation, highlighting a

significant difference between this model and mammalian models (Chamberlain et al, 1954). Chicks were used in an experiment confirming the role of *C. tarsalis* in continuous transmission between different generations of birds for a year (Bellamy et al, 1967).

Transmission

A mysterious and dramatic decrease in WEEV epidemics and epizootics has occurred over the last few decades. Reisen et al (2008) showed that the reduction in cases was not due to a change in WEEV's ability to infect either vectors or reservoir hosts. Vector competence of *C. tarsalis* in response to infection by viral isolates from 1953-2005 was not shown to be significantly different. The competence of white-crowned sparrows and house sparrows for different strains of WEEV was not found to be temporally dependent. A combination of effective equine vaccination and a decrease in the entomological inoculation rate for humans is the likely cause for the absence of epizootics and epidemics (Reisen et al, 2008). Forrester et al (2008) tested the virulence of ten strains isolated between the 1940s and 1990s in mice. Subcutaneous injection was used in an effort to mimic natural transmission by mosquito bite and failed to show a connection between strain virulence and date of isolation (Forrester et al, 2008). WEEV is able to persist between epizootics as a result of low-level transmission between *C. tarsalis* and avian hosts. Support for WEEV persistence was discovered by the capture of infected *C. tarsalis* and occasional infection of sentinel chickens (Reisen et al, 1995). Maintenance of WEEV transmission during interepizootic periods may also occur as a result of vertical transmission. Adult male *A. dorsalis* mosquitoes collected as larvae at a salt marsh in San Luis Obispo County, California were infected with three strains of WEEV. WEEV infected male *A. dorsalis* indicated the presence of vertical transmission (Fulhorst et al, 1994). Parenterally inoculated *A. dorsalis* failed to pass WEEV on to their offspring in a laboratory environment and a subsequent survey

failed to find WEEV in wild *A. dorsalis* (Reisen et al, 1996). Populations of *A. dorsalis* in the Coachella Valley of California have failed to yield isolates of WEEV while there have been historical isolates in the San Joaquin valley. *A. dorsalis* is more likely to feed on human hosts than *C. tarsalis* and is common in the western United States (Hammon et al, 1945; Reisen et al, 1998).

Free WEEV virions have been spotted in the lumen of the mosquito midgut as early as 1 hour after ingestion of an infected bloodmeal (Hardy et al, 1983). Electron microscopy was used by Houk et al in 1985 to document the entry of WEEV virions into midgut epithelial cells of *A. dorsalis* and *C. tarsalis* mosquitoes infected by infectious bloodmeal. Nascent fusion events and naked nucleocapsid structures were observed within 3 hours of bloodfeeding. Apparent nucleocapsids were also found to be contained within epithelial cells within minutes of finishing the blood-feed. Released virions were first seen at 22-24 hours post blood-meal and the release of mature virions continued through 35 hours post infection. The maturation phase of viral development was associated with the basal side of the midgut epithelial cells adjacent to the basolateral membrane. Virions were not attached to the hemocoel side of the basolateral membrane. A refractory strain of mosquito lacked production of nascent virions after *per os* infection with WEEV. This observation was supported by a significantly lower midgut titer following an infectious blood-meal compared to susceptible strains of *C. tarsalis* or *A. dorsalis* (Houk et al, 1985).

Kramer et al (1998) looked at the effect of temperature on the maintenance of WEEV titers in mosquitoes shown to be permissive or refractory to infection at 32°C. At 3 days post intrathoracic injection, permissive mosquitoes developed a BFS 1703 virus titer of $10^{6.3}$ PFU per mosquito. Up to 20% of refractory mosquitoes had detectable levels of virus between 3 and 17

days post-injection at 32°C. However, 80% of sampled mosquitoes at 15°C yielded detectable virus at day 17 post-injection and 100% from days 24 to 31 post injection. Both strains of *Culex tarsalis* were shown to have detectable virus at a higher rate after initial incubation at 15°C compared to 32°C. Kramer et al also looked at dissemination to the salivary glands in both strains of *C. tarsalis*. Ninety-three percent of the sampled members of the permissive strain infected salivary glands 4-5 days post infection compared to 7% of the refractory strain at 32°C thereby demonstrating a salivary gland infection barrier (Kramer et al, 1998). WEEV has been maintained in laboratory infected *C. tarsalis* for up to 8 months, highlighting this species' capability of transmitting virus after overwintering. Survival of infected *C. tarsalis* allowed for persistence of viral transmission (Bellamy et al, 1967). The amount of virus released in the saliva by infected *C. tarsalis* was determined to be between 1.0 and 1.7 $\log_{10}$ PFU with the BFS 1703 of WEEV (Reisen et al, 2000).

Mosquito-Virus Interactions

Arboviruses are largely maintained in transmission cycles through horizontal transmission between vertebrate hosts mediated by vector species. Infection of the vector occurs following the ingestion of a viremic blood meal. An extrinsic incubation period, wherein the virus undergoes replication and dissemination in the vector, leads to infection of the salivary glands and transmission. The arbovirus is introduced by the vector into the vertebrate host with the vector's saliva (Marquardt et al, 2005).

An arbovirus encounters an array of barriers to establishing a successful infection in the arthropod vector. The arbovirus must first infect and replicate in the midgut epithelium. Infection is initiated following virion interaction with a host-cell and subsequent entry into the cell by the virus. Viral binding is frequently species specific and small changes in the amino acid sequence

of the binding protein can alter host specificity. The site of receptor interaction or uptake in cell culture may also depend upon the cholesterol content of the host cell. CHIKV replication in cholesterol-depleted C6/36 cells was lessened compared to normal C6/36 cells (Tsetsarkin et al, 2007). The inability of a virus to infect the midgut is known as a midgut infection barrier (MIB).

Viral maturation and budding from the epithelial cells constitutes a potential midgut escape barrier (MEB). Arboviruses are unable to pass the basal lamina separating the midgut cells from the hemocoel, perhaps necessary for viral dissemination. The basal lamina is composed of glycoproteins arranged in a fine mesh weave (Lehane et al, 1997) that physically bars passage of arboviruses. *A. aegypti* strains have been genetically selected that have MEB's to DENV by selecting for high midgut infection rates and low dissemination rates over time (Bennett et al 2005). Weaver et al (1984) showed that a dissemination barrier can also be present in a strain-specific or concentration dependent manner. *Culex (Melanoconion) taeniopus* mosquitoes were refractory to dissemination of epizootic strains of VEEV and permissive to enzootic strains after oral infection. Twenty percent of mosquitoes examined showed infection with the epizootic strains of VEEV after a high titer blood meal. All mosquitoes were shown to be completely susceptible to infection by the epizootic strains of VEEV following intrathoracic injection of virus, circumventing the midgut. Oral infection with enzootic strains of VEEV at low virus titers resulted in a 91% midgut infection rate. Despite the presence of infection in the midgut, relatively few mosquitoes demonstrated evidence of dissemination compared to higher virus titer bloodmeals. This evidence serves to demonstrate a MEB to low concentrations of infecting VEEV (Weaver et al, 1984).

A new environment, the hemocoel, is encountered by the arbovirus after passage of midgut barriers. The hemocoel, the open circulatory system of the mosquito, allows the arbovirus

to infect susceptible tissues throughout the vector. Arboviruses travel through the hemolymph through transport by hemocytes. Intrathoracically injected SINV was found by Parikh et al (2009) to infect and replicate within *A. aegypti, A. albopictus, A. triseriatus,* and *C. pipiens* hemocytes. The injected SINV was engineered to express GFP under the control of a second subgenomic promoter in these cells. Expression of GFP suggested that active replication was occurring (Parikh et al, 2009).

Dissemination and transmission barriers are also determined by mosquito species. Paulson et al (1989) demonstrated that LaCrosse virus (LACV; *Bunyaviridae*: *Orthobunyavirus*) has different dissemination profiles depending upon which species of the *Aedes (Ochlerotatus) triseriatus* group it infects. *Aedes zoophilus* readily transmits LACV, displaying no significant midgut or salivary gland barriers to the virus. A MEB is evident in *Aedes (Ochlerotatus) triseriatus.* Transmission rates for LACV in *Aedes (Ochlerotatus) triseriatus* increased (from 37% to 79%) with intrathoracic injection as opposed to oral infection (Paulson et al, 1989). *Culex pipiens pipiens* was found to be resistant to oral infection by a Malaysian strain of SINV (MRE16), exhibiting a barrier to midgut infection. *Culex tritaeniorhynchus* is resistant to dissemination of SINV from midgut although the midgut has a high infection rate (Foy et al, 2004).

The posterior portion of the midgut is the site of initial infection for VEEV in *A. taeniorhynchus* (Smith et al, 2007) and EEEV in *Culiseta melanura* (Scott et al, 1984a). WEEV anad VEEV also infect the foregut, ventral diverticulum, and midgut of *Culex tarsalis* and *Culiseta melanura*, respectively (Weaver et al, 1993a; Weaver et al, 1991). O'nyong-nyong virus (ONNV) had foci of infection in both the anterior and posterior portions of the midgut of *A. gambiae* four days following ingestion of a viremic bloodmeal (Brault et al, 2004). At day seven,

dissemination was observed with foci of infection in the salivary glands, head, hindgut, or malpighian tubules (<30%). Midgut infection remained focal in nature and did not exhibit significant dispersal until days 10-14 of infection in a minority of mosquitoes tested. Dispersal throughout the midgut epithelium did not exhibit correlation with dissemination (Brault et al, 2004a). SINV was detected in the posterior midgut and portions of the anterior midgut and intussuscepted mosquito foregut of *A. aegypti* following ingestion of an infectious bloodmeal (Foy et al, 2004).

The salivary glands present the last barrier to transmission and potentially possess both an entry and exit barrier to invading virus (Marquardt et al, 2005). Infection of the salivary glands occurred fairly rapidly, with an extrinsic incubation period of less than or equal to 3 days for EEEV in *Culiseta melanura*. Enveloped virions were detected in the salivary matrix by electron microscopy and evidence of viral replication was seen in salivary gland tissue from 55 to 69 hours after oral infection (Scott et al, 1984b). Evidence of such a barrier was demonstrated using *O. triseriatus* with LACV. *Aedes hendersoni* and *Aedes brelandi* were found to be susceptible to infection with LACV. *A. hendersoni* and *A. brelandi* exhibited a low rate of transmission (7% and 27%) compared to *Aedes zoosophus* (85%) following ingestion of an infectious bloodmeal (Paulson et al, 1989). Arbovirus tropism for different anatomic portions of the salivary glands may be involved in determining the presence or absence of a salivary gland barrier. SINV preferentially infected the proximal lateral lobes of *O. triseriatus*. In *A. aegypti*, both the distal and proximal lateral lobes were infected by SINV. In *Culex pipiens*, the entirety of the salivary glands contained SINV antigen (Rayms-Keller et al, 1995). SINV, CO92 WEEV, and the McMillan strain of WEEV were not detected in the saliva of *C. tarsalis* after ingestion of an infectious bloodmeal containing 6-7 $\log_{10}$ plaque-forming-units (PFUs) of virus (Kenney et al,

2010). SINV exhibited high midgut infection and dissemination rates (100% and 95%, respectively) with only 20% of mosquitoes having detectable SINV in the saliva. The CO92 strain of WEEV had 85% and 70% midgut infection and dissemination rates, respectively. CO92 was not detected in the saliva of *C. tarsalis* exhibiting a disseminated infection. The McMillan strain of WEEV was not able to infect a strain of *C. tarsalis* by infectious bloodmeal (*per os;* Kenney et al, 2010). Salivary gland barriers have also been described for other Culicid mosquitoes that impact the transmission of RVFV (Turell et al 2007; Turell et al 2010).

Pathogenesis and infection

Alphaviruses produce pathologic effects in invertebrate cells. Vector species experience pathologic effects upon infection by alphaviruses. EEEV infection of *Culiseta melanura* results in sloughing off of infected midgut tissue, degeneration of midgut epithelial cells, and a loss of basal lamina integrity. The pathology associated with this interaction may aid the virus in accelerating dissemination and transmission as EEEV is able to disseminate throughout the mosquito after 2-3 days and can be transmitted to a vertebrate host 3 days following an infectious bloodmeal (Weaver et al, 1988). This pathology was not seen to be dosage dependent, as a 10,000 fold difference in EEEV titer injected intrathoracically into *C. melanura* failed to show significant difference in mosquito mortality. EEEV injected groups demonstrated a marked increase in mortality compared to controls (Cooper et al, 2000). Infectious blood meals with higher titers of WEEV in a susceptible strain (Fort Collins) of *C. tarsalis* did not show a significant increase in pathologic sloughing of virus in comparison to lower titers of virus in a less susceptible strain (Knight's Landing strain; Weaver et al, 1992).

Vertebrate-virus interactions

The clinical manifestation of alphaviral infection is characterized by headache, fever, rash, myalgia, diarrhea, vomiting, and joint pain. Old World alphaviruses such as SINV, O'nyong-nyong virus (ONNV), CHIKV, Semliki Forest virus (SFV), and Ross River virus (RRV) are associated with severe arthritis which can persist for years after clearance of virus. Infection by New World alphaviruses can cause similar symptoms with the addition of potentially fatal encephalitis. The major New World alphaviruses are western equine encephalitis virus (WEEV), eastern equine encephalitis virus (EEEV), and Venezuelan equine encephalitis virus (VEEV). EEEV is particularly deadly, with fatality rates in symptomatic patients ranging from fifty to seventy percent. Acute disease from EEEV can also result in debilitating neurological sequelae (Deresiewicz et al, 1997; Ryman and Klimstra, 2008).

The course of infection for mosquito-borne alphaviruses begins with intradermal inoculation of the vertebrate host with infectious saliva. The infection starts with viral replication at the site of introduction and by virus migration to lymph nodes responsible for draining that region. Virus migration could also occur as a result of transportation via migratory cells (such as macrophages or dendritic cells). Cell-free virus could also spread through the circulatory system without specific transport. Cells in the draining lymph node become infected and harbor viral replication and amplification. The lymph tissue then releases virus into the circulatory system along with normal venous fluid. Once in the circulatory system, the virus is able to spread throughout the host during primary viremia. A second period of viremia with higher virus titer is initiated following further replication at distant sites. High viremia titer mediates transmission to vector species that take a blood-meal during this time. Eventually, the virus may be capable of

reaching the CNS through either the blood or the peripheral nervous system (Ryman and Klimstra, 2008).

Introduction of arbovirus in the host

Conditioning of alphaviruses while in the mosquito is likely to optimize the ability to infect mammalian cells. Shabman et al (2006) contributed to this hypothesis by testing the ability of mosquito cell-derived VEEV and RRV to infect myeloid DCs and induce a type I interferon in these cells. Increased levels of infection were seen in human and murine primary DCs with VEEV, RRV, and Barmah Forest virus (BFV) grown in mosquito cell culture. Interestingly, mammalian derived virus induced a superior level of interferon production in infected cells. The use of type I interferon receptor deficient DCs was used by Shabman et al (2006) to test the relation between interferon induction and viral replication. Mammalian derived RRV demonstrated comparable levels of infection with insect cell derived RRV in the absence of an effective type I interferon response. With type I interferon, infection of DCs with mosquito cell derived RRV was augmented compared to infection with mammalian RRV. Interferon induction was correlated with different glycosylation of alphavirus E2 proteins. Complex glycosylation of E1 and E2 was associated with mammalian cell culture and interferon induction while high-mannose N-linked glycans were linked to mosquito cell culture and lower levels of interferon induction (Shabman et al, 2006).

Virus is introduced into the host with saliva secreted by the feeding mosquito. High virus titers of a number of different viruses have been found to be contained in mosquito saliva. Experiments in the 1960s measured virus concentrations in saliva by infecting mice with varying dilutions of saliva and measuring a dose sufficient to kill 50% of infected mice (LD_{50}). Depending upon the virus and vector, concentrations from 1,000 to 100,000 LD_{50} were measured

(Collins, 1963; Devine et al, 1965; Hurlbut, 1966; LaMotte, 1960; Thomas, 1963). A more recent experiment measured between 0.2 and 3.6 x 10^7 PFU of VEEV titrated from extracted mosquito saliva (Smith et al, 2005). While these assays allow a measure of virus titer in saliva, they do not completely provide an answer for the amount of virus introduced *in vivo*. Styer et al (2007) developed an *in vivo* assay for measuring the amount of WNV introduced into a chick or mouse during probing and feeding. Recovery of WNV from tissues following infection led to an estimation of introduced virus titers. *C. tarsalis* introduced about 1 x 10^5 PFU, *Culex pipiens* 1 x 10^6 PFU, *Aedes japonicus* 1 x $10^{4.7}$ PFU, and *Aedes (Ochlerotatus) triseriatus* was estimated to inject 1 x $10^{3.4}$ PFU of WNV. These estimates were based on approximately a one-third recovery of injected virus in controls (Styer et al, 2007). Once introduced into the host, arboviruses seem to follow an initially extravascular course of infection. This was shown by Turell et al (1992, 1995) who fed infected mosquitoes on the distal portions of suckling mouse tails. Amputation of the tail ten minutes after feeding was shown to significantly extend the survival time of mice following infection by RVFV, VEEV, and St. Louis encephalitis virus (SLEV). Tail amputation an hour after infection by mosquito bite was ineffective at delaying mortality (Turell et al, 1992; Turell et al, 1995). WNV appeared to exhibit both intravascular and extravascular dissemination in the host (Styer et al, 2007).

Early stages of infection and peripheral replication

DCs, while important for the immune response against an invading pathogen, are also targets for viral infection. Viruses achieve entry into DCs through two possible routes. Specific binding between a viral ligand and a DC receptor/co-receptor can initiate entry similar to a normal infection of a host cell. If the intracellular milieu is permissive, the virus will be endocytosed and taken to the endosome. Subsequent viral fusion, release of nucleic acid,

replication, maturation, and release from the DC will then occur. Some of the viral particles may be subjected to degradation by the proteasome and loaded on to major histocompatibility class II (MHC-II) molecules. The MHC-II molecules containing viral peptides are trafficked to the outer membrane where they can present the foreign antigen to T-cells. Alternatively, the virus may be internalized via binding to DC-specific intercellular adhesion molecule-3-grabbing non-integrin (DC-SIGN) or Langerin (for Langerhans' cells; Pohl et al, 2007).

VEEV is transported to draining lymph nodes as early as four hours post-inoculation by resident DCs. Viral titers of up to 10^7 PFU/gram were shown to occur in the draining lymph node 6 hours post-injection. Viral replication in the draining lymph node occurs 6-8 hours before amplification at the site of subcutaneous injection. MacDonald and Johnston (2000) conducted experiments with VEEV demonstrating that Langerhans' cells constituted the primary cell population to be infected with virus (MacDonald and Johnston, 2000). DCs differentiate into migratory DCs and travel to nearby draining lymph nodes after infection or ingestion of virus (Foti et al, 2004). Infection by WNV and SFV increased numbers of dermal DCs present in lymph nodes draining the site of injection. This increase is dependent upon the injection of live virus and was not seen following injection of UV-inactivated virus (Johnston et al, 2000).

WNV was shown to replicate in human DCs *in vitro*. A possible role for DCs in WNV infection was also illustrated by the enhanced replication of glycosylated strains of WNV in these cells. This enhanced replication correlates with the greater virulence associated with WNV strains possessing glycosylated envelope proteins (Beasley et al, 2005). Langerhans' cells and DCs have also been shown to be targets of DENV infection *in vitro*.

Differences in the site(s) of peripheral replication may account for differences in general pathogenesis. VEEV utilizes dermal DCs and macrophages for transport to draining lymph nodes

where it undergoes peripheral amplification. Alternatively, EEEV does not replicate well in lymphoid tissue, including draining lymph nodes and the spleen. EEEV replicated more efficiently in the mesenchyme of the host such as osteoblasts or fibroblasts for peripheral amplification. EEEV's replication in myeloid tissue is not dependent upon the activation of interferon by the host cells or receptor recognition. As EEEV was as virulent as VEEV in mice, infection of draining lymph nodes was not essential for systemic replication and neuroinvasion (Gardner et al, 2008). A relationship between virulence and the ability to replicate in macrophages was established with VEEV. While both a virulent (V3000) and an attenuated strain (V3032) of VEEV were capable of establishing infection in quiescent peritoneal macrophages, the virulent strain reached maximum titer in a shorter period of time. Activation of infected macrophages severely restricted replication of the attenuated strain of VEEV. V3000 did not demonstrate a significant reduction in growth kinetics as a result of macrophage activation by lipopolysaccharide. Activation of macrophages by IFNα/β did restrict V3000 replication to a lesser degree than V3032. Increased cell death was seen with infection by V3000 compared to V3032 VEEV (Grieder and Nguyen, 1996).

EEEV typically exhibits a course of infection characterized by two phases. The initial phase is self-limiting and involves peripheral amplification in fibroblasts proximal to the site of injection as well as in osteoblasts. Contrary to other arboviruses that use draining lymph nodes as the primary site of amplification, EEEV appears to utilize osteoblasts for this purpose. Extraneural amplification leads to a transient viremia that provides the impetus for viral replication in other tissues, including cardiac muscle, skeletal muscle, renal tissue, and dermal epithelium. EEEV most likely enters the CNS by passing through the blood-brain barrier without the involvement of the olfactory bulb. This is illustrated by the diffuse pattern of central nervous

infection and a relative absence of pathology in the olfactory neuroepithelium (Vogel et al, 2005).

Neurovirulent strains of SFV were found to infect the CNS by crossing the blood-brain barrier as evidenced by radiation of infection throughout the brain from perivascular foci (Fazakerley et al, 2006). VEEV infection progresses to encephalitis in less than 15% of symptomatic cases and rarely presents a fatal outcome. Usually, a mild to severe illness with nonspecific symptoms results from a case of VEE (Gardner et al, 2008). Of those who succumb to VEEV infection, most have significant pathologic changes to the brain, lungs, lymph nodes, and gastrointestinal tract. Most of the cadavers examined by De La Monte et al (1985) demonstrated follicular necrosis of the lymph nodes, edema and meningitis in the CNS, interstitial pneumonia, and edema of the lungs (De La Monte et al, 1985). EEEV infection begins with a similar picture of 'flu-like' symptoms. Following a short prodromal phase of illness there is a rapid onset of neurological deterioration. In one clinical study nearly 90% of patients became stuporous or comatose, 50% had seizures, and 36% succumbed to infection. Only one of the survivors recovered fully while 14/36 had mild sequelae, 3/36 had moderate sequelae, and 5/36 experienced severe debilitation as a result of infection (Deresiewicz et al, 1997).

The Old World alphaviruses present a very different clinical picture, with disease characterized primarily by rash, fever, and joint pain without significant CNS involvement in human beings. Neonatal mice, however, are highly susceptible to developing encephalitis caused by SINV with the outcome depending upon the neurovirulence of the strain (Griffin, 1989). ONNV and CHIKV have been responsible for massive epidemics of debilitating joint pain in Africa, Asia, and the Indian Ocean. An acute illness typified by headache, rash, fever, inflammation of lymph nodes, and arthralgia usually results from infection by these viruses.

RRV and Barmah Forest virus (BFV) are endemic to Australia and cause polyarthritis (Rulli et al, 2007).

Joint pain and arthritis during and after alphaviral infection could be caused by viral replication near or at the site of the joint, host immune response damage to the joint, or some combination of the two. Viral replication was shown to specifically occur along the periosteum and tendons adjacent to the joint without the presence of inflammation (Heise et al, 2000). Natural killer (NK), CD4+ and CD8+ T-cells, and macrophages have been found in the synovial fluid of patients infected with RRV. A mouse model of RRV induced arthritis was developed that demonstrates viral infection of the periosteum, muscle, and joint tissue along with an infiltrate of inflammatory macrophages into the synovial cavity of the joint. The resulting inflammation of the joints mirrors the symptoms described in human patients. The action of macrophages was demonstrated to contribute to the striated muscle and joint inflammation seen in RRV infection of mice (Rulli et al, 2007; Lidbury et al, 2000.) RRV RNA persisted a month after the presentation of symptoms in joint fluid (Soden et al, 2000).

Infection of the central nervous system

CNS involvement is a possible complication of alphaviral infection, especially with the New World alphaviruses. Different viruses utilize different routes to achieve entry into the CNS. The two main routes are through the peripheral nervous system and direct entry through the endothelial cells lining the blood vessels that supply the brain. The olfactory nervous system has been implicated as a possible route for neuroinvasion by both VEEV (Vogel et al, 2005) and SINV (Cook and Griffin, 2003). VEEV was detectable in the noses of intranasally infected guinea pigs before the onset of viremia in some cases and in all cases virus titers in the nasal mucosa outstripped virus titers in other tissues up to 18 hours post infection. VEEV infection

was not found in the nose significantly prior to other organs or at a higher titer in infected rabbits (Danes et al, 1973b). VEE virions were detectable in the olfactory bulb by electron microscopy (Jelinkova et al, 1974). In horses infected with EEEV the olfactory bulb was not found to be positive for virus (Hurst, 1934). With intranasal VEEV infection of Rhesus macaques, pathologic changes were first demonstrated in the olfactory bulbs (Danes et al, 1973a).

The death of infected neurons can come about through either necrosis or apoptosis. Necrotic cell death involves cell swelling, lysis, and induction of inflammation. Apoptosis is a physiologic process that results in an organized destruction of a cell and is associated with embryonic development, immune system maturation, and viral infection. Characteristics of apoptotic cell death include cell shrinkage, nuclear fragmentation, and segmentation into apoptotic compartments that are absorbed by neighboring cells (Kerr et al, 1972; Searle et al, 1982). SINV infection of neonatal mice results in apoptotic death of neurons while adult mice (who are resistant to SINV induced encephalitis) suffer necrotic damage to anterior horn motor neurons when infected by a neurotropic virus (Griffin, 2005). Intracerebral inoculation of neonatal mice with SINV elucidated a mechanism for migration using the brain's ventricular system. This results in viral spread throughout the grey matter and to the anterior horn of the spinal cord. Infection and death of these cells accounts for the hind-limb paralysis seen with infection (Jackson et al, 1987). Neurons proximal to necrotic cells are also killed in adult mice through the activation of neurotoxic pathways. It is also likely that different cell types infected by neurovirulent SINV are killed through the activation of different pathways. Apoptosis of neonatal neurons is induced as a result of viral membrane fusion which activates acidic sphingomyelinase. This enzyme is responsible for the degradation of sphingomyelin and subsequent release of the pro-apoptotic molecule ceramide (Griffin, 2005).

Vertebrate host immunity

Immune mediated clearance of viral infections is accomplished through a complicated process. Inhibition of viral spread to cells beyond the site of infection is initially important to the host. Cell free infectious virus must be limited and removed for this to occur in many viral infections. Sites of virus propagation must be cleared either through the removal of infected cells, macrophage phagocytosis, or cessation of intracellular viral replication. The innate arm of the immune response is essential for the completion of the first stages of clearance with antibody-mediated humoral immunity serving to clear or neutralize remaining virus (Griffin, 2003). Dendritic cells (DCs) serve an important role as mediators of innate immunity. They are noted for their capacity as antigen presenting cells and possess an array of pathogen recognition receptors coupled with a significant phagocytic activity. There are a number of DC sub-populations throughout the body. Resident DCs are found in non-lymphoid tissues and act as sentinels for the innate immune system. Langerhans' cells and dermal DCs form a network of sentinel cells in the skin by sampling the environment for microbial markers. The infecting microbe expressing these markers is phagocytosed. Following exposure to a potential pathogen, resident DCs mature into a migratory stage. Migratory DCs have a life-span limited by terminal differentiation and eventual apoptosis. Migratory DCs present foreign antigens to T-cells in the lymph tissue via major-histocompatibility protein II. This stimulates division of compatible T-cell populations and the release of cytokines that are involved in the initiation of the adaptive immune response (Foti et al, 2004). Toll-like receptors (TLRs) function to activate DCs in the presence of a pathogen or to mediate internalization, processing and presentation of pathogens. TLRs can be located on the surface of the plasma membrane and are responsible for the recognition of surface pathogen associated molecular patterns (PAMPs). TLR 3, 7/8, and 9 are

localized to low pH endosomal compartments and are capable of recognizing pathogen associated nucleic acids such as dsDNAs, ssRNAs, and dsRNAs (Diebold et al, 2004; Hiel et al, 2004; Krug et al, 2004). DCs also have cytoplasmic pathogen recognition receptors (PRRs) that can detect dsRNA and 5'phosphorylated RNA. Examples of these include retinoic acid induced gene 1 (RIG-1), melanoma-differentiation associated gene 5 (MDA-5), and protein kinase R (PKR). Upon binding a PAMP, these sensors are capable of initiating the production of interferon α/β (IFN-α/β; Kawai and Akira, 2006; Pohl et al, 2007).

IFN-α/β production was effective in combating VEEV pathogenesis as interferon α/β deficient mice exhibited a much shorter time to death (30 hours) compared to control mice (7.7 days) following subcutaneous inoculation. These results were confirmed *in vitro* and several cell types possessing the IFN-α/β pathway exhibited diminished production of an IFN-α/β sensitive VEEV compared to IFN-α/β deficient cell lines (White et al, 2001). Ryman et al (2000) showed that a strain of SINV (TR339) that normally causes a subclinical infection in adult mice adopted a different set of symptoms and tropism with the absence of IFN-α/β. Subcutaneous inoculation of IFN-competent adult Sv/Ev strain mice with 100 PFU of TR339 SINV resulted in clearance of infection by 96 hours post-infection. IFN-α/β deficient mice, however, experienced a significant increase in mortality with death occurring within 84 hours (Ryman et al, 2000). Interferon-γ (IFN- γ) produced by NK cells and activated T-cells is also important for preventing mortality. Mice lacking both IFN-α/β and IFN-γ developed a viral hemorrhagic syndrome after infection by TR339 (Ryman et al, 2007). Sensitivity to IFN was also associated with strains of EEEV that replicated poorly in the brains of infected mice. IFN sensitive EEEV replicated to a level of viremia titer ten-fold higher than a virulent, IFN insensitive strain of EEEV (Aguilar et al, 2008). Other viruses that infect the CNS are frequently cleared through the action of activated T-cells

and the function of IFN-γ. The actions of the innate immune system and released cytokines are important for clearance of peripheral viral infection. Innate immune system factors are deleterious to the health of the brain and so an antibody-mediated immune clearance is also vital for CNS infections (Griffin et al, 2003). Elevated levels of IFN were also found in the CNS of a patient who died following admission into a hospital with WEEV infection (Luby et al, 1971).

Neurons regulate protein levels through degradation of internal proteins in lysosomal compartments. This phenomenon is called autophagy and may also serve an immune function in addition to recycling cellular components. Autophagy occurs during alphaviral infection of the CNS, where clearance of viral components by host cell lysosomes may mitigate the pathologic effects of infection. Less neurovirulent SINV replication in the CNS, host mortality, and virus-associated apoptotic cell death were observed with expression of the lysosomal protein Beclin-1. Double-subgenomic SINV transducing system expression of Beclin-1 protected mice against mortality due to encephalitis. This evidence pointed towards clearance of virus from neurons as an important stage in avoiding encephalitic complications of infection (Levine et al, 1996; Liang et al, 1998; Orvedahl and Levine, 2008). Antibodies against the E2 protein were effective in clearing infectious virus from the CNS and preventing recrudescence (Levine and Griffin, 1992).

Despite active viral replication in the CNS, mortality in neonatal mice after SINV infection can occur in the absence of encephalitis. A severe hormonal stress response accounts for host death in some cases (Trgovcich et al, 1996; Trgovcich et al, 1997). Inflammation and apoptosis of neural tissue has also been observed with alphaviruses. Intracerebral infection by the A7 strain of SFV resulted in the necrotic death of mature oligodendrocites followed by apoptotic death of uninfected bystander cells. Cell death was followed by inflammation and demyelination

even after clearance of virus. It is likely that a T-cell response caused both the inflammatory damage and clearance of virus infected cells (Fazakerley et al, 2006).

Alphavirus infection can have lasting consequences for the host. This is especially evident in cases of EEEV infection that can leave survivors with debilitating neurological sequelae (Deresiewicz et al, 1997). In the case of SFV, an autoimmune reaction directed towards myelin protein induces demyelination of neurons after clearance of virus. In mice susceptible to SFV encephalitis, markers of inflammation and pathology were seen several months after the absence of infectious virus. SFV RNA persisted in mice up to 90 days following infection (Donnelly et al, 1997). SINV E2 and nsP1 RNA sequences were isolated from mice up to 17 months post-infection. Recrudescence of active viral replication was observed in severe combined immunodeficient (SCID) mice up to three months post-infection (Levine and Griffin, 1992).

Infectious cDNA clones of alphaviruses

Infectious cDNA clones are produced by reverse transcription of an RNA template to construct a full-length complementary DNA (cDNA). The cDNA is incorporated into a plasmid for amplification in transformed *Escherichia coli*. Full-length RNA is generated by in vitro transcription and transfected into cells to produce infectious virus. Infectious Qβ bacteriophage was produced by Taniguchi et al (1978) using this method, marking the first successful use of this technology. This process was first used for a mammalian RNA virus (poliovirus) by Racaniello and Baltimore (1981). Mammalian cells were transfected with genomic cDNA andwere able to produce infectious poliovirus that was serologically identical to naturally produced virus (Racaniella and Baltimore, 1981). Full-length infectious clones of alphaviruses have been produced for SINV (Rice et al, 1987), VEEV (Davis et al, 1989), WEEV (Schoepp et

al, 2002; Logue et al, 2009), EEEV (Schoepp et al, 2002), RRV (Kuhn et al, 1991), ONNV (Brault et al, 2004a), CHIKV (Vanlandingham et al, 2005), RUBV (Wang et al, 1994), and Sagiyama virus (SAV; Shirako and Yamaguchi, 2000). Virus produced from these infectious clones is nearly indistinguishable from naturally derived virus in mammalian and insect cell culture (Brault et al, 2004a). Infectious clone technology allows for consistent production of virus from a standardized template without mutations introduced through continued passage in cell culture.

Alphavirus transducing systems

Single virus systems capable of autonomous replication and packaging while expressing a gene of interest have been developed. These alphavirus transducing systems are generated from extant infectious clones and are constructed by duplicating the subgenomic promoter. The subgenomic promoter is cloned from the infectious clone using a polymerase chain reaction (PCR) with primers containing a multiple cloning site. If the second subgenomic promoter is inserted downstream of the structural genes, the resultant construct is referred to as a 3' double-subgenomic alphavirus transducing system (3'dsATS). Insertion of the duplicated 26S promoter between the original promoter and structural polyprotein codon resulted in a 5' double-subgenomic system (5'dsATS). With the 5'dsATS it is important to note that transcription of the structural genes is driven by the inserted promoter and the gene of interest is produced under the direction of the original promoter (Foy and Olson, 2008). The alphavirus genome possesses a certain level of fluidity regarding its length as evidenced by the variability in the length of the C-terminal end of the nsP3 gene (Lastarza et al, 1994). Up to 2,000 extra nucleotides added to the genome can be packaged. However, addition of a heterologous genetic sequence in excess of 1kb can significantly impair viral replication (Foy and Olson, 2008).

Alphavirus expression systems

SINV has been utilized in the construction of expression systems for a number of reasons. SINV's broad species tropism means that it can infect insect, avian, and mammalian cells. SINV cDNA infectious clones allow both the rapid construction of expression systems and the capacity for generation of infectious viral RNA using *in vitro* transcription. Once introduced into a host cell, the subgenomic promoter drives transcription of the desired RNA species which can lead to abundant expression of protein (Hahn et al, 1992).

Stability of insert expression is an important consideration for the use of these systems. Second subgenomic promoters located 5' of the structural genes have been demonstrated to be significantly more stable through cell culture passage compared to 3' double subgenomic systems. GFP expression in Vero cells infected by 3'SINV transducing systems dropped significantly from its original value over five passages while viral titres remained constant. The 5' double subgenomic system continued stably expressing GFP through the fifth passage (Pierro et al, 2003).

An initial difficulty with the use of expression systems derived from the prototypical AR339 strain of SINV was the destruction of mammalian cells *in vitro*. The genomes of these cytopathic SINV replicons were bipartite in nature. One portion would supply the nonstructural genes necessary for producing the RNA-dependent RNA polymerase and methyltransferase. These enzymes transcribe RNA from one or more subgenomic promoters to express genes of interest. With the addition of a second RNA that supplied the SINV structural genes *in trans* virions containing the original replicon were produced. SINV replication was still found to be cytopathic in mammalian cells, making this system fitted for only transient expression. Replicons were engineered to express a selection gene (puromycin) under the second subgenomic

promoter. Cells that showed diminished pathogenesis and resistance to puromycin were selected for. They sequenced the non-cytopathic vector and found that a proline to leucine mutation at location 726 in nsP2 reduced cytopathogenicity. When used to express β-galactosidase, this replicon was shown to have a 96% reduction in activity compared to the cytopathogenic SINV vector. There were diminished genomic and subgenomic RNA levels in cells infected with this replicon. The loss in activity was compensated for through the addition of a DI particle. This DI particle contained a tRNA-like secondary structure attached to the 5' end, a β-galactosidase gene, and a selection marker for G418. The DI particle rescued reporter gene expression compared to the replicon by itself (Agapov et al, 1998). VEEV and EEEV replicons were less cytopathic than similarly constructed SINV replicons. The VEEV replicons generated significant CPE and cell death in infected mammalian cell cultures. VEEV replicons were subjected to mutations in the 5' UTR and nsP2/nsP3 genes to diminish the production of CPE in BHK-21 cells (Petrakova, 2005).

Alphavirus transducing systems

Natural infection and proliferation in vector species is also an important consideration for the development of an alphavirus expression system. Initial studies utilizing SINV double subgenomic expression systems were based on the TE/3'2J double-subgenomic system made from a neural-adapted clone of the AR339 strain of SINV (Hahn et al, 1992; Lustig et al, 1988). The use of the double-subgenomic system was limited by the inability of TE/3'2J to infect *A. aegypti* orally. Seabaugh et al (1998) addressed this concern by replacing the structural genes of TE/3'2J with those of MRE16. The chimeric virus had increased tropism for mosquito midgut cells (Seabaugh et al, 1998). MRE16 was a strain of SINV isolated in Malaysia and was fully

capable of infecting *A. aegypti* midguts (Pudney et al, 1979). The MRE/ 3'2J construct was engineered to express GFP from the second subgenomic promoter (Olson et al, 2000).

Uses of double-subgenomic alphavirus expression systems

Double-subgenomic expression systems have expressed reporter genes, epitopes from foreign viruses, and molecules capable of stimulating specific cytotoxic T-lymphocyte responses against cells expressing a desired viral antigen (Hahn et al, 1992). Expression of fluorescent and bioluminescent reporters has been instrumental in illuminating the physiology of viral infection. The MRE/ 3'2J construct was engineered to transcribe GFP mRNA from the second subgenomic promoter (Olson et al, 2000).The expression of GFP by MRE/3'2J allowed researchers to track SINV infection throughout the mosquito (Pierro et al, 2003; Foy et al, 2004). The construction of a corresponding system for ONNV was used to describe the movement of virus through its natural vector, *Anopheles gambiae*. The 5' double subgenomic ONNV containing an insert was shown to possess diminished growth kinetics compared to the parental virus. Peak virus titer with 5'dsONNV containing an inserted sequence was 1.5 $\log_{10}$ PFU/mL lower and occurred 24 hours later in cell culture compared to virus lacking an insert (Brault et al, 2004a). Tsetsarkin et al (2006) developed a similar system for CHIKV and used it successfully to express GFP in cell culture and *Aedes* mosquitoes. The infection profile and growth kinetics of the engineered virus were shown to be similar to virus produced by the infectious clone and original virus isolate. Infection in *Aedes aegypti* mosquitoes was reduced for 5'dsCHIKV-GFP compared to the wild-type viruses (Tsetsarkin et al, 2006). The role of RNA interference in the vector immune response was described using two strains of SINV engineered to express GFP. The use of a reporter allowed investigation of how the two strains of SINV interacted with the mosquito midgut in response to a specific RNAi response primed by injection of dsRNA (Campbell et al,

2008). ONNV expressing GFP was used in a similar experiment to highlight the effect of a diminished RNAi response on the dissemination of the virus following intrathoracic injection (Keene et al, 2004). Firefly luciferase (FLUC) expression by a double-subgenomic system was used to illuminate the course of infection for a neurovirulent SINV. Following the injection of the enzyme substrate, D-luciferin, bioluminescence was detectable in SINV infected tissues using the *in vivo* imaging system (IVIS) from Caliper Biosciences. Virus infection of a vertebrate host was followed in a single animal over multiple time points using bioluminescence (Cook and Griffin, 2003).

Double subgenomic SINV was used to express non-reporter exogenous genes in mosquitoes. Expression experiments included the production of CAT in *C. pipiens pipiens* salivary glands and saliva (Olson et al, 1997), scorpion venom in *Aedes* and *Culex* mosquitoes (Higgs et al, 1995), single-chain antibodies in *A. aegypti* (de Lara Capurra et al, 2000), influenza hemagglutinin and cytotoxic t-lymphocyte hemagglutinins in murine cell lines (Hahn et al, 1992). The expression of antisense RNA by a SINV ATS was used to knock-down expression of FLUC in transgenic *A. aegypti*. The SINV ATS demonstrated the induction RNA interference (Johnson et al, 1999). Another example of the utility of this system was the elucidation of molecular mechanisms essential for antiviral defense in *A. aegypti*. The production of anti-sense RNAs by a SINV ATS was used to inhibit the replication of DENV-2, YFV, and LACV in mosquitoes and cell culture (Franz et al, 2006; Olson et al, 1996; Gaines et al, 1996; Adelman et al, 2001; Travanty et al, 2004; Higgs et al, 1998; Powers et al, 1996). Expression of DENV-2 genomic RNA fragments by SINV inhibited DENV-2 replication through the RNA interference pathway. This experiment helped show the importance of RNA interference in innate immunity

to viral infection (Sanchez-Vargas et al, 2004). SINV expressed pro-apoptotic genes were used to study the role of apoptosis in viral interactions with mosquito cells (Wang et al, 2008).

Fluorescent and bioluminescent reporters

Monomeric cherry fluorescent protein (mCherry) possesses an excitation wavelength of 587 nm, an emission wavelength of 610 nm, and forms monomers when expressed as a protein. When compared to a *Discosoma* red (DsRed), another monomeric red fluorescent protein derived from *Discosoma* spp. mCherry is four times as bright and six times as photostable. Shaner et al recommended mCherry as the best red fluorescent protein due to a combination of low molecular weight, brightness, and relative photostability (Shaner et al, 2004; Shaner et al, 2005).

FLUC was first isolated in a crystal form in 1957 from *Photinus pyralis*, a coleopteran commonly known as the firefly. The gene for FLUC was first cloned from *Photinus pyralis* and expressed in *Escherichia coli* in 1985. In the presence of the substrate luciferin and ATP, expression of the protein could be measured using a luminometer (de Wet, J.R. et al, 1985). The enzymatic half-life of FLUC in mammalian cells is approximately 3 hours (Thompson et al, 1991).The FLUC protein is a 62 kD enzyme that shows sequence homology to a number of other proteins that use ATP to catalyze adenylation reactions. Morphologically, the protein folds into two distinct domains, a β-barrel and two β sheets flanked by α-helices make up the N-terminal domain. A cleft separates the C-terminal domain of the protein. Active sites found on each domain suggest that the two sections come together during catalysis. Each individual luciferase enzyme turns over very slowly, initially emitting light then succumbing to product inhibition which slows the catalysis of the next reaction. The reaction is highly efficient, with nearly one photon of light produced from the oxidation of one molecule of luciferin (DeLuca and McElroy,

1974; Conti et al, 1996; Marques and Esteves da Silva, 2009). The production of light by FLUC is the result of a catalyzed oxidation of its substrate, luciferyl adenylate which is an anhydride of D-firefly luciferin and adenosine monophosphate (Hopkins et al, 1967). This reaction requires the presence of oxygen, and Mg_2ATP. The net product of this reaction is light in the form of a photon and oxyluciferin (Marques and Esteves da Silva, 2009).

Summary and Goals

Arboviruses present a continuous threat to human and veterinary health throughout the world. Emergence from enzootic into epidemic cycles of transmission has been reported for a number of arboviruses. Knowledge of the interactions between arbovirus and host during a natural infection is essential for complete understanding. Syringe and needle inoculation of vertebrate animals with virus has led to a great many advances in infectious disease research. Inoculation by syringe does not precisely mimic nature in the case of arboviruses, which are transmitted by arthropods during feeding or probing. Developments in imaging technology have allowed the resolution of light emission from the interior of an animal. The combination of *in vivo* imaging with the existing technology of alphavirus expression systems presents a unique opportunity to visualize the course of infection. The complete transmission cycle of an arbovirus can be imaged. The EIP from infection of the mosquito midgut to dissemination and transmission have been imaged by arboviral expression of reporter genes. The use of a dsATS in an animal model allows a potentially highly efficient and less expensive means of tracking an alphavirus infection. Further considerations include the development of an understanding of the physiologic response of an alphavirus infection to pre-immunization or antiviral therapy. WEEV presents an excellent and timely model for the study of these processes. Closely related alphaviruses, VEEV and EEEV, are Select Agents with the potential for use in biological warfare

by the U.S. Department of Health and Human Services as well as the U.S. Department of Agriculture. WEEV provides a model system to study VEEV and EEEV with a lesser degree of restriction. The construction of a double-subgenomic WEEV capable of expressing a reporter gene in both the vector and animal model would allow for a more detailed examination of timely and important biological questions. *In vivo* imaging can be used to assess the efficacy of antiviral prophylactic treatment in preventing WEEV infection. Expression of fluorescent proteins using double-subgenomic WEEV can be used to investigate salivary gland infection and determinants of transmission.

Chapter II: *In Vivo* Bioluminescent Imaging of Western Equine Encephalitis Virus Infection

Introduction

A recombinant WEEV was generated that expressed FLUC as a marker of infection. *In vivo* imaging technology was used to visualize bioluminescence during WEEV infection of *C. tarsalis* as well as outbred (CD-1) and inbred (C57/BL6) strains of mice. Infection of mice was followed by bioluminescent imaging in the living tissue of a single animal over time. Entry into the CNS appeared to be part of a generalized dispersal of signal without specific involvement of regions consistent with the spinal cord or olfactory nerves. This indicates a vascular route of entry into the CNS for the McMillan strain of WEEV which differs from neurovirulent strains of SINV and more closely resembles VEEV neuroinvasion. Bioluminescence was initially detected in regions consistent with peripheral lymph nodes and site of subcutaneous injection. The initial spread of bioluminescence was followed by emission of detectable light from the heads of some mice, signaling entry and replication in the CNS. In vivo imaging of infected *C. tarsalis* was not instructive due to the limited resolution of the IVIS camera and a lack of luciferin dispersal in infected mosquitoes. In vivo imaging was used to predict efficacy of a cationic lipid RNA complex (CLRC) immunomodulator in the suppression of WEEV infection. The utility of bioluminescent imaging in screening potential antivirals for activity against WEEV in vivo has been described for the first time in this work.

WEEV is capable of causing severe disease in humans, with the majority exhibiting a subclinical illness. With a minority of infected persons, disease can progress to symptoms such as somnolence, fever, seizures, disorientation, neck stiffness, coma, and death. WEEV has an

overall case fatality rate of 3-7% in humans (Zacks and Paessler, 2010). In survivors, there is a distinct possibility of neurologic sequelae (Earnest et al, 1971). Like other New World alphaviruses, WEEV can be delivered via aerosol and cause a lethal infection (Logue et al, 2009; Reed et al, 2005). The ability for WEEV to be virulent when delivered by aerosol highlights the virus' potential for use as a biological weapon.

Understanding the route of infection and tissue tropism of an arbovirus is crucial to completing the overall picture of the pathogen-host relationship. The technology of *in vivo* imaging promises to streamline the process of investigating the action of infectious agents in an animal model. FLUC and its substrate, luciferin, were first used in an animal model to describe bacteria in a living host (Contag et al, 1995) and have subsequently been used to describe the path of infection for herpesvirus type-I (Luker et al, 2002), neurovirulent SINV (Cook and Griffin, 2003), and human immunodeficiency virus (HIV) gene expression (Contag et al, 1997). Bioluminescence was used by others to investigate entry of neurovirulent SINV into the CNS via retrograde axonal transport either through the olfactory epithelium or spinal cord (Cook and Griffin, 2003). They were able to distinguish virulent and avirulent strains of SINV in a mouse model using *in vivo* imaging. Use of bioluminescent reporters contributed to the study of tumor cell growth (Contag et al, 2000), regression (Contag et al, 2000; Sweeney et al, 1999), and metastasis (Sahai, 2007). A combination of infectious disease and cancer imaging was utilized to monitor SFV infection in nude mice concomitant with the clearance of glioma tissue (Heikkila, 2010). Research applying *in vivo* imaging technology to vaccinia virus infection showed potential in predicting lethality of virus infection based on luminescence (Zaitseva et al, 2009). *In vivo* imaging allows the detection of luciferase expression in tissues specifically infected with the agent engineered to express the reporter.

Previous work demonstrated the efficacy of cationic lipid DNA/RNA complexes (CLDCs or CLRCs) in preventing mortality by the McMillan strain of WEEV (Logue et al, 2010; unpublished information). This study used the efficacy of CLRC administration to investigate the utility of *in vivo* imaging in evaluation of prophylactic treatment. CLRCs are composed of polyriboinosinic:polyribocytidylic acid (poly I:C) and 1,2-dioleoyl-3-trimethylammonium-propane (DOTAP) liposomes. Viral double-stranded RNA (dsRNA) and poly I:C are both potent activators of toll-like receptor 3 (TLR3)and inducers of type I interferon. Following interaction with poly I:C, TLR3 induces type I interferon, inflammatory cytokine production, and dendritic cell maturation as a result of interaction with Toll/Interleukin-1 receptor domain containing adapter inducing interferon-β (TRIF). Delivery of poly I:C was shown to induce interferon in cell culture (Silhol et al, 1986) as well as *in vivo*. Poly I:C is preferred to viral dsRNA for inducing TLR3 and also activates MDA-5 (Gauzzi et al, 2010). Cationic liposomes have been used to deliver TLR9 and TLR3 agonists, which induced strong CD8 and CD4 T-cell responses *in vivo* (Zaks et al, 2006). Cationic lipid RNA complex containing DOTAP liposomes and poly I:C are an attractive prospect for adjuvant or prophylactic therapy for RNA viruses. Prophylactic use of CLRCs would act by inducing interferon and activating dendritic cells. This creates an antiviral state in a potential host that would prevent the initial stages of infection. WEEV has been shown to be susceptible to interferon in a hamster model (Julander et al, 2007), and induction of interferon in mice by stimulation by CLRCs should be effective in reducing WEEV infection in CD-1 mice.

As an alphavirus transducing system was not constructed for WEEV prior to this study, the initial objective was to construct such a system and observe fluorescent and luminescent expression in infected vertebrate and invertebrate tissues. *In vivo* imaging using 5'dsMcM-FLUC

could be used to follow subcutaneous and intranasal infection of mice with neurovirulent WEEV. Effective control of infection by pre-administration of CLRCs should be reflected in a markedly reduced level of bioluminescence in untreated mice compared to CLRC treated mice challenged with 5'dsMcM-FLUC.

Materials and Methods

Virus Construction

Plasmid DNA containing the full-length infectious cDNA clone of the genome of McMillan strain WEEV was a kind gift of Dr. Thomas Welte (Colorado State University) and WEEV.McM was derived from virus obtained from the Arbovirus Reference Collection at the Centers for Disease Control and Prevention in Fort Collins, CO, USA. The infectious cDNA clone of IMP181 was provided by Dr. Aaron Brault (Centers for Disease Control and Prevention, Fort Collins, CO). An RsrII restriction site was introduced into pWEEV.McM at nucleotide 7505 (Capsid gene) by PCR with overlapping mutagenic primers (5'-CGTAGTAGACACGCACCTACGGACCGCCAAAATGTTTCCATACCC-3' and 5'-GGCGGTGGGTCGGTCCGTGTCTACTACGTCACC-3') using Pfu turbo DNA polymerase (Stratagene). Infectious cDNA clones were treated with DpnI to remove methylated DNA (residual, unaltered template plasmid DNA is methylated from growth in *E. coli*) and electroporated into XL-Blue *E. coli* (Stratagene) using an ECM 630 electroporator (BTX) at 2500 volts, 200 ohms, and 25 microfarads. Transformed bacteria from each reaction were spread on LB Agar with 200 µg/mL Ampicillin and incubated overnight at 37°C. Colonies were picked and grown in liquid LB medium with 200 µg/mL Ampicillin overnight at 37°C and plasmid DNA purified by MiniPrep (Qiagen). The full-length alphavirus subgenomic promoter (-98 to +14 nucleotides of the TAATA sequence, Wielgosz et al, 2001) of WEEV was amplified from

pWEEV.McM using a forward primer with a 5'RsrII-SacII-SbfI multiple cloning site at the 5' end (5'-AAAACGGACCGAACCGCGGAAAACCTGCAGGTACTGGCAGGCCTGATCATC-3') and the reverse primer used in site-directed mutagenesis. The PCR product was inserted into pMcM to generate a second subgenomic promoter 5' of the structural genes. The MCS allowed insertion of heterologous genes under control of the original subgenomic promoter.

The infectious cDNA clone of IMP181 was provided by Dr. Aaron Brault (Centers for Disease Control and Prevention, Fort Collins, CO). Similar methods were used to alter the genomic DNA to contain a MCS. SacII and XmaI (New England Biolabs) restriction site sequences were introduced as the genomic IMP181 DNA contained a SbfI restriction site. Using similar primers, a FLUC gene was introduced into the MCS downstream of the native 26S promoter (Table 2.1).

Table 2.1 Primers used to clone the FLUC gene into 5'dsMcM-FLUC, Renilla luciferase into 5'dsMcM-RLUC, and FLUC into 5'dsIMP-FLUC.

Virus	Forward	Reverse
5'dsMcM-FLUC	Aaaaccgcggatggaagacgccaaaaacataaa	aaaacctgcaggttacacggcgatctttccgcc
5'dsMcM-RLUC	Aaaaccgcggatggctagcaaggtgtacgaccc	aaaacctgcaggttactgctcgttcttcagcac
5'dsIMP-FLUC	Aaaccgcggatggaagacgccaaaaacataaa	aaacccgggttacacggcgatctttccgcc

Once cloned and sequenced, constructed plasmids were linearized and treated with proteinase K. Linearized plasmids were purified by chloroform extraction and ethanol precipitation. Purified, linearized plasmids were subjected to *in vitro* transcription using a T7 RNA polymerase and MAXIscript™ kit (Ambion, Austin, TX). BHK cells were washed in PBS (Mediatech, Inc., Manassas, VA) and electroporated with *in vitro* transcribed RNA using an ECM 630 electroporator (BTX Inc, San Diego, CA) at 450 volts, 720 ohms, and 100 microfarads

by mixing 20 µL of *in vitro* transcribed RNA and 400 µL of 1 x 10^7 cells/mL BHK cell suspension. Cell culture supernatant was taken from electroporated cells and passaged once in BHK cells to make a stock virus (Figure 2.1). Supernatant was collected at 48 hours post infection, aliquoted, and stored at -80°C. The stock virus was quantified by plaque titration (typical virus titer was 10^6-10^7 PFU/mL) in Vero cells and used for subsequent experiments.

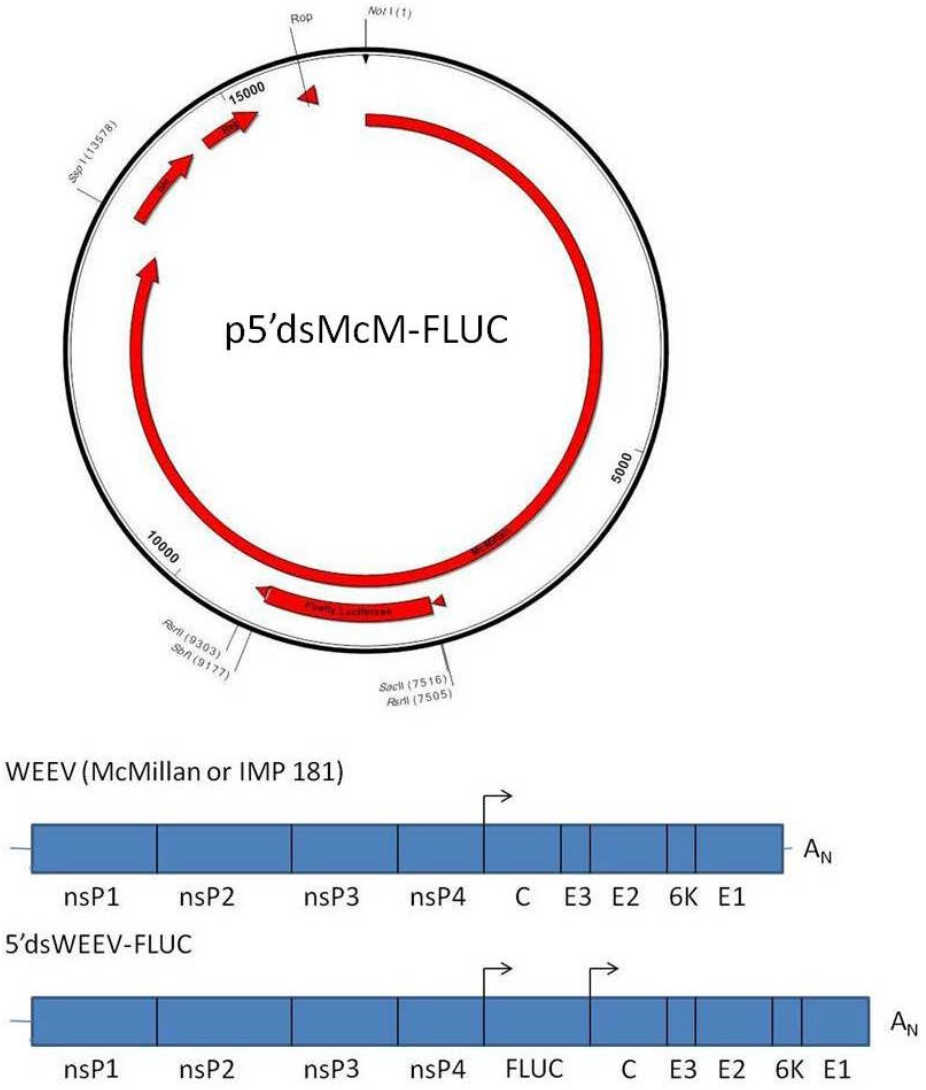

Figure 2.1 Plasmid map of 5'dsMcM-FLUC containing the McMillan infectious cDNA clone, introduced restriction sites, subgenomic promoters, linearization site, and ampicillin resistance gene (above). Genomic structure for native WEEV and double-subgenomic viruses.

Virus quantification through reporter expression

The correlation of infectious virus titer and reporter expression was determined by infecting four rows of a 24-well plate containing confluent monolayers of BHK cells with 1 ml of $1x10^5$ PFU/mL 5'dsMcMR-FLUC and serially diluting 10-fold to 10^1 PFU/mL. D-luciferin diluted in PBS was added to each well 8 hours later to a concentration of 150 µg/mL. Each plate was imaged using the *in vivo* imaging system (IVIS; Caliper Life Sciences). The Living Image 3.0 software's region of interest (ROI) tool was used to measure light emitted from each well in radiance ($p/s/cm^2/sr$) and the data plotted against initial concentration of virus. Each ROI was set as a circle in the imaging software large enough to circumvallate a single well of the plate and record bioluminescence only from that region.

Maintenance of FLUC expression in 5'dsMcM-FLUC and 5'dsIMP-FLUC

The stability of FLUC expression in cell culture was analyzed by passaging supernatant from electroporated BHK cells at a MOI of 1.0 in BHK or C6/36 cells at two day intervals. Supernatant from each passage was titrated in Vero cells and then used to infect the next passage at the same MOI. A milliliter of each virus at a titer of 10^5 PFU/mL was aliquoted into individual wells of a black 24-well plate (Greiner Bio-One, Monroe, NC) containing confluent monolayers of BHK cells and assayed for luminescence 12 hours after infection. Mean luminescence for each passage was compared to stock 5'dsMcM-FLUC as a positive control to measure the change in luminescence for each passage.

Maintenance of FLUC expression was also measured by the percent of 5'dsMcM-FLUC and 5'dsIMP-FLUC virus populations containing functional FLUC. Stock virus was passaged at a MOI of 1.0, 0.1, and 0.01 in BHK, Vero, and C6/36 cells at two day intervals. Each passage was titrated using an end-point assay (Reed and Muench, 1938) in Vero cells. The $TCLD_{50}$ titer

exhibiting luminescence was divided by the titer of virus expressing cytopathic effect ($TCID_{50}$) to derive a percentage of the viral population expressing the insert.

Stability of the FLUC gene in the viral genome was assayed by continuous passaging of virus in cultured cells or CD-1 mice and isolating viral RNA from supernatant or brain homogenates using a Viral RNA isolation kit (Qiagen). Isolated RNA was reverse transcribed with SuperScript™ reverse transcriptase (Invitrogen) and amplified using polymerase chain reaction (PCR) with the FLUC primers (Table 2.1). Each amplified insert segment was electrophoresed on a 1% agarose gel and compared to full length insert amplified from p5'dsMcM-FLUC or p5'dsIMP-FLUC. Each cDNA amplimer was sequenced and compared to full-length insert using ClustalW alignment software (Lasergene).

Mosquito infection and imaging

C. tarsalis CA strain of mosquitoes were a generous gift from William Reisen (UC Davis). *C. tarsalis* mosquitoes were incubated at 25°C and 74% humidity while *A. aegypti* were incubated at 30°C and 95% humidity in a Caron 9300 incubator (Caron). Prior to injection, mosquitoes were anesthetized by delivery of CO_2 and refrigerated on a glass plate resting on a bed of ice.

Mosquitoes were infected by intrathoracic injection of virus or by an infectious bloodmeal. Female *C. tarsalis* were injected with 6 x 10^2 PFU of McMillan, 5'dsMcM-RLUC, or 5'dsMcM-FLUC viruses diluted in MEM with a Nanoject II (Drummond Scientific) apparatus two days post-eclosion. Alternatively, mosquitoes were fed infectious blood-meals containing 2 x 10^6 PFU/mL diluted 1:1 in defibrinated sheep blood (Colorado Serum Company, Denver, CO; 1 x 10^6 PFU/mL final concentration) using a Hemotek™ (Discovery Workshops, Accrington, UK) feeding chamber calibrated to 35°C ± 1. Mosquitoes were allowed to feed until repletion

and blood-fed females were sorted until imaging. Following infection, mosquitoes were stored in 0.5-liter containers with organdy netting covering the open end.

Bioluminescent imaging of adult mosquitoes was performed in infected and non-infected *C. tarsalis* injected intrathoracically with 150 ug/mL D-luciferin in PBS. Imaging of 5'dsMcM-RLUC infection in *A. aegypti* was conducted by intrathoracic injection of 67 nL of ViviRen (Promega) suspended in 60mM dimethylsulfoxide (DMSO). For biosafety reasons, each mosquito had legs and wings removed prior to imaging. Mosquitoes were stored at -80°C for plaque titration of WEEV.

Infectious virus titrations

Confluent monolayers of Vero cells in a 12-well plate were overlaid with 200 µL of WEEV suspension. The WEEV suspension was serially diluted ten-fold in MEM with 10%FBS, NEAA, L-glutamine, and antibiotics. Plates containing virus and cells were rocked gently every 15 minutes for 45 minutes to ensure complete coverage of the monolayer. Nutrient medium overlay was made by mixing H_2O, Medium 199 (Mediatech, Inc., Manassas, VA), 20% FBS, 0.6% NaHCO3 (Mediatech, Inc., Manassas, VA), MEM Vitamins, NEAA, penicillin/streptomycin, and 2% agarose (Sigma-Aldrich) to give a final concentration of 1X Medium 199 and 10% FBS. After equilibration to 42°C, agarose was added to the wells. The plates were incubated at room temperature until the agar solidified and then incubated at 37°C, 5% CO_2. After four days, 200 µL of 3 mg/mL MTT (3-(4,5-Dimethylthiazol-2-yl)-2,5-diphenyltetrazolium bromide; USB) was added to the wells and the plates were incubated at 37°C overnight prior to being read (Liu et al, 1970).

WEEV isolated from mosquitoes was titrated following homogenization of *C. tarsalis* whole bodies and filtration of homogenates to remove contaminants. Infected mosquitoes were

individually homogenized in a 2 mL Eppendorf tube containing 500 µL MEM-10% FBS with a plastic pestle and a cordless mixer motor (Kontes, VWR). Homogenates in MEM 10% FBS were filtered using a 0.2 µm Acrodisc filter (Pall Life Sciences) prior to plaque titration.

Mouse infection and imaging

All animal use in these experiments was reviewed and approved by the Animal Care and Use Committee at Colorado State University. Mice were handled in compliance with the PHS Policy and Guide for the Care and Use of Laboratory Animals. Two laboratory strains of mice were used in this study. Female outbred (CD-1) or inbred (C57/BL6) 4-5 week old mice (Charles River Labs) were acclimated to the facility for 3-6 days prior to experiments. Subcutaneous (s.c.) injections were performed at a dose of 1-1.5 x 10^4 PFU of 5'dsMcM-FLUC or 1.5 x 10^4 PFU McMillan WEEV derived from infectious clones. Unless otherwise described, injections were performed s.c. in a volume of 100 µL delivered dorsal to the cervical spine of anesthetized mice. Intranasal (i.n.) inoculation was conducted at a dose of 1-5 x 10^3 PFU McMillan or 5'dsMcMFLUC in a volume of 10 µL delivered drop wise onto the nostrils of lightly anesthetized animals. Imaging was conducted after 150 mg/kg of D-luciferin diluted in PBS was injected s.c. dorsal to the cervical spine of each infected animal. *Renilla* luciferase bioluminescence was imaged after interperitoneal (i.p.) injection of 100 µL of ViviRen (Promega) coelenterazine substrate suspended in 60mM dimethylsulfoxide (DMSO). CD-1 and C57/BL6 mice were imaged 10-15 minutes after injection of substrate. Uninfected mice were used as an imaging control to adjust for background and each animal was imaged both dorsally and ventrally to account for signal occluded by the body. Mice were kept anesthetized through the administration of isoflurane (Minrad Inc, Bethlehem, PA) using an XGI-8 anesthesia system (Caliper Life Sciences, Hopkinton, MA) connected to the IVIS 200 camera. Exposure time was 3

minutes under standard settings for the camera. Living Image 3.0 (Caliper Life Sciences, Hopkinton, MA) software was used to analyze and process images taken with the IVIS 200 camera. A threshold for significant bioluminescence was established using imaging of non-infected controls to determine levels of background emission. At a detection threshold of 5×10^3 p/s/cm^2/sr, background luminescence was eliminated. Total light emission from each mouse was accomplished by creating an ROI of standard size for each mouse and collecting light emission data using the software.

Rapid detection of CLRC efficacy

Cationic lipid RNA complexes were generated by diluting the 1,2-dioleoyl-3-trimethylammonium-propane (DOTAP) liposomes 1:10 in buffered 5% dextrose in water. The liposome suspension was mixed well and poly I:C (Sigma) was added to a final concentration of 0.1 mg/ml. The CLRCs were made less than one hour prior to injection into CD-1 mice. At 24 hours prior to infection with WEEV, each mouse in groups 1, 3, and 4 was injected s.c. with 250 µL poly I:C complexed with DOTAP liposomes. Animals in groups 1 and 2 were injected s.c. with 1.5×10^3 PFU of 5'dsMcM-FLUC in 100 µL. Animals in groups 4 and 5 were injected with the same dose of neurovirulent McMillan strain WEEV. Group 3 was kept as an uninfected control and was only inoculated with CLRCs.

Every 24 hours post infection for five days each animal in groups 1 and 2 and a negative imaging control mouse was injected under anesthesia with 100 uL 30 mg/mL luciferin in PBS (for a dose of 150 mg/kg). Each mouse was allowed to rest for 10 minutes prior to imaging to allow maturation of bioluminescence. Each animal was imaged twice (dorsally and ventrally) using the IVIS 200 at an exposure of 3 minutes on standard settings with a set minimum of luminescence at 1×10^4 p/s/cm^2/sr. At each time point a ROI box was drawn around each animal

and the amount of luminescence emitted from each animal quantified to that region using the IVIS Living Image analysis software (Caliper Life Sciences). Each animal was also scored at each day post infection using the rubric outlined below:

- 0: no significant signal detected in the mouse.
- 1: signal detected at a single defined location in the mouse.
- 2: signal detected at two defined locations in the mouse.
- 3: signal detected at three defined locations in the mouse.
- 4: signal detected at four defined locations in the mouse.
- 5: signal detected at five or more defined locations in the mouse.

The maximum score was set to five due to the difficulty of distinguishing more than five discreet sites of bioluminescence in a sample because of light pollution from neighboring sites. Any moribund animals were euthanized according to IACUC protocol and the day recorded to calculate time to death. At two weeks post-infection surviving animals were euthanized. Dissected brain from two mice in group 2 was harvested for infectious virus detection and analysis of 5'dsMcM-FLUC genome stability.

Statistics

All titration data were $\log_{10}$ transformed and compared using unpaired Student's *t* test. Luminescent score, mean-time-to-death (MTD) for animals that succumbed to infection, and titration data were tested for normality using the Shapiro-Wilk and Kolmogorov-Smirnov methods. Analysis was conducted using statistical analysis software (SAS) version 9.2. Survival

curves were subjected to Kaplan-Meier (log rank test) analysis using Prism version 4.00 for Windows (GraphPad).

Results

Characterization and quantification of virus in cell cultures

The parental double subgenomic (5'dsMcM) and FLUC-expressing (5'dsMcM-FLUC) viruses were compared to virus produced from the McMillan infectious clone by analyzing viral growth kinetics in cell cultures. Confluent monolayers of Vero, BHK, and C6/36 cells were infected with a 0.01 MOI of each virus. Growth kinetics assays resulted in a maximal titer of 3.1 x 10^7 PFU/mL in BHK cells, 1.5 x 10^7 PFU/mL in Vero cells, and 5.33 x 10^9 PFU/mL in C6/36 cells for McMillan (Figure 2.2). Growth kinetics of 5'dsMcM-FLUC did not appear to be inhibited in C6/36 cells (Figure 2.2B). In Vero and BHK cells, however, 5'dsMcM-FLUC reached a maximal titer approximately one $\log_{10}$ less than McMillan and 5'dsMcM (Figure 2.2A and 2.2C). There was no significant difference in viral propagation between 5'dsMcM and McMillan strain viruses in Vero, BHK, or C6/36 cell cultures.

Correlation between viral titer and luminescence was established in cell culture using the ROI tool of the IVIS 200 system. Ten-fold serial dilutions of virus starting at 10^5 PFU/mL in a 24-well plate format were layered onto confluent BHK cells and imaged 8 hours later. Luminescence correlated well with virus concentration added with an R^2 value of 0.9673 (Figure 2.2D).

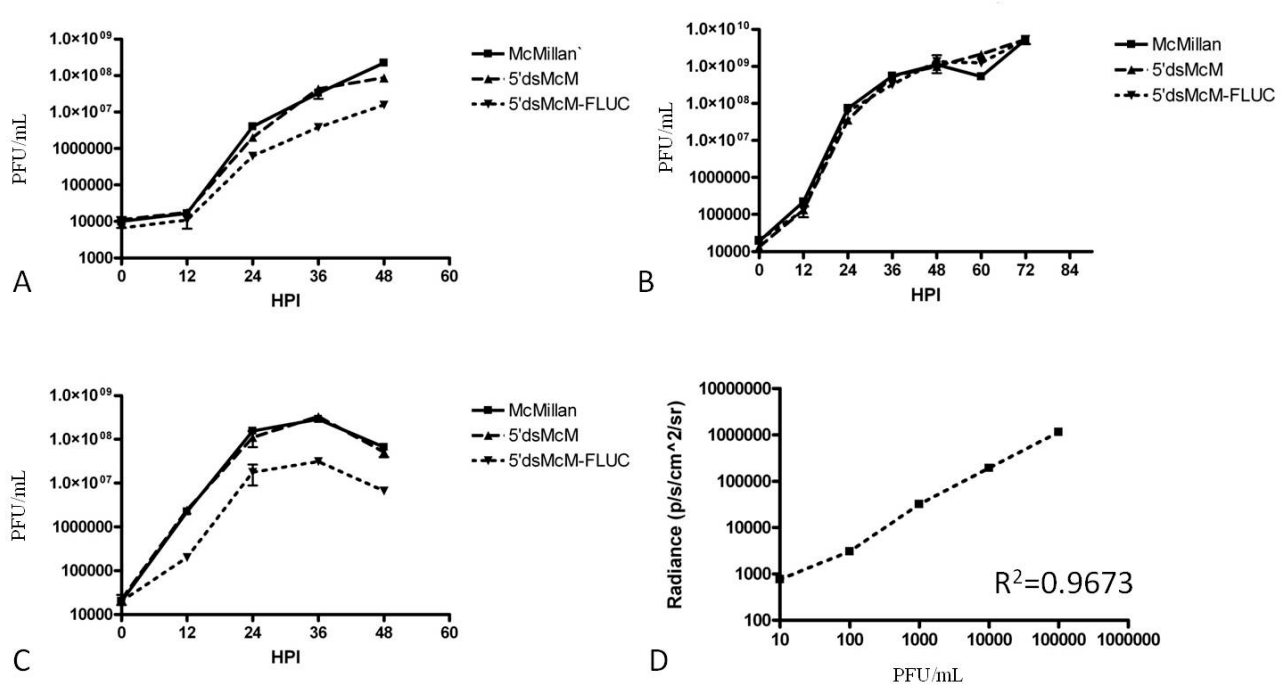

Figure 2.2: Growth curves of McMillan, 5'dsMcM, and 5'dsMcM-FLUC after infection at a MOI of 0.01 in Vero (A), C6/36 (B), and BHK cells (C). Cell culture supernatant was harvested at time of infection and every 12 hours thereafter for 48 hours and titrated in Vero cells to compare McMillan, 5'dsMcM, and 5'dsMcM-FLUC virus titer at each time point. The relationship between virus titer of 5'dsMcM-FLUC added (PFU/mL) and amount of light emitted from expressed FLUC in BHK cells was examined by correlating 5'dsMcM-FLUC titer (10^5, 10^4, 10^3, 10^2, and 10^1 PFU/mL) with bioluminescence at 8 hours post infection as measured by radiance (p/s/cm^2/sr).

Growth curves of 5'dsMcM-mCherry were also compared to McMillan, 5'dsMcM, and 5'dsMcM-FLUC (Figure 2.3). Inclusion of the gene for mCherry fluorescent reporter protein in the viral 5'dsMcM-mCherry genome led to reduced growth kinetics in Vero (Figure 2.3A) and BHK cells (Figure 2.3B). The FLUC gene also resulted in diminished growth kinetics for 5'dsMcM-FLUC in all three cell types (Figure 2.3A, 2.3B, and 2.3C). The use of end-point assays for 5'dsMcM-mCherry virus titration were necessary due to a shortage of Medium 199, precluding the use of plaque titration to determine virus titer. For proper comparison, growth curves of McMillan, 5'dsMcM, and 5'dsMcM-FLUC were redone in Vero, BHK, and C6/36 cells using end-point assays in Vero cells (Figure 2.3).

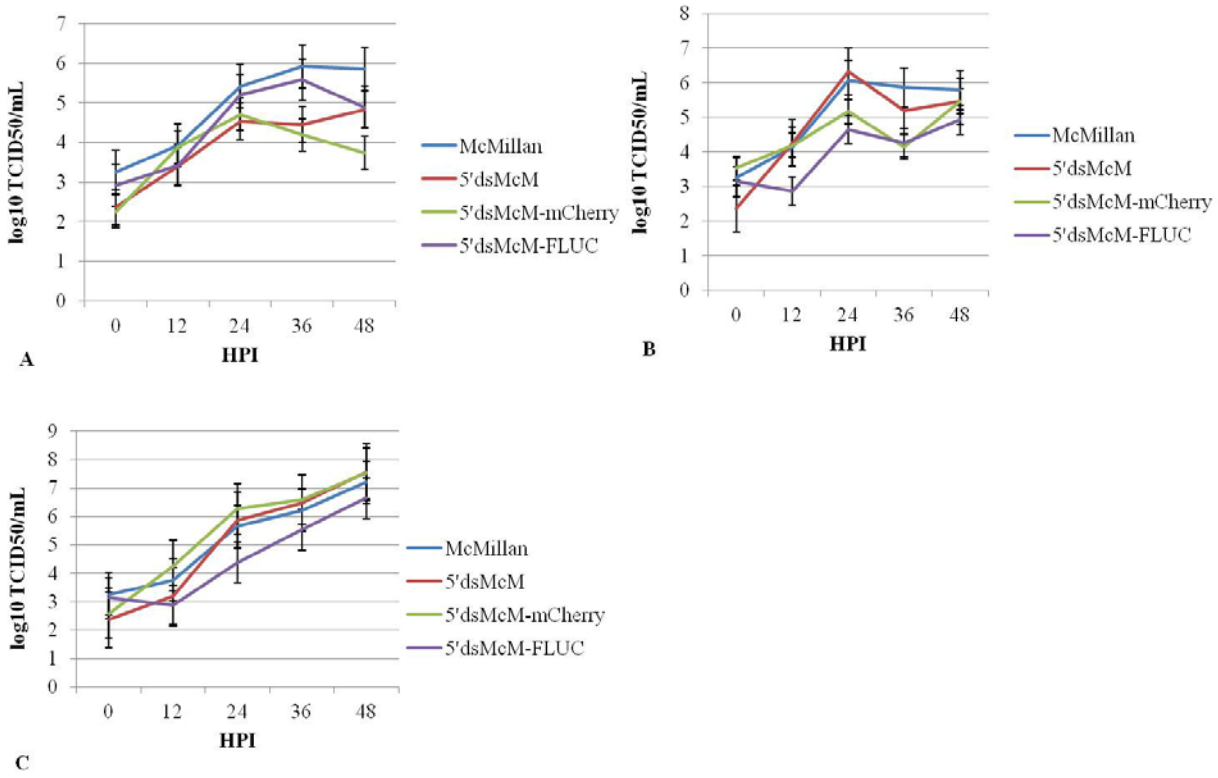

Figure 2.3: Growth curves of McMillan, 5'dsMcM, 5'dsMcM-mCherry, and 5'dsMcM-FLUC after infection of Vero (A), BHK (B), and C6/36 (C) cells at a MOI of 0.01. Supernatant was harvested at time of infection and every 12 hours thereafter for 48 hours and titrated by end-point assay on Vero cells to compare infectious virus titers of McMillan, 5'dsMcM, 5'dsMcM-mCherry, and 5'dsMcM-FLUC.

IMP181-derived viruses grew to lower maximal virus titers in BHK and Vero cells (Figure 2.4A and 2.4B) compared to McMillan-derived viruses. No increase in virus titer was observed over the course of the experiment for 5'dsIMP-FLUC in BHK cells. IMP181 was observed to grow to a higher maximal virus titer and replicate more rapidly in an invertebrate cell line (C6/36) compared to vertebrate cell lines (BHK and Vero).

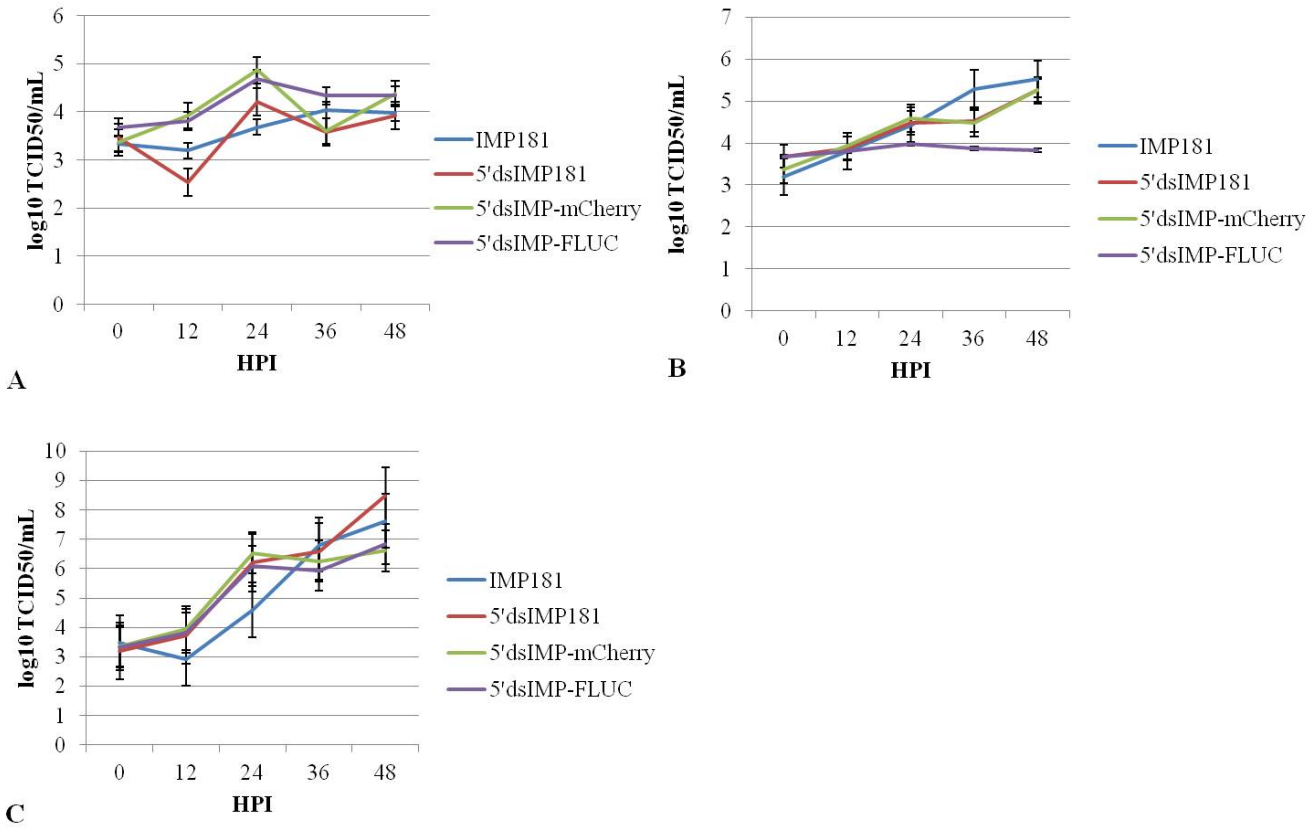

Figure 2.4: Growth curves of IMP181, 5'dsIMP181, 5'dsIMP-mCherry, and 5'dsIMP-FLUC after infection of Vero (A), BHK (B), and C6/36 (C) cells at an MOI of 0.01. Supernatant was harvested at time of infection and every 12 hours thereafter for 48 hours and titrated in Vero cells to compare infectious virus titers of IMP181, 5'dsIMP181, 5'dsIMP-mCherry, and 5'dsIMP-FLUC.

Stability of reporter expression

Repeated passage of recombinant viruses in BHK and C6/36 cells demonstrated a stable level of reporter expression for two passages with declining expression starting with the third passage (Figure 2.5). Virus taken from electroporated BHK cells was passaged at a MOI of 1.0 in BHK and C6/36 cells for a two day period before being transferred to a fresh flask of cells. At each of five passages, supernatant was stored at -80°C prior to titration by plaque and end-point assays in Vero cells.

Maintenance of the FLUC insert is crucial for experiments in cell culture and *in vivo*. Bioluminescence for each passage of 5'dsMcM-FLUC was compared with the original stock

virus passage as a positive control at the same viral concentration. Interestingly, 5'dsMcM-FLUC appeared to be more stable in C6/36 cells than BHK cells (Figure 2.5). In C6/36 cells at a MOI of 1.0, luciferase expression was maintained into the second passage, dropped to 54% in the third passage, then 25% with the fourth passage before becoming indistinguishable from background in the 5th passage. A MOI of 1.0 was chosen for this experiment because it was found to be associated with optimal retention of FLUC by 5'dsMcM-FLUC (Table 2.2). The 5'dsMcM-FLUC virus had superior stability and maximal virus titers in C6/36 cells compared to Vero or BHK cells. Prolonged replication in Vero and BHK cell cultures resulted in truncation of the FLUC insert and loss of detectable luciferase expression.

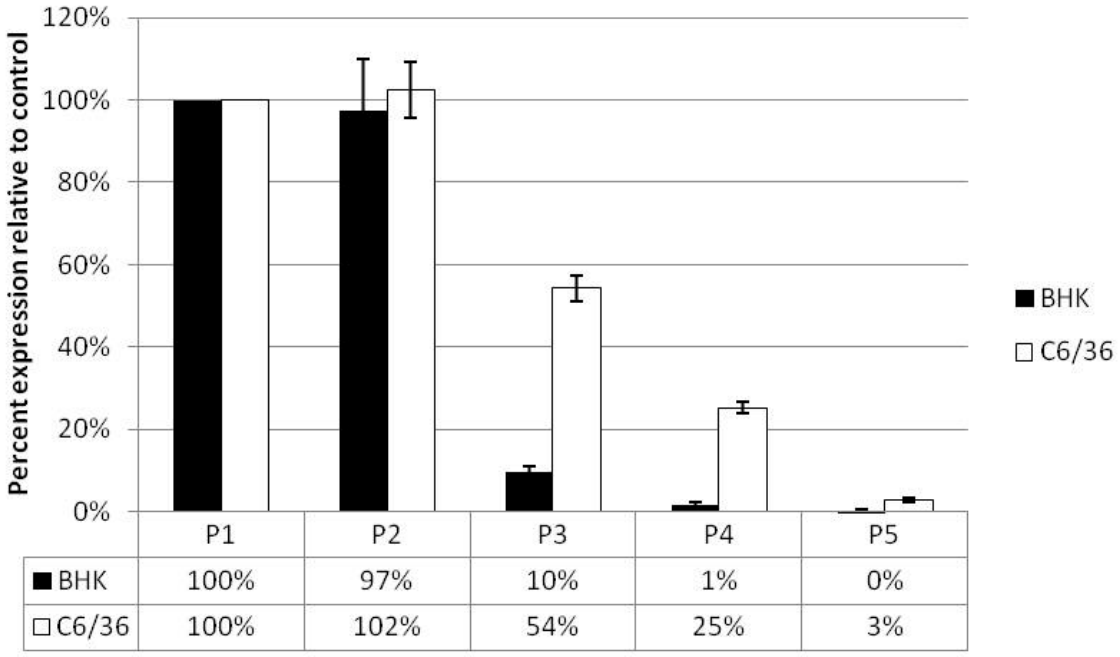

	P1	P2	P3	P4	P5
■ BHK	100%	97%	10%	1%	0%
□ C6/36	100%	102%	54%	25%	3%

Figure 2.5: FLUC expression after serial passage in BHK and C6/36 cells. Measurement of FLUC activity over sequential passages in BHK and C6/36 cells demonstrated a loss of activity over time. 5'dsMcM-FLUC was serially passaged at 2 day intervals in BHK and C6/36 cells at an MOI of 1.0. Supernatant taken from each passage (passage 1 through passage 5) was titrated in Vero cells and equal concentrations of virus (1 x 10^5 PFU/mL) were compared in terms of radiance (p/s/cm^2/sr) during infection of BHK cells 12 hours post infection.

The proportion of 5'dsMcM-FLUC infectious virions containing functional FLUC insert was investigated using end-point assays for cytopathic effect relative to luciferase expression following repeated cell passage in BHK and C6/36 cells. The population of 5'dsMcM-FLUC containing functional FLUC insert started to diminish at the third passage. In agreement with the experiments measuring luciferase activity, 5'dsMcM-FLUC appeared to be more stable in C6/36 cells than in BHK cells. In BHK cells at an MOI of 1.0, the proportion of infectious 5'dsMcM-FLUC that retained full-length FLUC dropped to .55 in the second passage, then .25 with the third passage. In the 4^{th} passage of 5'dsMcM-FLUC at a MOI of 1.0 in BHK cells, the virus population completely lost expression of FLUC. Lower MOI of 5'dsMcM-FLUC in BHK cells resulted in a complete loss of virus expressing FLUC by the third passage. When 5'dsMcM-FLUC was passaged in C6/36 cells, the entire viral population expressed FLUC into the 4^{th} passage. At MOI's of 0.01, 0.1, and 1.0, the proportion of 5'dsMcM-FLUC expressing FLUC in Vero cell cultures dropped from 0.9-1.0 in passage 2 to zero in passage 3 (Table 2.2). Infectious 5'dsMcM-FLUC or 5'dsIMP-FLUC titer at 48hpi did not significantly increase with sequential passage in BHK, Vero, or C6/36 cells.

Table 2.2 Proportion of infectious virus expressing FLUC in 5'dsMcM-FLUC passaged at MOI of 1, 0.1, and 0.01 in BHK, Vero, or C6/36 cells. Virus titers were determined by plaque assay in Vero cells. The virus titers were used to inoculate the subsequent culture at an MOI of 1.0, 0.1, or 0.01. Following two days of incubation the medium was subjected to end-point titration for both CPE and bioluminescence. The ratio of bioluminescence to CPE end-point titers was used to calculate the proportion of 5'dsMcM-FLUC virus with FLUC expression in the total viral population.

5'dsMcM-FLUC	Passage 1	Passage 2	Passage 3	Passage 4
BHK 1.00 MOI	1.0	.55	.25	.00
BHK 0.10 MOI	1.0	.64	.00	.00
BHK 0.01 MOI	1.0	.48	.00	.00
Vero 1.00 MOI	1.0	1.0	.00	.00
Vero 0.10 MOI	1.0	1.0	.00	.00
Vero 0.01 MOI	1.0	.90	.00	.00
C6/36 1.00 MOI	1.0	1.0	1.0	1.0
C6/36 0.10 MOI	1.0	1.0	1.0	1.0
C6/36 0.01 MOI	1.0	1.0	1.0	1.0

When passaged in the same cell types at the same MOI, 5'dsIMP-FLUC was highly unstable. The 5'dsIMP-FLUC virus demonstrated significantly diminished bioluminescence after two passages in BHK cells (Figure 2.3). One passage of 5'dsIMP-FLUC in Vero cells resulted in no detectable bioluminescence. Persistance of 5'dsIMP-FLUC associated bioluminescence was observed into the third passage in C6/36 cells at a greatly decreased ratio ($p<0.0001$). While 5'dsIMP-FLUC was more stable in C6/36 cell culture compared to other cell types, it was less stable than 5'dsMcM-FLUC in C6/36, BHK, and Vero cells (Table 2.3).

Table 2.3 Proportion of virus expressing FLUC in 5'dsIMP-FLUC passaged at MOI of 1, 0.1, and 0.01 in BHK, Vero, and C6/36 cells.

5'dsIMP-FLUC	Passage 1	Passage 2	Passage 3	Passage 4
BHK 1.00 MOI	1.0	.22	.00	.00
BHK 0.10 MOI	1.0	.00	.00	.00
BHK 0.01 MOI	1.0	.00	.00	.00
Vero 1.00 MOI	1.0	.00	.00	.00
Vero 0.10 MOI	1.0	.00	.00	.00
Vero 0.01 MOI	1.0	.00	.00	.00
C6/36 1.00 MOI	1.0	1.0	.11	.00
C6/36 0.10 MOI	1.0	1.0	.02	.00
C6/36 0.01 MOI	1.0	1.0	.01	.00

Maintenance of bioluminescence in 5'dsMcM-FLUC infected CD-1 mice was observed over the course of infection. When imaged *in vivo*, 5'dsMcM-FLUC persisted and expressed detectable luciferase for up to 2 weeks in CD-1 mice at the site of inoculation. Loss of visible reporter expression occurred in approximately half of infected animals imaged with occasional virulence signified by symptoms of encephalitis without accompanying bioluminescence. Persistent bioluminescence *in vivo* was observed for 14 days post infection in *C. tarsalis* adult females intrathoracically injected with 10^3 PFU of 5'dsMcM-FLUC (Data not shown).

Electrophoresis of 5'dsMcM-FLUC viral RNA isolated from infected BHK cell culture supernatant and subjected to RT-PCR showed bands at the expected size (~1700 nucleotides) for passages 1 and 2 with faster-migrating bands of varying size occurring with the third passage in BHK cells and no detectable FLUC insert RNA or activity in subsequent passages (Figure 2.6).

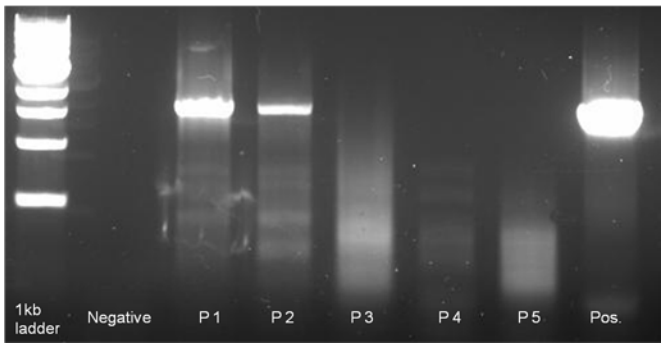

Figure 2.6 RT-PCR of FLUC inserts from 5'dsMcM-FLUC viruses. RT-PCR products amplified from viral RNA extracted from serial passages in BHK cells of 5'dsMcM-FLUC. The first passage had the full length insert present with smaller amplicons occurring in the second (and additional) passages.

Sequencing of viral FLUC insert RNA generated from infected BHK cell supernatant resulted in the detection of the 5' 118 nucleotides of the FLUC coding sequence in proper relation to the multiple cloning sequence restriction site (SacII) followed by 92 nucleotides homologous to the section of nsP4 gene found in the full length subgenomic promoter with the 3' cloning site (SbfI) absent. In total, 1,583 nucleotides are absent from the FLUC insert of 5'dsMcM-FLUC passaged 3 times or more in BHK cells. Loss of FLUC expression occurred as a result of a deletion of viral genomic RNA sequence between the restriction endonuclease sites used to clone the gene into the infectious cDNA clone of McMillan (Figure 2.7). This deletion was observed with 5'dsMcM-FLUC in BHK cells, Vero cells, and in CD-1 mice (data not shown). Deletion of FLUC was also observed in sequenced FLUC insert RNA from cell cultures infected with 5'dsIMP-FLUC (data not shown).

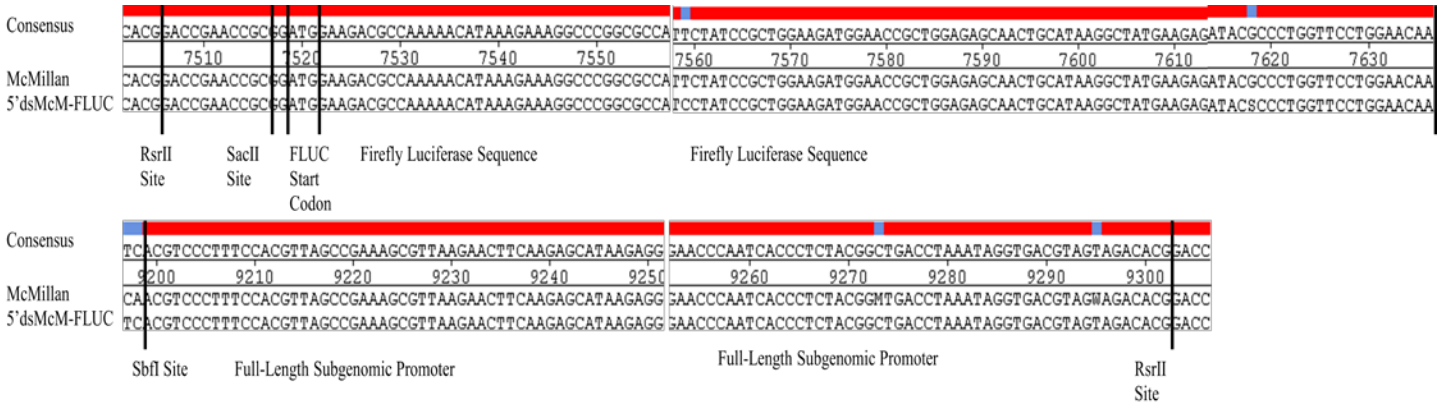

Figure 2.7 Nucleotide sequence of a RT-PCR product amplified from 5'dsMcM-FLUC RNA after passage 3 times in BHK cells at a MOI of 1.0. Sequenced viral genomic RNA possessed the RsrII site flanking the multiple cloning site, the SacII site flanking the FLUC insert, a section of the 5' end of the FLUC sequence, and the SbfI site at the 3' end of the FLUC insert. Most of the FLUC insert was deleted except for the 5' ~130 nucleotides.

Characterization of recombinant virus in mice

Viral infection in a murine model was followed by inoculating CD-1 and C57/BL6 mice s.c. or i.n. with 5'dsMcM-FLUC. Each animal was injected s.c. with 150 mg/kg luciferin diluted in 100 µL PBS and imaged every 12 hours post infection. The 5'dsMcM-FLUC virus established persistant luciferase expression at the site of inoculation in CD-1 mice. Detectable bioluminescence persisted for up to 2 weeks in surviving animals (background radiance threshold was set at 1 x 10^4 p/cm^2/s/sr; not shown). FLUC has a half-life of 3-4 hours in mammalian cells (Thompson et al, 1991), therefore bioluminescence was produced from a continuously active enzyme.

CD-1 mice that were inoculated i.n. with 5 x 10^3 PFU of 5'dsMcM-FLUC expressed bioluminescence consistent with infection of the nares at one day post inoculation and were euthanized following presentation of symptoms within 3 to 4 days of infection concomitant with strong (1 x 10^7 p/s/cm^2/sr) bioluminescence from the head region (Figure 2.8). Intranasally infected mice did not demonstrate bioluminescence outside of the head region. CD-1 mice were

intranasally inoculated with 5 x 10^3 PFU 5'dsMcMFLUC (n=6) or McMillan (n=5) to investigate the comparative lethality of the FLUC expressing virus. Neither 5'dsMcM-FLUC nor McMillan induced 100% mortality at that dose. Twenty percent of McMillan infected mice and 33% of 5'dsMcM-FLUC infected mice survived to 10 days post inoculation. MTD was 3.75 days in McMillan-infected and 4 days in 5'dsMcM-FLUC infected animals. The McMillan and 5'dsMcM-FLUC survival curves for intranasal inoculation were not significantly different by Kaplan-Meier analysis (χ^2= 0.6878, p=0.4069; Figure 2.8). Survival of mice following intranasal inoculation with McMillan was unusual (Logue et al, 2009) compared to previous results and could have been due to loss of inoculum during infection, or resistance by individuals belonging to an in-bred mouse strain (CD-1 mice).

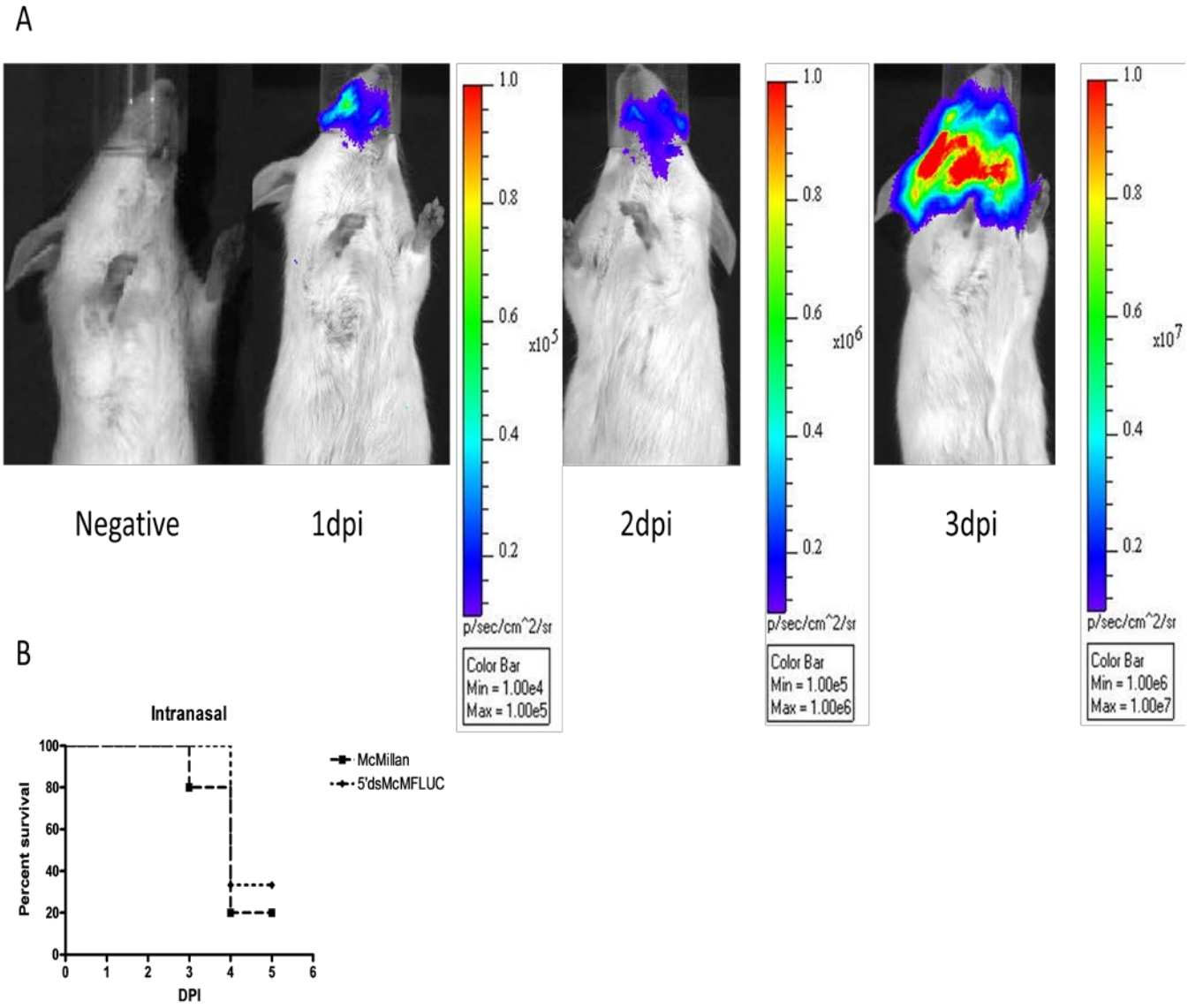

Figure 2.8 Bioluminescence in CD-1 mice infected by the intranasal route. CD-1 mice were inoculated with 5 x 10^3 PFU of 5'dsMcM-FLUC and imaged following injection of D-luciferin at 1, 2, and 3 days post infection (A). Survival curves of McMillan (n=5) and 5'dsMcM-FLUC (n=6) infected CD-1 mice over time (B).

CD-1 mice injected s.c. with 1.5 x 10^4 PFU of 5'dsMcM-FLUC demonstrated two typical routes of dissemination detected by bioluminescence. During the initial stages of infection in animals that were euthanized due to signs of illness we detected bioluminescence at the site of injection. The bioluminescence in 5'dsMcM-FLUC infected CD-1 mice spread to regions consistent with infection of local lymph nodes and virus dissemination terminating in infection

of the CNS (Figure 2.9). The same inoculation regimen conducted with inbred C57/BL6 mice showed a similar pattern of dissemination.

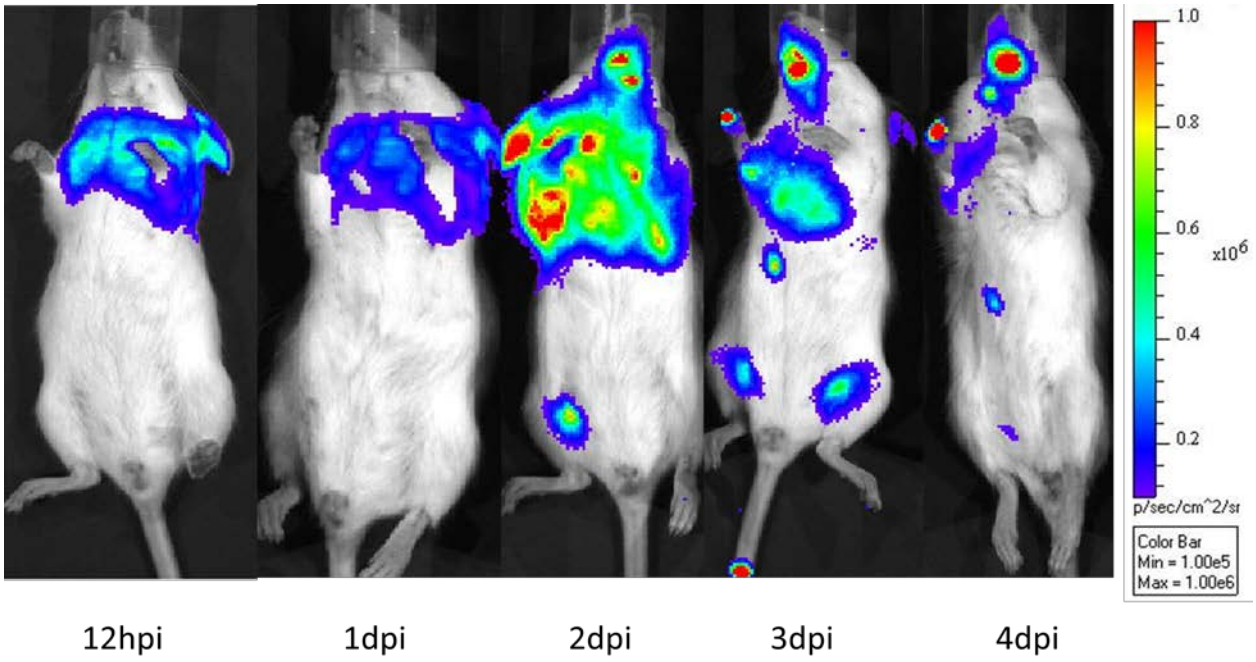

Figure 2.9 CD-1 mouse infected by the s.c. route. CD-1 mice were injected s.c. with 1.5 x 10^4 PFU of 5'dsMcM-FLUC and imaged at 12 hours and at 24 hour intervals post injection to follow the route of virus dissemination. Bioluminescence caused a disseminated pattern consistent with spread to lymph nodes and the CNS at 2 days post infection in 3 out of 10 animals.

In CD-1 mice infected s.c. with 5'dsMcM-FLUC, three out of ten injected animals showed a disseminated infection with bioluminescence consistent with replication in the inguinal lymph nodes and abdominal organs. It is possible to image bioluminescence from dissected organs (*Ex vivo*) after injection of luciferin and euthanasia of the experimental subject. *Ex vivo* imaging confirmed bioluminescence in the brain, liver, and spleen of infected CD-1 mice. In three out of 10 of 5'dsMcM-FLUC-infected CD-1 mice diminished bioluminescence compared to the first group and occasional light emission from the head was observed. In the remaining four infected CD-1 mice, bioluminescence was absent except at the site of inoculation. Possibly due to loss of the FLUC gene as the virus replicates in successive tissues, mice died without

demonstrating FLUC activity except at or near the site of injection. Viral genomic RNA extracted from the dead mice without signal showed a loss of FLUC insert. Imaging of disseminated infection at 2 days following injection of 5'dsMcM-FLUC agreed with prior work (Logue et al, 2009), which demonstrated a sharp rise in McMillan titers in the inguinal lymph node, spleen, and brain at 2 days following injection into the inner left thigh of the mice.

The effect of firefly luciferase gene insertion on WEEV virulence was determined *in vivo* through analysis of CD-1 or C57/BL6 mouse survival after McMillan or 5'dsMcM-FLUC infection. CD-1 and C57/BL6 mice were s.c. inoculated with 1.5×10^4 PFU 5'dsMcM-FLUC or McMillan. Each group of mice was monitored twice daily for signs of illness and euthanized after showing symptoms of severe illness such as ruffled fur, hind limb paralysis, or seizures. Prior to euthanasia, each animal was imaged to determine presence of bioluminescence. In both strains of mice, 5'dsMcM-FLUC was demonstrated to cause mortality, with 46% of CD-1 mice surviving infection compared to 7% with McMillan. Kaplan-Meier analysis of the survival curves confirmed a significant difference between McMillan and 5'dsMcM-FLUC infected groups (χ^2=15.78, $p<0.0001$; Figure 2.11). C57/BL6 mice infected s.c. had a MTD of 3.8 days with McMillan compared to 4 days with 5'dsMcM-FLUC. In C57/BL6 mice, the lack of significant difference in survival between McMillan and 5'dsMcM-FLUC indicated that C57/BL6 mice were more susceptible to infection and mortality with 5'dsMcM-FLUC than CD-1 mice. Similar to CD-1 mice, C57/BL6 mice exhibited symptoms of neuropathology prior to being euthanized (Figure 2.10).

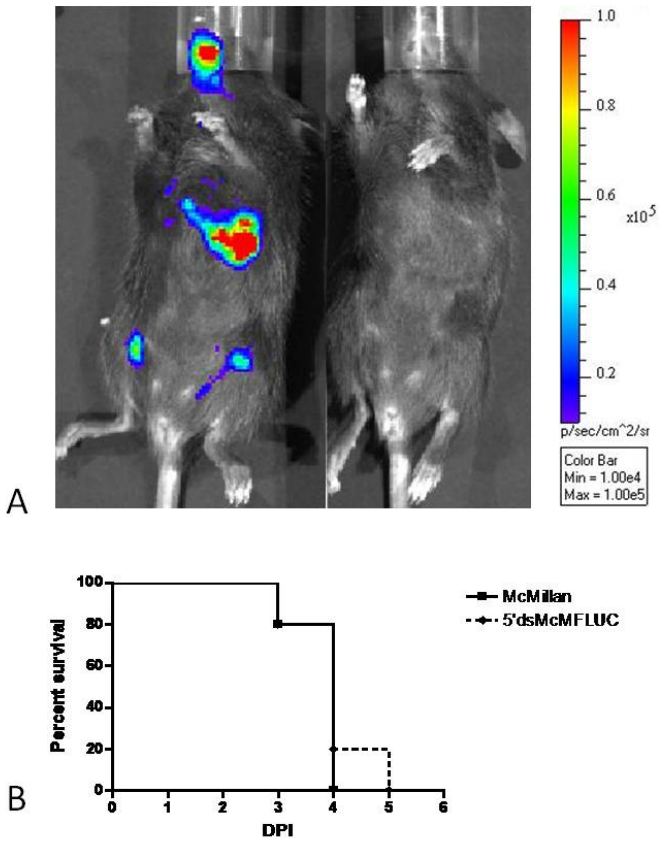

Figure 2.10 C57/BL6 mice infected by the s.c. route. C57/BL6 mice were injected with 1.5 x 10^4 PFU of McMillan or 5'dsMcM-FLUC to image the route of dissemination for 5'dsMcM-FLUC. In vivo imaging of a C57/BL6 mouse (left) 4 days post s.c. injection showed a patternof dissemination comparable to that seen in CD-1 mice infected with 5'dsMcM-FLUC. Bioluminescence from infected animals was distinct from an uninfected control (right) injected with D-luciferin at the same time (A). Survival curves of C57/BL6 (n=5) mice infected s.c. with McMillan or 5'dsMcM-FLUC were compared over 6 days to assess potential attenuation of 5'dsMcM-FLUC in C57/BL6 mice (B).

CLRC treatment of infected mice

CLRC pre-treatment of 5'dsMcM-FLUC infection was assayed using *in vivo* imaging techniques alongside traditional survival curve analysis. Survival was compared with Kaplan-Meier analysis of survival curves using a Bonferroni adjustment (which changed α and significant p-values to 0.0100) for McMillan or 5'dsMcM-FLUC infection between groups of CD-1 mice treated once with CLRCs one day prior to infection or untreated. Comparison of survival curves assessed the efficacy of CLRC prophylaxis. Analysis of survival curves was

compared with *in vivo* imaging of 5'dsMcM-FLUC infected CD-1 mice. Survival was significantly greater in treated animals relative to untreated. In the group treated with CLRCs and infected with McMillan virus, 50% of animals survived while 7% of the untreated control group survived. The McMillan infected, CLRC treated group was not found to be significantly different (χ^2=6.367, p=0.0116) due to a higher α from the Bonferonni adjustment compared to the uninfected, CLRC treated control. The McMillan infected, untreated group exhibited a significantly different survival curve compared to untreated CD-1 mice (χ^2=11.65, p=0.0006). In the 5'dsMcM-FLUC infected group, 46% survived without treatment while all animals survived if treated with CLRCs. The 5'dsMcM-FLUC infected, treated group was found not to be different from the uninfected, treated group (χ^2=0, p=1.0000). The 5'dsMcM-FLUC infected, treated group was significantly different when compared to the 5'dsMcM-FLUC infected, untreated survival curve (χ^2=14.98, p=0.0001). CLRC pre-treatment in this study was not as effective against McMillan in CD-1 mice as reported previously for CLDC (Logue et al, 2010) or CLRC (Phillips and Olson, unpublished). The higher doses of McMillan and 5'dsMcM-FLUC used in this study were most likely responsible for this observation (Figure 2.11).

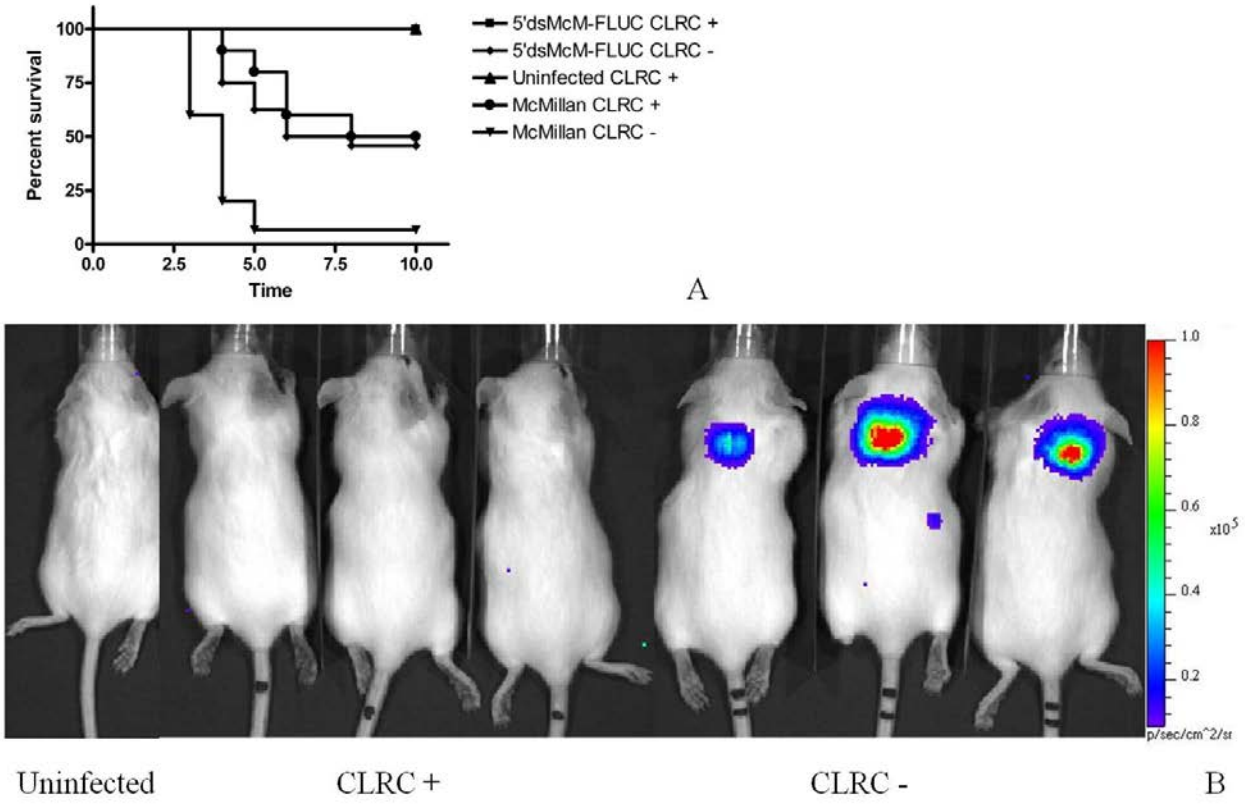

Figure 2.11 CLRC pre-treatment of McMillan and 5'dsMcM-FLUC infection.Survival curves of CD-1 mice treated or untreated with CLRCs 1 day prior to infection with McMillan or 5'dsMcM-FLUC (A). Imaging of uninfected and 5'dsMcM-FLUC infected CD-1 mice treated or untreated with CLRCs. The set of representative images show an uninfected negative control, CD-1 mice infected with 5'dsMcM-FLUC and treated 1 day prior with CLRCs, and CLRC untreated mice infected with 5'dsMcM-FLUC. Mice were imaged 1 day post infection with 5'dsMcM-FLUC (B).

In vivo imaging assessed the efficacy of CLRC administration by scoring each animal based on the number of discrete sites of luminescence or through direct measurement of the light emitted using a region of interest tool in the Living Image 3.0 IVIS software. Imaged animals exhibited a clear demarcation in the number of sites of bioluminescence between treated and untreated groups at a single day after infection. A significantly larger number of untreated animals exhibited bioluminescence compared to treated animals by Satterthwaite t-test ($p=<0.0001$). Quantitative scoring of each group infected with 5'dsMcM-FLUC revealed that the untreated group emitted a significantly greater amount of light one day post infection compared

to the CLRC treated group (p=0.0119, Satterthwaite t-test; Table 2.4). Untreated and treated groups did not demonstrate a significant difference in radiance at 2 (p=0.4414, Satterthwaite t-test), 3 (p=0.7381, Satterthwaite t-test), 4 (p=0.8506, Satterthwaite t-test), and 5 (p=0.1595, Satterthwaite t-test) days post infection. MTD was significantly delayed in 5'dsMcM-FLUC infected animals. In CD-1 mice, the MTD for mice injected s.c. with McMillan was 3.7 days compared to 5.0 days with 5'dsMcM-FLUC (p=0.0019, Satterthwaite t-test; Table 2.4).

Table 2.4 Survival, mean time to death, mean radiance, and mean bioluminescent scores for each group of mice treated with CLRCs or untreated. Each mouse in groups 1 and 2 was injected s.c. with 100 µL 1.5 x 10^5 PFU/mL of 5'dsMcM-FLUC, groups 4 and 5 were injected s.c. with 100 µL 1.5 x 10^5 PFU/mL of McMillan, groups 1, 3, and 4 were treated 24 hours prior to infection by s.c. injection of 250 µL CLRC suspension. Mean time to death was calculated for all CD-1 mice that died during the course of the experiment. Survival percentage was calculated after a period of 2 weeks following infection. Mean radiance is the average amount of light emitted by each animal at 1 day post infection. Mean score is the mean bioluminescent score generated by imaging each group of mice 1 day after infection with 5'dsMcM-FLUC and counting separate sites of bioluminescence. N/A: Not applicable due to all test animals surviving the course of the experiment (MTD) or not imaged (mean radiance and mean score).

Group	CLRC	Virus	Sample Size	MTD	Survival	Mean Radiance	Mean Score
1	+	5'dsMcM-FLUC	20	N/A	100%	842	0.05
2	-	5'dsMcM-FLUC	24	5.0	46%	1446	1.10
3	+	Not Infected	10	N/A	100%	704	0
4	+	McMillan wild-type	10	5.8	50%	N/A	N/A
5	-	McMillan wild-type	15	3.7	7%	N/A	N/A

Characterization of recombinant virus in mosquitoes

In vivo imaging experiments were conducted with 5'dsMcM-FLUC to detect bioluminescence in *C. tarsalis*. Adult, female mosquitoes were fed an infectious bloodmeal containing 2 x 10^6 PFU/mL of 5'dsMcM-FLUC. Seven days later, following injection of D-

luciferin, *in vivo* imaging was used to separate infected mosquitoes from uninfected controls. At 7 days following *per os* infection of *C. tarsalis* with 5'dsMcM-FLUC, 15 of 16 demonstrated bioluminescence above background. However, no saliva samples (n=8) taken from infected mosquitoes contained detectable virus or luciferase activity, suggesting a transmission barrier. Imaging of mosquitoes also did not reveal signal from the head except in 1 of 16 mosquitoes and bioluminescence was most often localized to the abdomen (Figure 2.12). Similar to experiments conducted with 5'dsMcM-dsRed and 5'dsMcM-mCherry, 5'dsMcM-FLUC was not observed to readily escape the midgut as luminescence was not observed from sites outside of the abdomen.

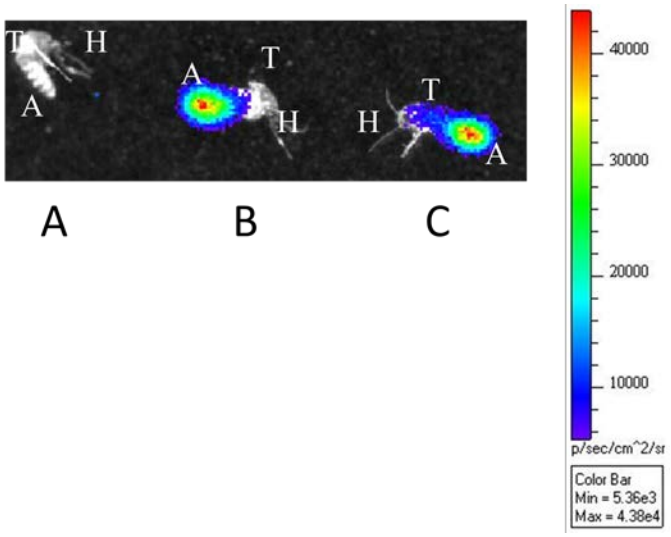

Figure 2.12 *In vivo* imaging of *C. tarsalis*. Images of C. tarsalis given an infectious bloodmeal containing 2 x 10^6 PFU/mL 5'dsMcM-FLUC and imaged 7 days post infection (B and C) in comparison to an uninfected negative control (A). H: Head, A: Abdomen, T: Thorax.

Bioluminescence was detected in *C. tarsalis* infected by a bloodmeal containing 5'dsMcM-FLUC. The effect of FLUC insertion into the genome of McMillan was assessed by comparing replication of 5'dsMcM-FLUC and McMillan in *C. tarsalis. C. tarsalis* mosquitoes were infected by intrathoracic injection of 500 PFU 5'dsMcMFLUC or McMillan and harvested at 1, 5, and 7 days post infection for *in vivo* imaging. Infectious virus titer was compared with *C.*

tarsalis infected with the parent McMillan strain of WEEV. Titers were significantly higher in McMillan-infected compared to 5'dsMcM-FLUC infected mosquitoes at 5 days post infection ($p=0.0002$) but not at 1 ($p=0.2089$) or 7 ($p=0.2084$) days post infection by Satterthwaite t-test (Figure 2.13A).

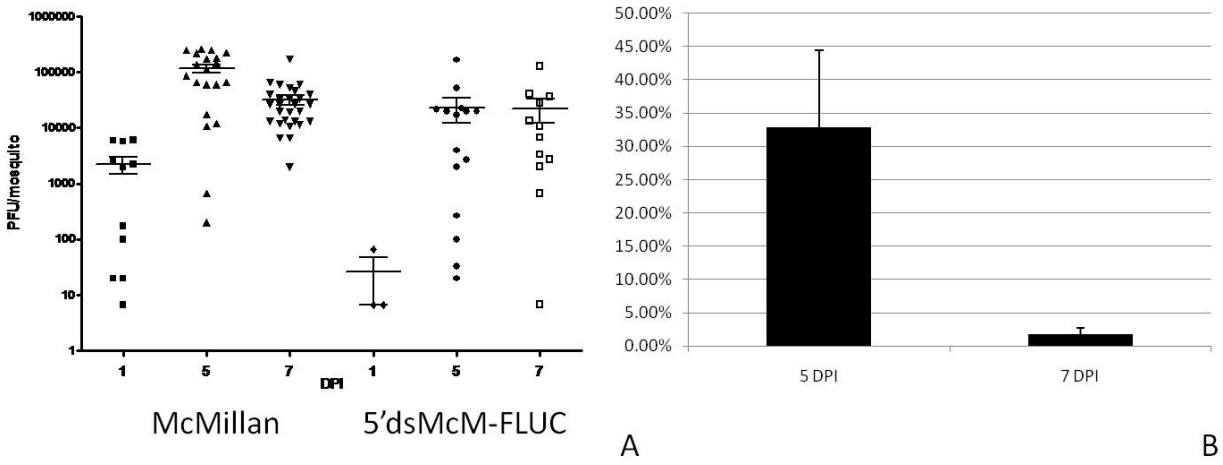

Figure 2.13 Growth and genomic stability of 5'dsMcM-FLUC in C. tarsalis. Viral titers for McMillan and 5'dsMcM-FLUC in individual i.t. injected C. tarsalis whole bodies 1, 5, and 7 days post inoculation (A). Percent of 5'dsMcM-FLUC virus population expressing FLUC from infected *C. tarsalis* at 5 and 7 days post injection as determined by a ratio of end-point titers for luminescence and cytopathic effect ($TCLD_{50}/TCID_{50}$; B).

Analysis of FLUC insert stability was conducted by comparing ratios of bioluminescent and CPE endpoint virus titers. An average of 32.82% of the 5'dsMcM-FLUC population expressed functional luciferase at 5 days and 1.82% at 7 days post infection. An approximately 18-fold decrease in the proportion of 5'dsMcM-FLUC expressing FLUC was observed from this experiment. This decrease was significant by Satterthwaite t-test ($p=0.0111$; Fig, 2.13B). Mosquito homogenates were titrated by plaque assay in Vero cells and the virus titer was log transformed and tested for correlation with bioluminescence (as measured by log transformed radiance). Bioluminescence failed to correlate significantly with virus titer ($R^2=0.653$ after $\log_{10}$ transformation of both parameters).

Renilla reniformis luciferase

The use of an alternate source of bioluminescence to FLUC was considered in the form of *Renilla reniformis* luciferase (RLUC). The gene encoding this enzyme is smaller (932 nucleotides compared to 1653 nucleotides for FLUC). RLUC has been reported to be brighter with *in vivo* imaging applications (Bhaumik et al, 2004) when compared to FLUC. As a putatively ideal candidate for use with *in vivo* imaging, 5'dsMcM-RLUC expressed RLUC in cell culture after addition of the substrate (coelenterazine; ViviRen, Promega). Characterization in cell culture was performed before preliminary experiments in CD-1 mice. Vero cells infected with 5'dsMcM-RLUC produced abundant light when imaged *in vitro* compared to uninfected control cells. Virus was characterized through growth curves conducted in 25 cm^2 flasks containing confluent monolayers of Vero or C6/36 cells. The maximal titer of 5'dsMcM-RLUC was comparable to McMillan in both Vero and C6/36 cells. However, 5'dsMcM-RLUC was slower in reaching maximal titer in Vero cells compared to unaltered McMillan (Figure 2.14).

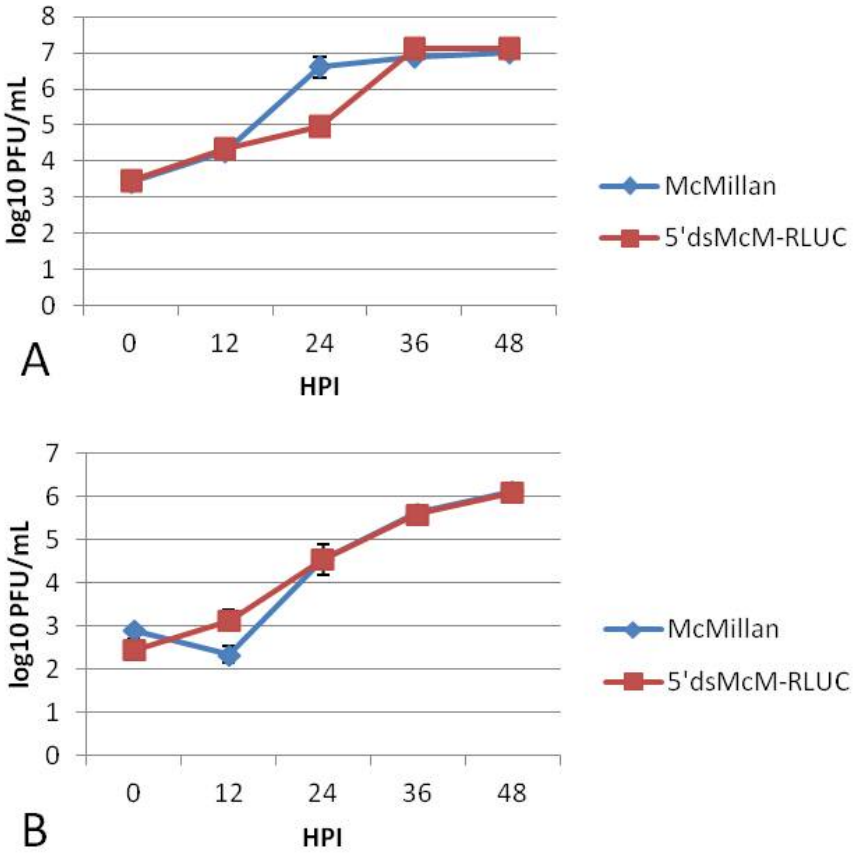

Figure 2.14 Growth curves of McMillan or 5'dsMcM-RLUC in Vero (A) and C6/36 (B) cells. All cultures were infected at an MOI of 0.01. Medium was taken from the infected cell cultures at time of inoculation and every 12 hours thereafter for 48 hours and titratedby plaque assay in Vero cells. At 24 hours post infection, 5'dsMcM-RLUC exhibited a significantly lower (p=0.0019) titer than McMillan in Vero cells. There were no significantly different virus titers at any time between McMillan and 5'dsMcM-RLUC infected C6/36 cells. The maximal titers for McMillan and 5'dsMcM-RLUC were not significantly different.

In the interest of developing a transmission model for WEEV utilizing mosquito transmission, CD-1 mice were inoculated either with 25 uL of 1 x 10^7 PFU/mL 5'dsMcM-RLUC in the right hind footpad or by exposure to 10 *A. aegypti* mosquitoes injected 10 days previously with 5'dsMcM-RLUC. Infected was confirmed in mosquitoes through in vivo imaging following injection of coelenterazine (not shown). Mice infected by the s.c. route succumbed to infection (n=2) and 5'dsMcM-RLUC recovered from brain homogenates retained expression of RLUC by

cell culture assay. When infection of a CD-1 mouse was attempted through infected mosquito feeding, signs of WEEV infection were not observed despite successful feeding. Considerable background bioluminescence from the RLUC substrate administered via the i.p. route prevented successful imaging. *A. aegypti* that were injected with 500 PFU of 5'dsMcM-RLUC and subsequently with ViviRen substrate at 10 days post infection were positive for bioluminescence and lacked significant background bioluminescence in a ViviRen injected, uninfected negative control (Figure 2.15). Nonspecific bioluminescence was detected in non-infected CD-1 mice but not in cell culture or *A. aegypti* mosquitoes 10 days after intrathoracic injection with 5'dsMcM-RLUC.

Experiments with 5'dsMcM-RLUC showed bioluminescence in absence of the enzyme, the substrate was poorly soluble in water, and prolonged bioluminescence (1-3 days) in CD-1 mice at the site of coelenterazine injection. RLUC use was discontinued for these reasons. Various formulations of the diluents and substrate were attempted using manufacturer's recommendations (suspension in ethylene glycol or DMSO) *in vivo* without success. Imaging was possible with limited background bioluminescence from the substrate in mosquitoes and in cell culture. However, 5'dsMcM-RLUC virus isolated from the brains of moribund mice expressed RLUC in BHK cell culture, indicating superior stability to FLUC *in vivo*.

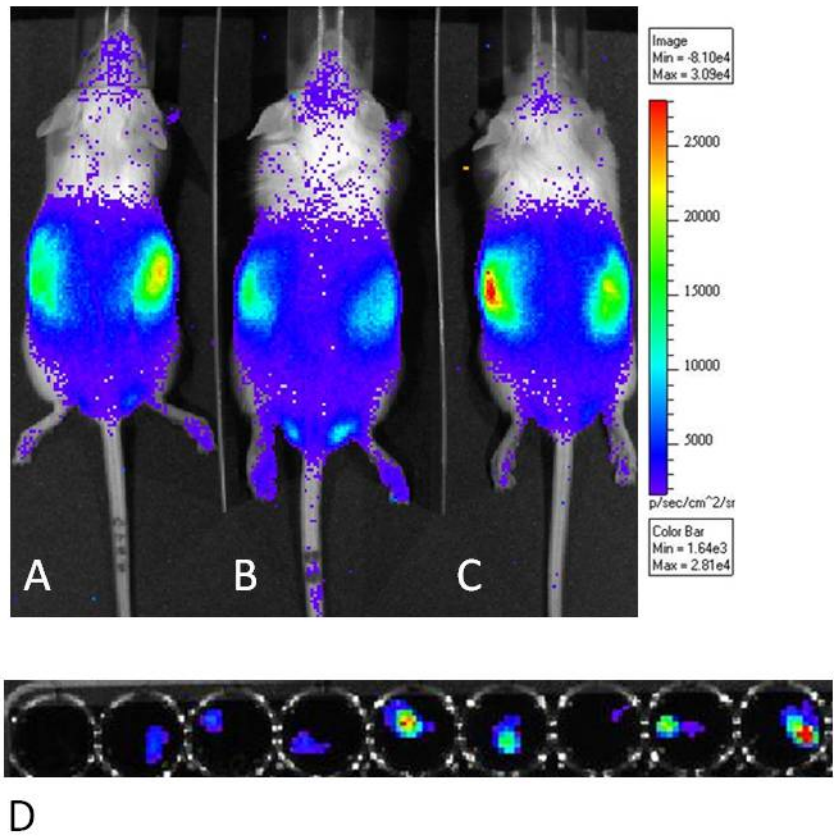

Figure 2.15 RLUC expression in mice and mosquitoes. CD-1 mouse injected s.c. in the right hind footpad with 2.5 x 10^5 PFU 5'dsMcM-RLUC (A), mouse fed upon by 5'dsMcM-RLUC infected A. aegypti mosquitoes (B), or non-infected mouse (C). Nonspecific bioluminescence was detected in non-infected CD-1 mice but not in cell culture or *A. aegypti* mosquitoes 10 days after intrathoracic injection with 5'dsMcM-RLUC (D). The left-most well contained a non-infected mosquito injected with an identical amount of ViviRen.

Discussion

Multiple approaches were followed to determine which reporter was optimal for *in vivo* imaging of mice and mosquitoes. Desirable traits for a reporter included low genomic stress of the insertion on the recombinant virus, easily recognizable and measurable signal with *in vivo* imaging using the IVIS, and low background signal during imaging. The use of mCherry fluorescent protein was considered due to the short length of the insert. *In vivo* imaging is problematic with fluorescent proteins as living tissue provides a barrier to both the excitation light emitted by the IVIS and the light emitted by the fluorophore. The IVIS 200 camera lacked a

filter specific to mCherry emission wavelengths (the dsRed filter was used) and was found to be generally incapable of clearly imaging biologically expressed fluorescent proteins either *in vitro* (in cell culture) or *in vivo*. Significant background was also observed with imaging fluorescent expression. The expression of mCherry is difficult to quantitate due to the extended half-life of the protein. While 5'dsMcM-FLUC infected, replicated, and expressed bioluminescence in *C. tarsalis* after intrathoracic injection or infectious bloodmeal, insertion of the FLUC gene attenuated viral replication in adult mosquitoes. The loss of FLUC expression in *C. tarsalis* contraindicated transmission studies using this system as 5'dsMcM-FLUC would need to retain the FLUC gene in both the mosquito and mouse. The utility of 5'dsIMP-FLUC in transmission studies was found to be more unlikely than 5'dsMcM-FLUC. The 5'dsIMP-FLUC virus lost functional insert one passage sooner in cell culture. While IMP181 may be better able to infect the invertebrate host, IMP181's lack of virulence in the CD-1 mouse model and inability to maintain bioluminescent expression in the 5'dsIMP-FLUC system make an undesirable virus for study.

In most cases, s.c. injection of CD-1 mice with 5'dsMcM-FLUC was variable in terms of mortality and bioluminescence. The genomic stress that such a large insert (FLUC; 1653 nucleotides) carried in the viral genome resulted in attenuation of virulence and loss of functional insert. Intranasal inoculation proved to be more dependable. The lethality and bioluminescence exhibited following the intranasal route of infection indicated the utility of this system for testing antiviral strategies in the CNS. Intranasally inoculated animals demonstrated a more uniform detection of bioluminescence with rapid progression towards high levels of bioluminescence (>1 x 10^6 p/s/cm^2/sr) in the head. When 5'dsMcM-FLUC was given ready access to the CNS, the virus was able to invade and express bioluminescence one day after inoculation. Less mortality

was observed in these studies with intranasal inoculation compared to previous experiments with intranasal inoculation using McMillan. This could be due to the outbred nature of the mouse strain or loss of inoculum during delivery. Rapid mortality seen with CD-1 mice infected with McMillan may be less than optimal for testing antiviral strategies. WEEV infections in humans often occur over weeks instead of days and the death of an infected mouse in four days may provide too virulent of a model for the initial screening of an antiviral compound. The attenuated infection in CD-1 mice seen with 5'dsMcM-FLUC may be more sensitive to treatment or vaccination by providing more time to cure an initial infection or prevent CNS involvement.

Significant bioluminescence was reliably present shortly after injection of 5'dsMcM-FLUC, enabling the use of *in vivo* imaging in validating a previously established prophylactic treatment for McMillan in CD-1 mice. The approximately 40% increase in the survival of CD-1 mice infected with 5'dsMcM-FLUC compared to McMillan is similar to that described in albino B6 and BALB/c mice infected with neurovirulent SINV strains with or without the FLUC gene. In previous work a 10%-60% increase in survival was observed with neurovirulent SINV containing FLUC (Cook and Griffin, 2003). The incorporation of FLUC is therefore associated with the attenuation of the host WEEV or SINV strain used to express it.

The selective pressure against the FLUC insert in vertebrate cell lines was not observed in C6/36 cells infected with 5'dsMcM-FLUC. At 48 hours post infection at MOIs from 0.01 to 1.0 in BHK and Vero cells, there are CPE with significant detachment of cells from the monolayer. C6/36 cells did not show obvious signs of 5'dsMcM-FLUC infection throughout the course of the 48 hour passages used to assess stability. It is possible that the combination of an intracellular environment permissive to the replication of a larger viral genome combined with the morphologically healthier cells seen in C6/36 culture contribute to retention of the FLUC

insert. The absence of cell death possibly allowed retention of full-length 5'dsMcM-FLUC and 5'dsIMP-FLUC genomic replication in healthy cells for a longer period of time. Truncation of FLUC during viral replication would result in the incapsidation of infectious WEEV with nonfunctional FLUC in cell culture. With C6/36 cells existing in a healthy state for a longer period of time, more replication from the original infectious 5'dsMcM-FLUC or 5'dsIMP-FLUC virus would occur, with more WEEV produced containing functional FLUC. In BHK and Vero cells, initially infected populations of cells would perish. Subsequent generations of infection would be caused by a mixture of virus with or without FLUC and continued expression of full-length 5'dsMcM-FLUC would suffer as a result.

This study used two techniques that were distinct from previous work with New World alphaviruses: measuring total light emission from each animal and scoring each animal based on discrete sites of bioluminescence. Both methods agreed with traditional survival curve analysis in this study. At 24 hours post infection, there was a clear difference between groups treated and untreated with CLRCs. This is a marked improvement over the days to weeks needed to make a decision based on survival curves and has the potential to assist evaluation of potential antivirals or prophylactic treatments by streamlining the animal model testing phase of development. *In vivo* imaging technology successfully predicted the efficacy of CLRC treatment 24 hours prior to infection with a virus engineered to express FLUC. Use of bioluminescent scoring as well as quantitative measurement of light emitted from each animal was used to show reduced reporter expression in treated animals compared to untreated. A significant degree of protection was observed in treated animals after survival curve analysis. This technology highlighted the utility of *in vivo* imaging in the testing of antiviral strategies in single living animals imaged over time.

This study showed the possibility of reducing the total number of animals needed in such a study, thereby alleviating economic and ethical concerns associated with this process.

Currently no other models exist for using bioluminescence to study the spread or pathogenesis of New World alphaviruses. Studies aimed at examining WEEV dissemination to peripheral sites of replication or neuroinvasion following different methods of infection could benefit from the use of bioluminescent imaging. Neurovirulent McMillan strain WEEV in CD-1 mice is a good model for testing antivirals, prophylactic treatments, and pathogenesis that could in turn be applicable for studying other neurovirulent alphaviruses such as EEEV and VEEV in the future.

Chapter III: Fluorescent Reporter Expression by a Western Equine Encephalitis Transducing System

Introduction

Western equine encephalitis virus is maintained in an enzootic cycle through transmission by *Culex tarsalis* to passerine bird species. Transmission to equine or human hosts has been associated with severe outbreaks of disease in the past. Understanding the determinants of transmission to the vector from the host, dissemination within the vector, and secretion in saliva of this virus are crucial to understanding the overall cycle. An alphavirus transducing system has facilitated the study of WEEV interaction with the midgut and salivary gland tissues of *C. tarsalis* utilizing in vivo methods. The expression of monomeric cherry fluorescent protein was used to examine infection, dissemination, and transmission with the IMP181 and McMillan strains of WEEV. Salivary gland infection rate was initially hypothesized to be different between IMP181 and McMillan, allowing the strain with fewer passages since isolation from a mosquito to be transmitted at a higher rate. *C. tarsalis* has been shown to be refractory to midgut infection by McMillan and the existence of a similar salivary gland barrier was investigated using expression of mCherry fluorescent protein.

The use of chimeric recombinant viruses revealed the association of McMillan structural proteins with lower virus titers in expectorated saliva. Intrathoracic injection of McMillan and IMP181 into mosquitoes resulted in no significant difference between the two strains of WEEV in terms of salivary gland infection or transmission rates at 7 and 14 days post infection. The transmission rate, but not the salivary gland infection rate was found to be dose dependent with both strains of WEEV. Dose dependence of transmission suggested the relation of a threshold

virus titer in the hemocoel to the likelihood of virus escape from the salivary glands into the saliva of infected mosquitoes.

To develop an effective model to study the interactions of WEEV with its natural vector, double subgenomic recombinant viruses expressing mCherry were constructed and used to infect a laboratory colony of *C. tarsalis* mosquitoes. Alphavirus transducing systems, as infectious and replication-competent viruses engineered to express reporter genes, have yet to be used to study New World alphavirus interactions with vector species. The two principal strains of WEEV used in this study were isolated originally either from a human (McMillan) or *C. tarsalis* (IMP181) and propagated in mouse brains or Vero cells respectively (Bianchi et al, 1993; Reisen et al, 2008; Zhang et al, 2011). McMillan and IMP181 have 99.7% identity at the nucleotide sequence level and significant amino acid sequence homology. McMillan and IMP181 differ greatly in their ability to cause disease in an outbred mouse model of infection. While both strains were neuroinvasive, IMP181 lacked neurovirulence sufficient to cause disease in adult mice (Logue et al, 2009). Enzootic strains have been associated with a lack of neurovirulence in mice (Bianchi et al, 1993). The McMillan strain was originally isolated in 1941 and has been used in numerous studies of WEEV (Bianchi et al, 1993; Logue et al, 2009; Trent and Grant, 1980; Hayes 1978).

WEEV infects the vertebrate host through saliva secreted by an infected mosquito. High concentrations of arboviruses can be detected in mosquito saliva. Experiments in the 1960s measured WEEV concentrations in saliva by infecting mice with varying dilutions of saliva and determining the dose sufficient to kill 50% of infected mice (LD_{50}). Depending upon the virus and vector, WEEV concentrations from 1,000 to 100,000 LD_{50} per mosquito were detected (Collins, 1963; Devine et al, 1965; Hurlbut, 1966; LaMotte, 1960; Thomas, 1963). A more recent

experiment detected between 0.2 and 3.6 x 10^7 PFU per mosquito of VEEV isolated from extracted mosquito saliva (Smith et al, 2005).

The expression of mCherry fluorescent protein and FLUC by WEEV is an alternative to immunofluorescence assay (IFA) for tracking infection of *C. tarsalis*. Initially, DsRed fluorescent protein was evaluated for use in mosquitoes. Brighter fluorescence with mCherry fluorescent protein resulted in its adoption for the salivary gland infection and transmission experiments. Fluorescent marker expression by 5'dsMcM-mCherry and 5'dsIMP-mCherry is stable following infection of mosquitoes. Several hypothetical barriers to WEEV transmission were evaluated using 5'dsMcM-mCherry and 5'dsIMP-mCherry. The principal barrier to McMillan transmission is a documented midgut infection barrier in multiple strains of *C. tarsalis*. The salivary gland barrier for the McMillan strain of WEEV was hypothesized to be a result of an inability to effectively infect *C. tarsalis* salivary glands following intrathoracic inoculation (Kramer, 1981; Kenney et al, 2010). This study investigated the hypothesis of salivary gland infection posing a significant barrier to McMillan transmission. A salivary gland escape barrier was also hypothesized to exist that allows a greater proportion of IMP181 transmission into the saliva of intrathoracically inoculated mosquitoes than McMillan. A barrier to expectoration of McMillan in intrathoracic (i.t.) injected *C. tarsalis* CA strain mosquitoes was hypothesized to generate higher IMP181 virus titers in saliva.

Materials and Methods

Virus construction

A reporter gene encoding *Discosoma* red fluorescent protein (DsRed) or monomeric cherry fluorescent protein (mCherry) was inserted into the MCS of the 5'dsMcM plasmid to make different alphavirus expression systems (Table 3.1). Using similar primers, the gene for

mCherry fluorescent protein was introduced into the MCS downstream of the native 26S subgenomic promoter of 5'dsIMP181 plasmid (Table 3.1).

Table 3.1 Primers used to amplify mCherry and DsRed gene inserts for the production of p5'dsMcM-mCherry, p5'dsMcM-DsRed, and p5'dsIMP-mCherry.

Reporter	Forward	Reverse
mCherry	Aaaaccgcggatggtgagcaaggg	aaaacctgcaggttacttgtacagctcg
DsRed	Aaaccgcggatgaggtcttccaagaatgt	aaacctgcaggttaaaggaacagatgg
mCherry	Aaaccgcggatggtgagcaaggg	Aaacccgggttacttgtacagctcg

Once amplified and sequenced, plasmids were linearized by incubation overnight with MfeI (McMillan; New England Biolabs) or NotI (IMP181; New England Biolabs) at 37°C and treated with proteinase K (New England Biolabs) to destroy residual proteins such as RNases. Linearized plasmids were purified by chloroform extraction and ethanol precipitation. Between 500 and 1000 ng of purified, linearized plasmids were used as templates for *in vitro* transcription using a T7 RNA Polymerase and MAXIscript™ kit (Ambion). BHK cells were washed in PBS (Cellgro) and electroporated twice using an ECM 630 electroporator (BTX) at 450 volts, 720 ohms, and 100 microfarads by mixing 20 µL of *in vitro* transcribed RNA and 400 µL of 1 x 10^7 cells/mL BHK cell suspension. Medium was taken from the cells two days after electroporation and passaged once in C6/36 cells to make a stock virus that was stored in aliquots at -80°C in MEM containing 10% FBS plus non-essential amino acids, L-glutamine, and antibiotics. This stock virus was quantified by plaque titration in Vero cells (virus stock titers ranged from 1 x 10^6 to 1x 10^7 PFU/mL), aliquoted, stored at -80°C, and used for subsequent experiments.

Infectious clones 39, 40, 41, and 42 were a generous gift from Dr. Eric Mossel (CSU). They were constructed using standard molecular techniques and represent reciprocal domains of

genomic sequence from IMP181 and McMillan. Clone 39 has a backbone (5'UTR, nsP1-4) from IMP181 with 6K, E1, and 3'UTR sequences from McMillan. Clone 40 has a backbone from McMillan but has the 6K, E1, and 3'UTR sequences derived from IMP181. Clone 41 has an IMP181 backbone with the C, E3, and E2 genes derived from McMillan. Clone 42 is the opposite with a McMillan backbone and the C, E3, and E2 genes of IMP181 (Figure 3.1).

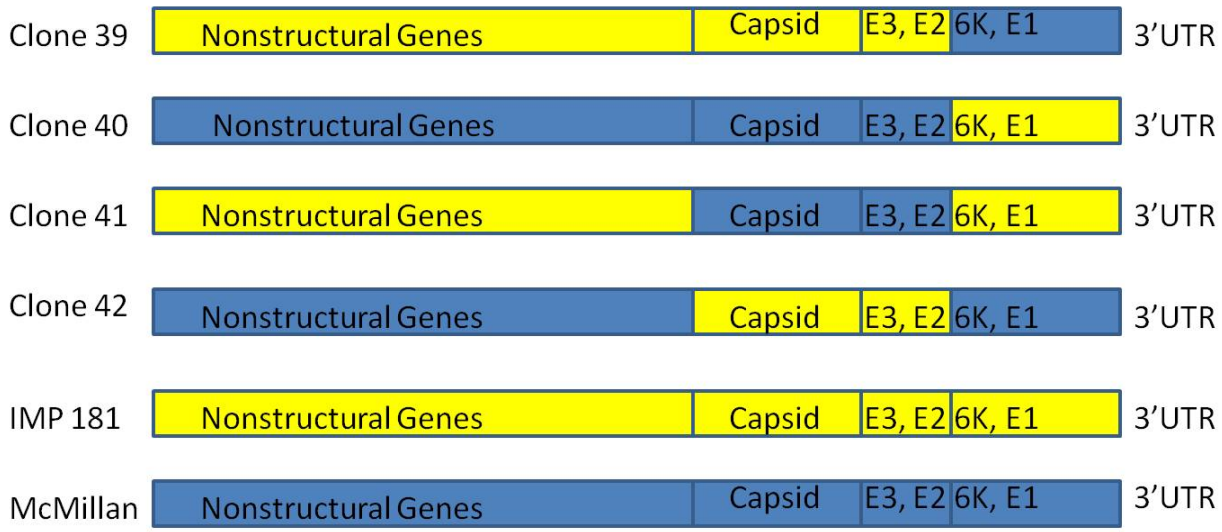

Figure 3.1 Diagram of each infectious cDNA clone used in the transmission experiments, with components of each derived from McMillan (Blue) or IMP181 (Yellow) strains of WEEV.

Growth curves

Growth kinetics of 5'dsMcMillan-dsRed were assayed in 24-well plates (VWR International) in cells over 48 (BHK and Vero) or 60 (C6/36) hours post infection at 5% CO_2, 37°C, and 95% humidity (BHK and Vero) or 5% CO_2, 28°C, and 95% humidity (C6/36). Aliquots of 100 µL were taken in triplicate from each cell type over 6 time points and replaced with DMEM containing 10% FBS. Slower growth kinetics with WEEV in C6/36 cells (Dennis Pierro, personal communication) resulted in time points at 0, 12, 24, 36, 48, and 60 hours post infection while samples were taken at 0, 6, 12, 24, 36, and 48 hours for growth curves in Vero and BHK cells. Virus titers were $\log_{10}$ transformed and compared between parameters (virus or

cell type origin) following histogram and QQ-plot tests for normality with a student's t-test using statistical analysis software (SAS).

Growth curves of recombinant and wild-type infectious clone derived virus were conducted in C6/36, Vero, and BHK cells. Confluent monolayers of each cell type were infected with at a MOI of 0.01 for each virus and aliquots of supernatant taken every 12 hours for 48 or 60 hours for quantitation. Virus was quantified using replicate ten-fold serial dilutions in 90 µL MEM 7% FBS followed by addition of Vero cell suspensions and calculation of $TCID_{50}$/mL using the method of Reed and Muench (1938).

Mosquito infection

C. tarsalis CA strain mosquitoes were a generous gift from Dr. William Reisen (UC Davis) and the colony was incubated at 28°C and 80.6% humidity in a Caron 6030 environmental growth chamber. Mosquitoes were infected with WEEV by either intrathoracic injection or infectious bloodmeal.

Mosquitoes were fed infectious virus in blood-meals consisting of a 1:1 mixture of defibrinated sheep blood (Colorado Serum Company) and 1.5 x 10^5 $TCID_{50}$/mL WEEV in a Hemotek™ (Discovery Workshops) feeding chamber calibrated to 35°C ± 1. Adenosine tri-phosphate (ATP; 100 µM) was added to the mixture to enhance feeding. Mosquitoes were allowed to feed until repletion and blood-fed females were sorted prior to imaging. Following infection, mosquitoes were incubated in 0.5-liter containers with organdy netting covering the open end. Other groups of mosquitoes were artificially bloodfed a 1:1 mixture of virus in DMEM 10% FBS and defibrinated sheep blood, providing 5'dsMcM-FLUC or 5'dsMcM-DsRed at a dose of 1-2 x 10^6 PFU/mL. ATP was added as described previously to enhance feeding.

Mosquitoes were bloodfed, sorted and incubated at 28°C and 80.6% humidity in a Caron 6030 environmental growth chamber.

The following procedures were used to test the hypothesis that the IMP181 strain of WEEV was expectorated at both a higher rate and greater titers compared to McMillan. Two-day-old female *C. tarsalis* were i.t. injected with 500, 250, or 125 $TCID_{50}$ of McMillan, 5'dsMcM-mCherry, IMP181, 5'dsIMP-mCherry, clone 39, clone 40, clone 41, or clone 42. At 7 and 14 days post infection injected mosquitoes were induced to secrete saliva by fixing each mosquito to laboratory tape and inserting the proboscis into a capillary tube containing 5 µL of 50% FBS:glycerol solution (Hurlbut et al, 1966; Smith et al, 2005). Expectoration occurred for 30-45 minutes before salivary glands were dissected for virus detection. The proportion of *C. tarsalis* transmitting virus was determined as the number of saliva samples positive for infectious virus divided by the total number of saliva samples. Infected mosquitoes were identified by fluorescence microscopy or IFA. Any mosquitoes found to be negative for viral infection were excluded from analysis of saliva.

Negative controls consisted of saliva collected from non-infected mosquitoes and diluted in MEM with 7% FBS. Known doses of McMillan (5×10^6 PFU) strain WEEV were added to saliva collected from non-infected mosquitoes either in the capillary tube or after dilution in medium as positive controls.

Midgut infection and dissemination

At 7 days following infection of *C. tarsalis* with 5'dsMcM-FLUC in an infectious blood-meal, 16 adult female mosquitoes were injected i.t with 150 µg/mL luciferin and imaged *in vivo* (IVIS, Caliper Life Sciences). Saliva samples were obtained from infected mosquitoes using capillary tube salivation with mineral oil (Hurlbut, 1966)**.** Saliva in mineral oil was immediately

inoculated onto Vero cells in a black-well 12-well plate for viral detection and examination for FLUC expression. Cells were monitored daily for 6 days for CPE by microscopic examination and bioluminescence using the IVIS 200. Poor plaque titration results with saliva extracted using mineral oil led to the adoption of 50% FBS/glycerol as a collection medium.

Prior to transmission experiments, *C. tarsalis* were blood-fed 5'dsMcM-mCherry and 5'dsMcM-DsRed to observe fluorescence *in vivo*. Dissected midguts were examined using fluorescence microscopy at 3 and 5 days following infection. Midguts, salivary glands, and heads from *C. tarsalis* infected with wild-type or chimeric viruses were fixed in 4% para-formaldehyde and examined with an immunofluorescence assay (IFA). IFA of mosquito tissue was conducted with 1:150 anti-SINV E1 mouse primary antibodies (30.11a), 1:200 biotinylated goat anti-mouse secondary antibodies (Sigma), and streptavidin-fluorescein (Sigma). Fluorescent protein infection and IFA were compared in terms of efficacy in identifying infected tissues. Expression of mCherry and DsRed were assessed for brightness and clarity of signal for future experiments.

Statistics

At each time point, virus titers from plaque titrations or end-point assays were compared using a Student's T-test for data with normal distributions and Satterthwaite T-test for data lacking a normal distribution. Infectious virus titers in saliva were log transformed and subjected to statistical analysis using Student's t-test with a post hoc Bonferroni adjustment. The Bonferroni adjustment was used to counteract the loss of statistical power inherent in making multiple statistical comparisons and resulted in an alpha (and a significant p-value) of 0.01.

Rates of transmission were compared between each set of related groups (14dpi versus 7dpi, McMillan versus IMP181, 5'dsIMP-mCherry versus IMP181, 5'dsMcM-mCherry versus

McMillan, mosquitoes inoculated with 500 $TCID_{50}$ versus 250 $TCID_{50}$ and 125 $TCID_{50}$ infected mosquitoes) using confidence intervals of binomial proportions and Z-tests.

Results

Growth curves

The maximal viral titers for IMP181, McMillan and the viruses derived from infectious clones 39-42 (referred to as clones 39-42) were compared in Vero, BHK, and C6/36 cells. In Vero cells, McMillan and viral clones 39-42 had similar maximal titers while IMP181 had lower titers than McMillan at each time point (24hpi $p= 0.0099$, 36hpi $p=0.0056$, and 48hpi $p= 0.0025$). Peak virus titers generally occurred at the 36 hour time point (Figure 3.2A). In BHK cells, McMillan, IMP181, and clones 39-42 exhibited similar viral growth kinetics (Figure 3.2B). In C6/36 cells, each virus demonstrated similar growth kinetics with a logarithmic increase in titers through the 48 hour time point. McMillan, IMP181, and clones 39-42 reached much higher viral titers in these cells than either Vero or BHK cells when infected at the same MOI (Figure 3.2C).

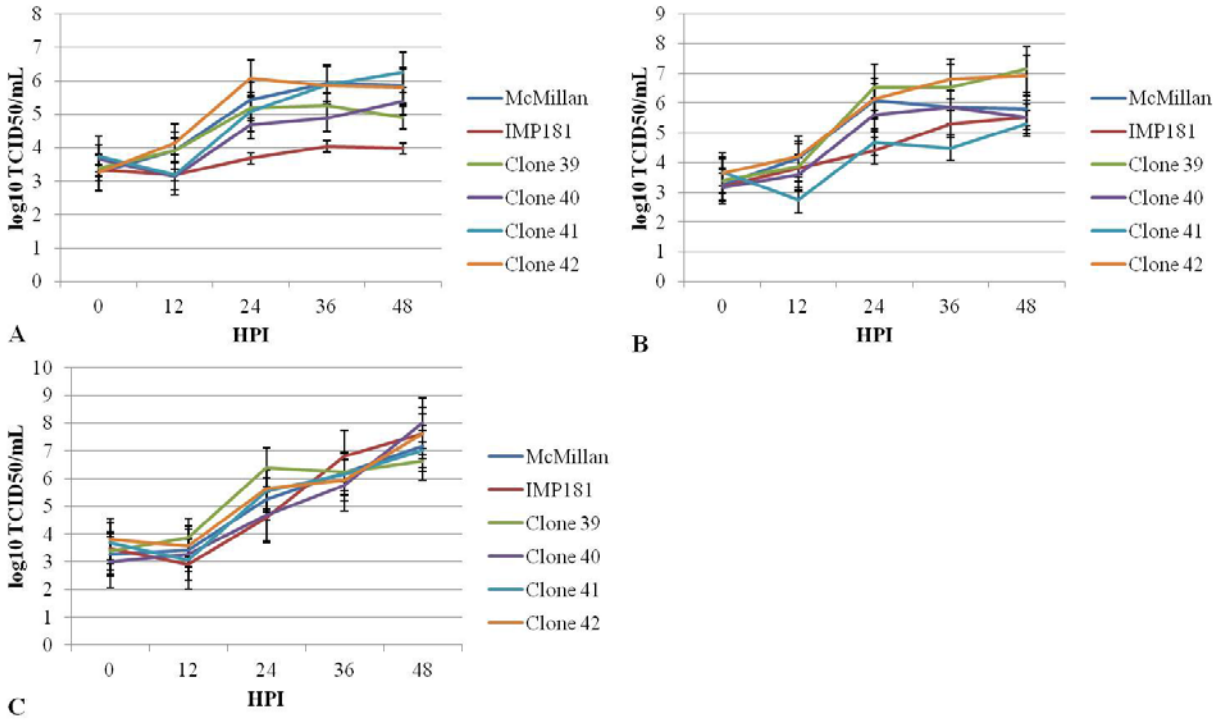

Figure 3.2 Growth curves of McMillan, IMP181, Clone 39, Clone 40, Clone 41, and Clone 42 viruses in Vero (A), BHK (B), and C6/36 (C) cells infected at an MOI of 0.01. Supernatant was harvested at time of infection and every 12 hours thereafter for 48 hours and titrated by end-point assay in Vero cells to compare infectious virus titers.

In Vero cells, 5'dsMcM-dsRed reached a maximal titer of 5.56 x 10^6 PFU/mL. Maximal virus titers for 5'dsMcM-dsRed were 3.11 x 10^6 PFU/mL in BHK cells and 4.87x10^8 PFU/mL in C6/36 cells. This was similar to McMillan WEEV except in Vero cells at the 36hpi time-point, where 5'dsMcM-dsRed exhibited significantly lower virus titers ($p<0.0002$; Figure 3.3).

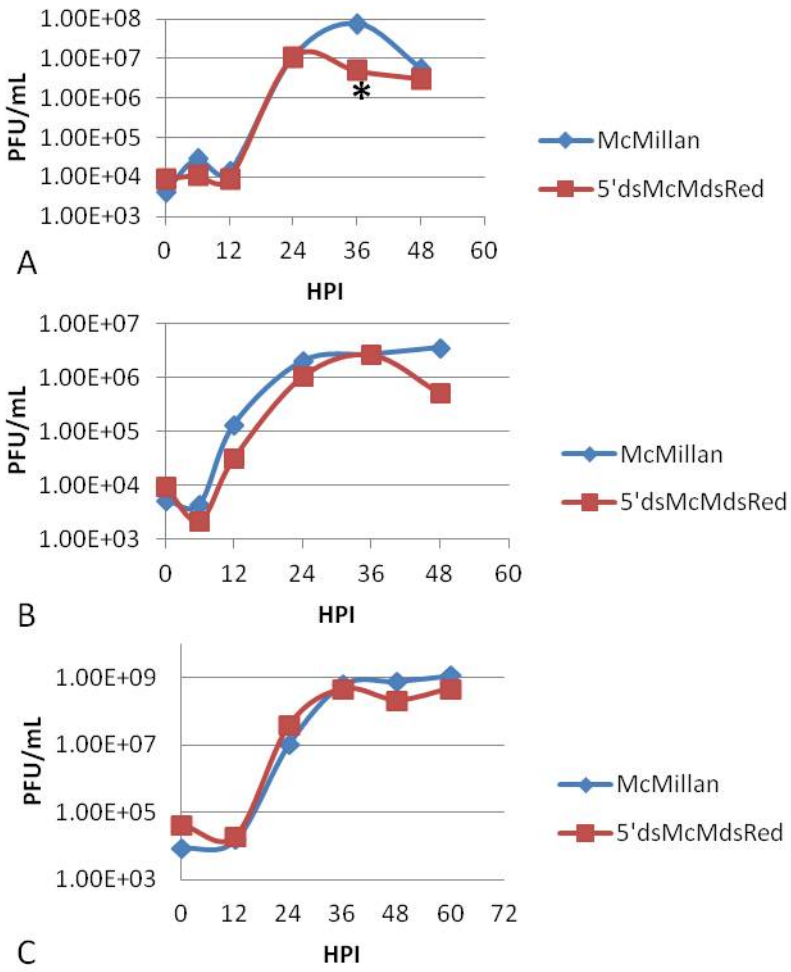

Figure3.3 Growth curves of McMillan and 5'dsMcM-dsRed in Vero (A), BHK (B), and C6/36 (C) cells infected at an MOI of 0.01.

Prior to s.c. injection of mosquitoes for transmission, McMillan and 5'dsMcM-dsRed from Vero, BHK, and C6/36 cells were assayed for growth in C6/36 cells to achieve optimum replication in mosquitoes. McMillan and 5'dsMcM-dsRed grown in BHK (vertebrate) or C6/36 (invertebrate) cells were compared in terms of growth kinetics in cultures of the same or alternate cell type. No significant difference was seen between BHK or Vero cells infected with 5'dsMcM-dsRed of either BHK or C6/36 cell origin. In C6/36 cells, BHK and C6/36 cell-derived 5'dsMcM-dsRed virus titers were significantly different at 24 hours post infection ($p=0.0002$) and 36 hours post infection ($p<0.0001$). C6/36 cell-derived 5'dsMcM-dsRed demonstrated lower

virus titers in C6/36 cells compared to BHK cell-derived virus (Figure 3.4). This is possibly due to differences in the host-cell derived membrane for 5'dsMcM-dsRed produced in BHK compared to C6/36 cells conferring an advantage in infecting C6/36 cells when introduced at the same MOI.

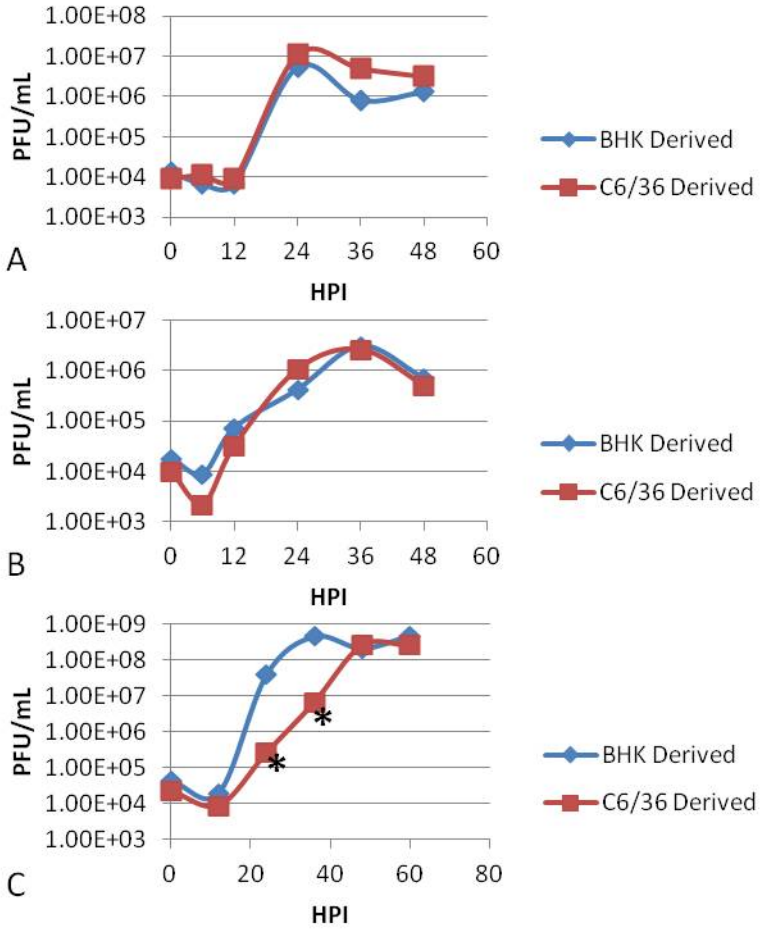

Figure 3.4 Growth curves of 5'dsMcM-dsRed in Vero (A), BHK (B), and C6/36 (C) cells infected at an MOI of 0.01. Each virus was derived from either BHK or C6/36 cells. BHK derived 5'dsMcM-dsRed replicated to a higher maximal titer in C6/36 cells compared with C6/36 cell-derived 5'dsMcM-dsRed, with higher titers at 24 ($p=0.0002$) and 36 ($p<0.0001$) hours post infection.

Midgut infection and dissemination

Following virus characterization in cell culture, *C. tarsalis* were infected with 5'dsMcM-mCherry or 5'dsIMP-mCherry in a blood-meal. Mosquito malpighian tubules, midguts, and

ovaries were dissected at 3, 5, and 7 days post infection to track dissemination of 5'dsMcM-mCherry and 5'dsIMP-mCherry. Midgut infection was uncommon with McMillan. Fluorescence was occasionally detected in portions of some tissues such as the malpighian tubules and ovaries (Figure 3.5).

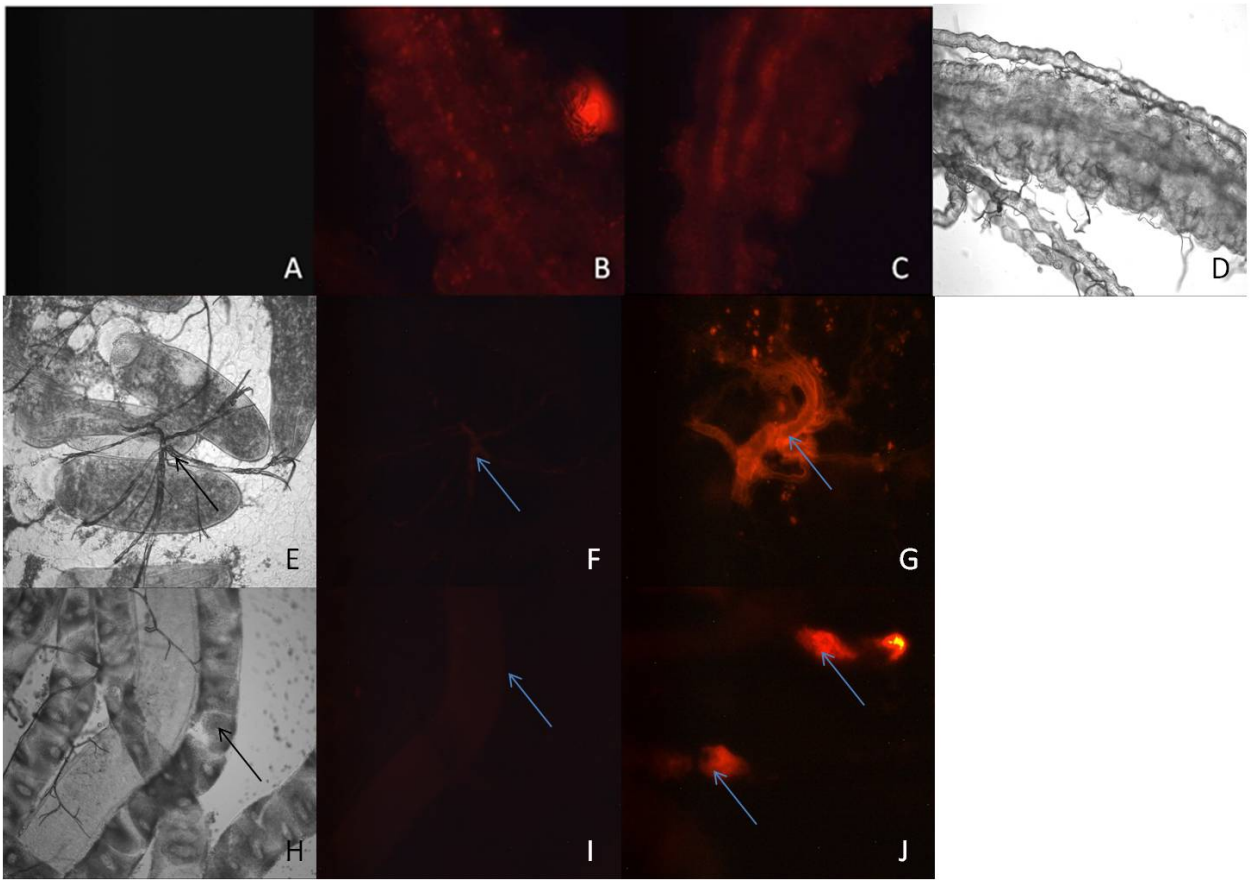

Figure 3.5 Epifluorescent imaging of mosquito tissues after feeding upon infectious blood-meals containing 5'dsMcM-mCherry or 5'dsIMP-mCherry at an infectious virus titer of 1-2 x 10^6 PFU. Images were taken at 20x magnification. Posterior midgut tissue at 7dpi for 5'dsMcM-mCherry (B) and 5'dsIMP-mCherry (C), ovarian tracheolar tissue 3dpi with 5'dsMcM-mCherry (G; arrow indicates ovarian skien), and malpighian tubules 5dpi (J; arrows indicate malpighian tubules) fluoresced. Images were compared to images of non-infected *C. tarsalis* midguts (A: Epifluorescent; D: Light), ovaries (E: Light; F: Epifluorescent; arrows indicate ovarian skiens), or malpighian tubules (H: Light; I: Dark; arrows indicate tubules) as negative controls.

At 5, 7, and 9 days after ingestion of an infectious blood-meal containing 5'dsMcM-dsRed virus, *C. tarsalis* were assayed for DsRed expression by fluorescence microscopy.

Midguts, legs, and heads were assayed for virus in Vero cells. At 3 days post infection, microscopy detected DsRed fluorescence in the bodies of 3 out of 20 mosquitoes while 1 out of 10 displayed fluorescence at 7 days post infection. At 9 days post infection, 0 out of 36 mosquitoes were positive for virus dissemination in the head. Plaque assay of infectious 5'dsMcM-dsRed from midguts, legs, and heads of individual mosquitoes at 5, 7, and 9 days post infection detected a similar proportion of infected mosquitoes, with a midgut infection rate of 20% and a dissemination rate of 10% to the legs and 5% to the head (Table 3.2).

Table 3.2 Proportions of midguts, legs, and heads from *C. tarsalis* infected orally with 5'dsMcM-dsRed at a blood-meal titer of 1-2 x 10^6 PFU. Midgut infection was detectable by plaque titration in Vero cells at day 5 and dissemination to the legs and head of infected mosquitoes occurred at 7 days post infection.

DPI	Midgut	Legs	Head
5	5/35 (.14)	0/35 (.00)	0/35 (.00)
7	8/40 (.20)	3/40 (.08)	2/40 (.05)
9	8/40 (.20)	4/40 (.10)	2/40 (.05)

Midgut, leg, and head virus titers were not found to be significantly different at each day using a Satterthwaite t-test. Infectious 5'dsMcM-dsRed was not detected in the legs or heads of mosquitoes at 5 days post infection. Starting at 7 days post infection, infectious virus in legs and heads were detected. Virus titers were not significantly different between 7 and 9 days post infection (Figure 3.6).

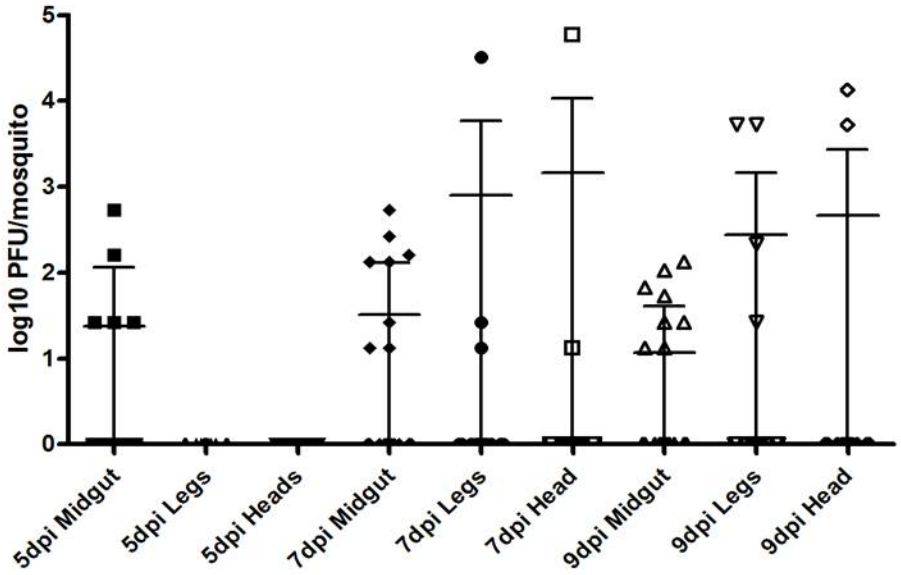

Figure 3.6 WEEV (5'dsMcM-dsRed) titrated from the midguts, legs, and heads of C. tarsalis infected 5, 7, or 9 days prior by infectious blood-meal at a dose of 1-2 x 10^6 PFU (Data on Table 3.2).

Salivary gland infection

A method for imaging the infection of *C. tarsalis* salivary glands by WEEV was developed using 5'dsMcM-mCherry and 5'dsIMP-mCherry to test a hypothetical salivary gland infection barrier. Adult *C. tarsalis* mosquitoes were intrathoracically injected to avoid midgut barriers to infection with WEEV. In salivary glands, the infection rate for McMillan, IMP181, 5'dsMcM-mCherry, and 5'dsIMP-mCherry viruses were not significantly different (Table 3.3). Fluorescent imaging of salivary glands dissected from mosquitoes injected with 5'dsMcM-mCherry and 5'dsIMP-mCherry viruses displayed similar patterns of mCherry expression. Uniform expression of mCherry occurred in the distal and proximal lateral lobes and the medial lobe of each positive set of glands examined (Figure 3.7).

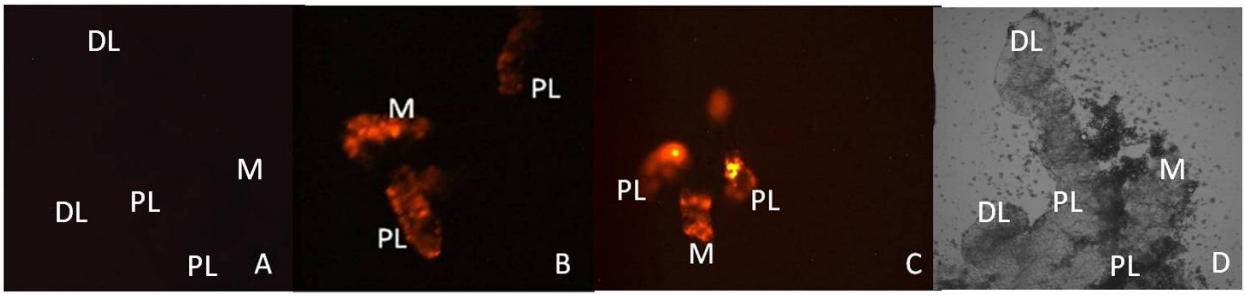

Figure 3.7 Epifluorescent imaging of *Culex tarsalis* salivary glands. Salivary glands were imaged at 20x magnification using fluorescence microscopy. Salivary glands were compared to negative control epifluorescent (A) and light (D) images of non-infected *C. tarsalis* salivary glands. *C. tarsalis* salivary glands 14 days post intrathoracic injection with 500 $TCID_{50}$ 5'dsMcM-mCherry (B) and 5'dsIMP-mCherry (C). M, medial lobe; PL, proximal-lateral lobes, DL, distal-lateral lobes.

Expression of mCherry was compared to IFA as a method of detecting 5'dsMcM-mCherry and 5'dsIMP-mCherry infection of *C. tarsalis* salivary glands. IFA using an anti-SINV E1 antibody (30.11a) revealed an almost complete infection of the salivary glands by both strains of virus at 7 days post injection. In salivary glands that were incompletely infected, the distal tips of the lateral lobes exhibited a lack of fluorescence. Prominent tissues expressing viral antigen include acinar cells and duct tissue connecting the glands to the proboscis. There were no visible differences in the pattern of salivary gland infection between 5'dsIMP-mCherry and 5'dsMcM-mCherry (Figure 3.8).

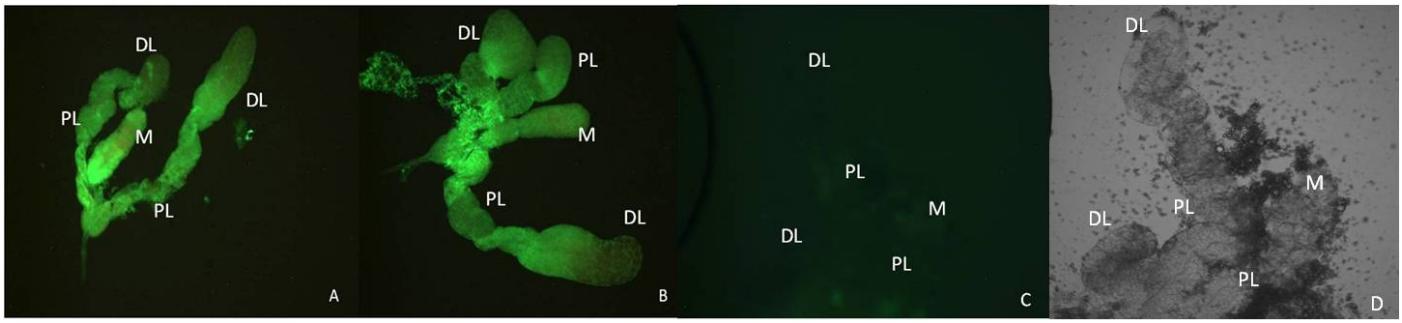

Figure 3.8 IFA of *Culex tarsalis* salivary glands. *C. tarsalis* salivary glands stained immunohistochemically for WEEV and imaged at 20x (A) and 40x (B) magnification using epifluorescent microscopy 14 days post intrathoracic injection with 500 $TCID_{50}$ McMillan (A) and IMP181 (B). Images were compared to non-infected salivary glands as a negative control (Epifluorescent: C; Light: D). WEEV E1 was detected by IFA using monoclonal 30.11a (anti-SINV E1) as the primary antibody. DL, distal-lateral lobe; M, medial lobe; PL, proximal-lateral lobe.

Salivary glands taken from mosquitoes 7 or 14 days post infection were tested for 5'dsMcM-mCherry or 5'dsIMP-mCherry virus through examination for antigen fluorescence. Epifluorescent imaging of salivary glands from intrathoracically injected *C. tarsalis* was conducted to determine the presence or absence of a salivary gland infection barrier for 5'dsMcM-mCherry. Lack of 5'dsMcM-mCherry positive salivary glands would indicate a significant infection barrier in the CA strain of *C. tarsalis*. However, a salivary gland infection barrier was not detected at any dose or time post infection assayed in this study. Salivary gland infection rates ranged from 69% to 89%, indicating a lack of a major barrier to entry. The rates of salivary gland infection were not significantly different between i.t. doses of 5'dsMcM-mCherry and 5'dsIMP-mCherry at any concentration or time point (Table 3.3).

Table 3.3 Rates of salivary gland infection 7 and 14 days after intrathoracic injection with 5'dsMcM-mCherry or 5'dsIMP-mCherry at doses of 125, 250, or 500 $TCID_{50}$. Rates are given as a percentage with a 95% confidence interval. Infection was determined by epifluorescent imaging of dissected salivary glands.

7dpi			
	Total Infected	Salivary Gland (%)	95% CI
5'dsIMP-mCherry			
125 TCID50	73	88%	[0.75, 1.01]
250 TCID50	70	86%	[0.72, 1.00]
500 TCID50	72	89%	[0.76, 1.01]
5'dsMcMmCherry			
125 TCID50	70	74%	[0.57, 0.92]
250 TCID50	72	86%	[0.72, 1.00]
500 TCID50	73	79%	[0.63, 0.95]
14dpi			
	Total Infected	Salivary Gland (%)	95% CI
5'dsIMP181-mCherry			
125 TCID50	32	69%	[0.43, 0.95]
250 TCID50	40	85%	[0.66, 1.04]
500 TCID50	48	81%	[0.62, 1.00]
5'dsMcMmCherry			
125 TCID50	36	72%	[0.47, 0.98]
250 TCID50	35	89%	[0.71, 1.07]
500 TCID50	72	89%	[0.76, 1.01]

Transmission of IMP181 and McMillan in C. tarsalis saliva

Mosquitoes with fluorescent salivary glands (detected through IFA or mCherry expression) were selected for cell culture assay of saliva to determine rates of viral transmission. These saliva samples were assayed for infectious virus and by end-point titration using Vero cells. Mosquitoes injected i.t. with McMillan, 5'dsMcM-mCherry, IMP181, 5'dsIMP-mCherry, clone 39, 40, 41, and 42 viruses were induced to salivate into capillary tubes. Percent transmission in each group was calculated using the number of saliva samples positive for infectious virus compared to number of infected mosquitoes (by IFA or mCherry expression). Percent transmission was found to not be significantly different between IMP181 and McMillan

injected groups. Attenuation of transmission rate was not observed in association with insertion of mCherry. Infection of *C. tarsalis* by 5'dsIMP-mCherry and 5'dsMcM-mCherry was not associated with a significant reduction in the proportion of infected mosquitoes that expectorated virus (Table 3.4).

Two sets of controls were run for the cell culture assay used to detect virus in collected mosquito saliva. Vero cells were used to detect WEEV by adding 3×10^3 $TCID_{50}$/mL of McMillan virus diluted in 7% FBS MEM and saliva collected in 50% FBS/Glycerol from non-infected *C. tarsalis*. Saliva collected from non-infected mosquitoes diluted in 7% FBS MEM was used as a negative control. In all cases (n=56) where virus was present, CPE developed in Vero cells. None of the negative controls (n=44) showed CPE. Experiments to evaluate the use of Vero cell culture in detection and measurement of a known concentration in saliva were also conducted. The concentrations of virus detected when mixed with saliva were not significantly different from concentrations of virus detected when mixed with medium ($p=0.6435$ by Satterthwaite t-test). This suggests that no virus was lost during incubation with the collection medium (50% FBS/Glycerol).

Table 3.4 Rates of infectious virus detected in saliva samples collected from *C. tarsalis* at 7 days post intrathoracic infection with McMillan, 5'dsMcM-mCherry, IMP181, 5'dsIMP-mCherry, clone 39, clone 40, clone 41, and clone 42 viruses at a dose of 500 $TCID_{50}$. Rates are given with sample sizes (total infected by positive IFA or mCherry expression), numbers of mosquitoes with positive saliva samples by Vero cell assay (saliva positive), proportion of infected saliva samples, and a 95% confidence interval for the proportion.

Virus	Total Infected	Saliva Positive	Transmission	95% CI
IMP181	83	19	0.23	[0.14, 0.32]
5'dsIMP-mCherry	73	19	0.26	[0.16, 0.36]
McMillan	89	14	0.16	[0.08, 0.23]
5'dsMcM-mCherry	73	10	0.14	[0.06, 0.22]
Clone 39	78	16	0.21	[0.12, 0.29]
Clone 40	96	29	0.30	[0.21, 0.39]
Clone 41	96	18	0.19	[0.11, 0.27]
Clone 42	96	19	0.20	[0.12, 0.28]

Recombinant viruses (5'dsIMP-mCherry and 5'dsMcM-mCherry) were used to assess the impact of varied dosage and duration of infection on transmission rates. Rates of transmission were not found to vary significantly between mosquitoes injected with 125, 250, or 500 $TCID_{50}$ of 5'dsIMP-mCherry. With 5'dsMcM-mCherry, however, there was a significant increase in transmission rate from doses of 250 to 500 $TCID_{50}$ at 7 ($p=0.02380$) and 14 ($p=0.0147$) days post injection. Transmission rates were significantly greater for 5'dsIMP-mCherry than 5'dsMcM-mCherry at 7 days post injection with 125 and 250 $TCID_{50}$ ($p= 0.0080$ for 125, $p=0.0003$ for 250 using Satterthwaite t-test). The two groups were not significantly different after injection of 500 $TCID_{50}$ (Table 3.5).

Table 3.5 Virus detection in saliva samples collected from C. tarsalis after 7 or 14 days of infection (determined by IFA or mCherry expression) with 5'dsMcM-mCherry or 5'dsIMP-mCherry at doses of 125, 250, or 500 $TCID_{50}$. Transmission rates are given as proportions with 95% confidence intervals.

7dpi				
	Total Infected	Saliva Positive	Transmission	95% CI
5'dsIMP-mCherry				
125 TCID50	73	32	0.44	[0.32, 0.55]
250 TCID50	70	29	0.41	[0.30, 0.53]
500 TCID50	72	19	0.26	[0.16, 0.37]
5'dsMcM-mCherry				
125 TCID50	70	2	0.03	[-0.01, 0.07]
250 TCID50	72	2	0.03	[-0.01, 0.07]
500 TCID50	73	10	0.14	[0.06, 0.22]
14dpi				
	Total Infected	Saliva Positive	Transmission	95% CI
5'dsIMP181-mCherry				
125 TCID50	32	5	0.16	[0.03, 0.28]
250 TCID50	40	6	0.15	[0.04, 0.26]
500 TCID50	48	12	0.25	[0.13, 0.37]
5'dsMcM-mCherry				
125 TCID50	36	1	0.03	[-0.03, 0.08]
250 TCID50	35	5	0.14	[0.03, 0.26]
500 TCID50	72	13	0.18	[0.09, 0.27]

Virus titers were found to be significantly higher in IMP181 compared to McMillan injected mosquitoes at 7 days post injection (p=0.0011). Following up on this difference, saliva virus titers were also measured from *C. tarsalis* injected i.t. with clones 39-42. Clones 40 (p=0.0010) and 42 (p=0.0066) had higher infectious virus titers in saliva compared to McMillan at 7 days post injection. Neither clone 40 nor 42 demonstrated significantly different saliva titers when compared to IMP181 (Figure 3.9).

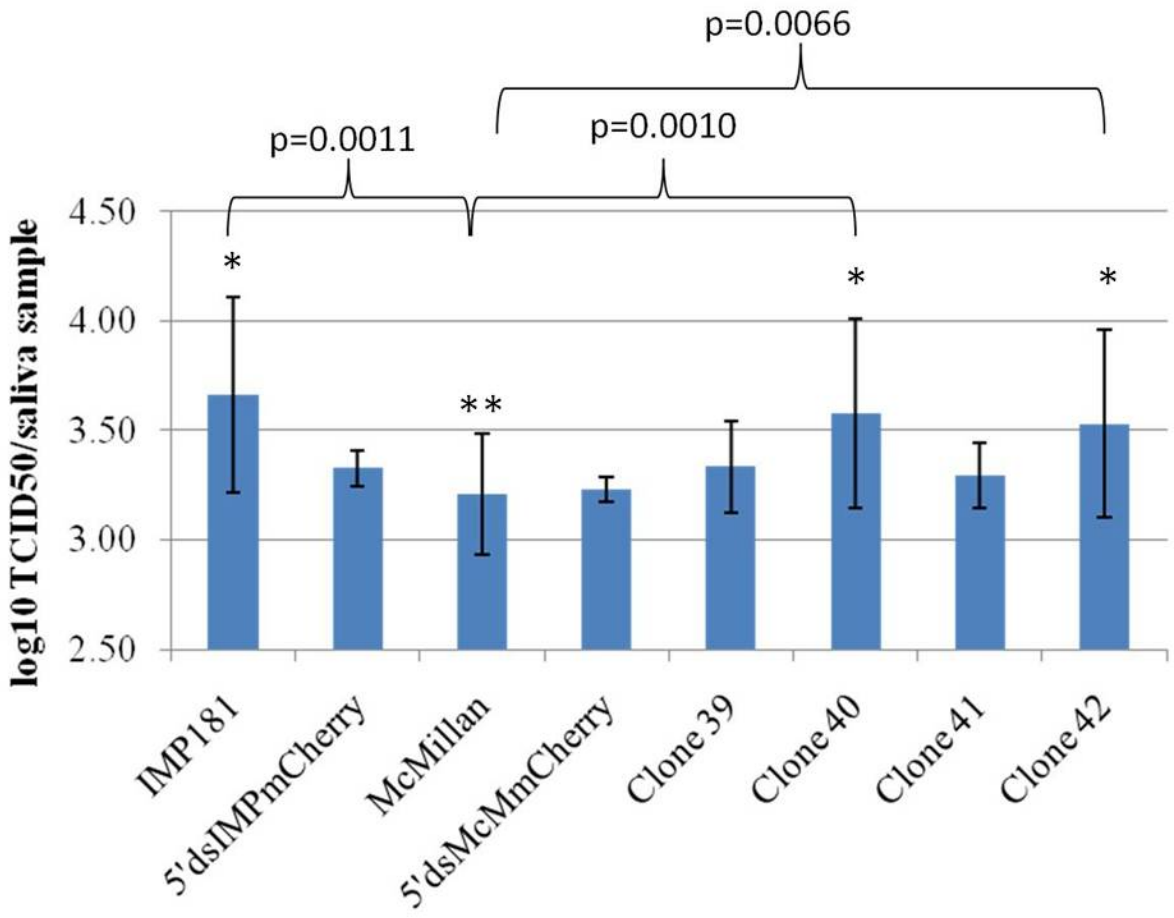

Figure 3.9 WEEV titers in saliva. Infectious virus titers of IMP181, 5'dsIMP-mCherry, McMillan, 5'dsMcM-mCherry, clone 39, clone 40, clone 41, and clone 42 WEEV in saliva collected from *C. tarsalis* 7 days after intrathoracic injection with 500 $TCID_{50}$. IMP181 (p=0.0011), Clone 40 (p=0.0010), and Clone 42 (p=0.0066) -injected mosquitoes expectorated higher log-transformed titers of virus in saliva compared to McMillan-injected mosquitoes.

While 5'dsIMP-mCherry titers in saliva were lower compared to IMP181 (p=0.0011) after injection of 500 $TCID_{50}$, 5'dsIMP-mCherry did not reach a higher virus titer in saliva collected from mosquitoes injected with 250 $TCID_{50}$ compared to 5'dsMcM-mCherry at the same dose. Saliva virus titers for the 125 $TCID_{50}$ and 500 $TCID_{50}$ injected groups of the 5'dsIMP-mCherry and 5'dsMcM-mCherry mosquitoes were not significantly different as well

(Figure 3.10). *C. tarsalis* infected with 5'dsMcM-mCherry had similar virus titers in saliva when compared to McMillan infected *C. tarsalis* (Figure 3.9).

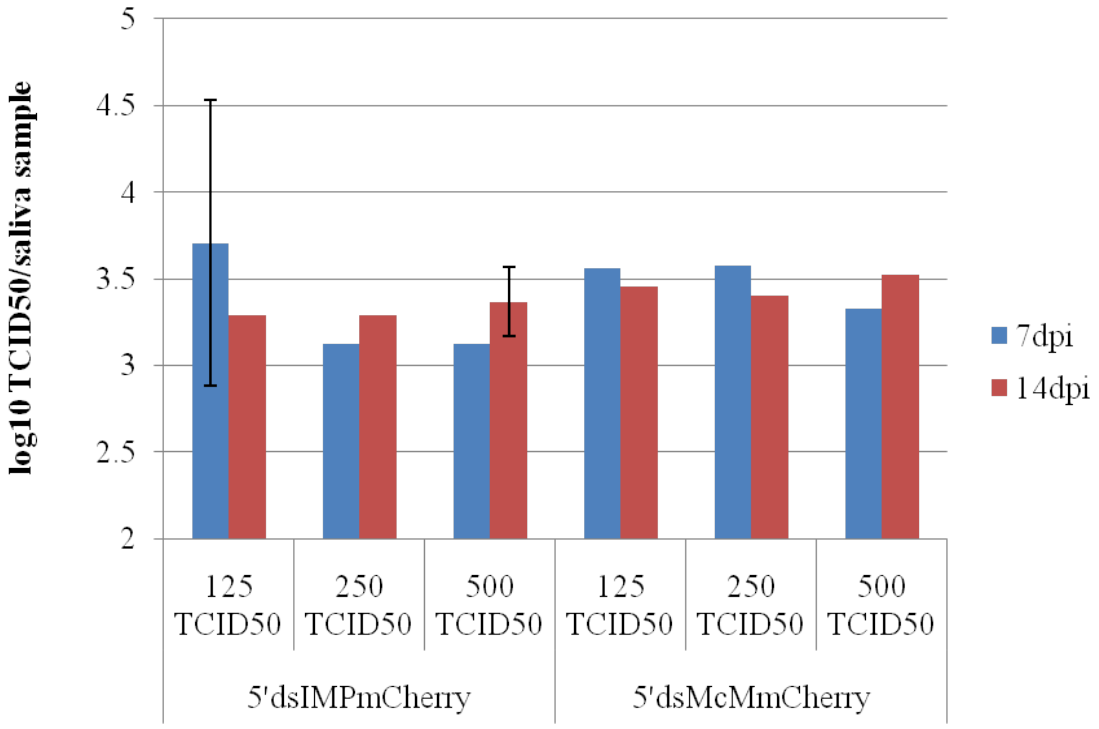

Figure 3.10 Saliva virus titers from intrathoracically injected *C. tarsalis*. Infectious virus titers of 5'dsMcM-mCherry and 5'dsIMP-mCherry in saliva collected from *C. tarsalis* 7 or 14 days after intrathoracic injection with 125, 250, or 500 $TCID_{50}$ of each virus. There was no significant difference in saliva virus titers between 5'dsMcM-mCherry and 5'dsIMP-mCherry infected mosquitoes.

Discussion

Fluorescent proteins (DsRed and mCherry) were expressed by 5'dsMcM-dsRed, 5'dsMcM-mCherry, and 5'dsIMP-mCherry viruses to investigate potential barriers to WEEV transmission in *C. tarsalis*. Epifluorescent microscopy is useful for providing rapid, qualitative evidence of virus infection in mosquito tissue that complements more quantitative methods such as plaque titration. In infected cell culture, DsRed and mCherry fluorescence was readily detected with all three viruses. Viral replication was slowed in BHK cells but not Vero or C6/36 cells with 5'dsMcM-dsRed compared to McMillan. Inclusion of the mCherry reporter did not

impair growth of 5'dsIMP-mCherry or 5'dsMcM-mCherry in Vero, BHK, or C6/36 cells. Brighter fluorescence was observed with mCherry expression in mosquitoes. Expression of fluorescence and infectious virus titration of midgut tissue confirmed the previously reported midgut infection barrier for the McMillan strain of WEEV in *C. tarsalis* (Kenney et al, 2010). As midgut infection can vary by mosquito strain, the susceptibility of the Bakersfield, CA strain of *C. tarsalis* to McMillan was determined before deciding to use intrathoracic injection.

DsRed expression by 5'dsMcM-dsRed demonstrated the utility of marker proteins for identifying arbovirus midgut infection, replication, and exit barriers in vectors. Virus infection was limited to 20% of *C. tarsalis* midguts that were exposed to an infectious bloodmeal. A midgut infection barrier was seen with 5'dsMcM-dsRed in terms of fluorescent marker expression and production of infectious virus. An escape barrier was demonstrated by failure to detect infectious virus from the legs or the heads of midgut-infected mosquitoes. Limited viral dissemination was seen in a small proportion of the heads of mosquitoes infected with either 5'dsMcM-mCherry or 5'dsMcM-dsRed.

Fluorescent microscopy was employed to examine the dissemination and salivary gland infection of *C. tarsalis* by McMillan and IMP181. The lack of resolution of the IVIS 200 camera and the need to inject each mosquito twice (once with virus, once with D-luciferin) made that approach inefficient for studying viral dissemination.

A salivary gland infection barrier was not seen with the *C. tarsalis* CA strain for McMillan or IMP181 after i.t. injection. Both 5'dsMcM-mCherry and 5'dsIMP-mCherry were able to infect *C. tarsalis* salivary glands and express a fluorescent reporter. Expression of mCherry fluorescent protein allowed for a clear demarcation of infected versus uninfected tissue. The ability to readily examine freshly dissected tissue without the fixing and staining steps

needed for IFA facilitated the study of salivary gland infection. Salivary gland infection was not shown to vary by dose, time, or strain of virus in this study. The salivary glands of the CA strain of *C. tarsalis* did not possess an infection barrier to McMillan or IMP181 derived viruses. The midgut played a major role in preventing transmission of WEEV, as the salivary glands of *C. tarsalis* CA strain appear to be permissive to invasion and replication by WEEV. Microscopy of salivary glands showed viral replication in cells adjacent to the duct responsible for carrying saliva to the proboscis. IFA detected viral antigen along the lining of the duct. An escape barrier was likely responsible for the lack of virus secreted in the saliva of infected mosquitoes as rates of transmission varied between 10-30% while salivary gland infection averaged around 80% for both strains of WEEV. Previous work (Kramer et al, 1998) identified a salivary gland barrier in a different strain of *C. tarsalis* that involved salivary gland infection (as identified by IFA) and lower replication of WEEV (Kramer et al, 1998). This work identified salivary gland exit barriers to WEEV in response to varied dosage and infection by IMP181 and McMillan. Time after infection (7 or 14 days post intrathoracic injection) was not shown to affect salivary gland infection, transmission rate in saliva, or amount of WEEV expectorated). This study discovered a mosquito-mediated salivary gland barrier that prevents both IMP181 and McMillan virus escape from the salivary glands into the saliva. Equal prevention of IMP181 or McMillan expectoration suggests that the CA strain of *C. tarsalis* possesses a barrier to WEEV transmission. The salivary gland escape barrier impeded infectious virus shedding into the saliva. While the proportion of infected mosquitoes expectorating virus was equal for IMP181 and McMillan, the amount of virus detected in saliva was significantly greater for IMP181, clone 40, and clone 42 virus infected mosquitoes. This implicates the McMillan structural proteins as being involved with decreased expectoration of infectious virus. IMP181-derived structural genes appeared to have a

dominant effect with regards to the phenotype of increased expectoraton of virus in saliva. Enhanced transmission (higher virus titers in saliva) was mediated by either the 5' or 3' section of the IMP181 genome 3' of the subgenomic promoter. Both sections were equally important to replication or egress in the salivary gland tissue of *C. tarsalis*.

The involvement of structural proteins in egress of WEEV into the saliva of *C. tarsalis* indicated that the receptor-binding, uncoating, encapsidation, or budding steps of infection were important for the McMillan-associated decline in expectorated virus. The equivalent ability of both IMP181 and McMillan derived viruses to infect the salivary glands suggested that the receptor binding or uncoating stages of infection were not significantly inhibited. Binding, uncoating, and initial production from the subgenomic promoter were inferred to occurr in the salivary glands due to the expression of mCherry fluorescent protein. IFA revealed the presence of WEEV E1 along the walls of the salivary gland duct for McMillan and IMP181 i.t. injected mosquitoes. As IFA is not quantitative, it is not possible to separate the roles of budding and encapsidation in determining the amount of WEEV egress in this study. Infectious virus titer in the saliva did not increase significantly with dose of 5'dsIMP-mCherry or 5'dsMcM-mCherry injected into the mosquito. This indicated that the limiting step for WEEV egress occurred within the salivary gland as the amount of WEEV in the hemocoel did not alter the amount of expectorated virus. The lack of significant difference with WEEV titer in the saliva indicated that the salivary gland barrier to expectorated WEEV was not dose dependent. Future studies using IFA with antibodies specific for different WEEV structural proteins and confocal microscopy could contribute enhanced visualization to the study of viral escape from infected salivary glands.

The hypothesis of higher rates of IMP181 transmission as a result of a salivary gland infection barrier to McMillan was not observed by these studies. Instead, evidence supported a salivary gland exit barrier to IMP181 and McMillan WEEV by *C. tarsalis* CA strain mosquitoes. Transmission rate was shown to be related to inoculation dosage in 5'dsMcM-mCherry as rates were higher in 500 $TCID_{50}$ injected mosquitoes compared to the lower dosages. Virus dose dependence was not observed with intrathoracic injection of 5'dsIMP-mCherry. Homogenous presentation of 5'dsIMP-mCherry transmission was possibly due to injection doses being higher than the minimum threshold for salivary gland infection, replication, or exit. Also, *C. tarsalis* has been shown to be more susceptible to IMP181 compared to McMillan in terms of midgut infection (Powers, unpublished data) and expectoration in saliva. As salivary gland infection rates for 5'dsIMP-mCherry and 5'dsMcM-mCherry were equivalent, the dose-dependence of 5'dsMcM-mCherry transmission rate was likely associated with a salivary gland replication or escape barrier.

This work demonstrated the importance of vector and pathogen mediated barriers to transmission, providing a system to determine which step is particular to each participant in transmission. Technologies such as viral reporter expression shed light on previous studies by allowing a more in-depth analysis of salivary gland infection, replication, and escape. IMP181 and McMillan strains of WEEV engineered to express mCherry were capable of infecting *C. tarsalis* midguts and salivary glands. Expression of mCherry fluorescent protein was maintained over the course of the study by both 5'dsMcM-mCherry and 5'dsIMP-mCherry viruses. Both were transmitted in the saliva of the natural vector at rates and virus titers comparable to the parent strains. An alphavirus expression system allowed imaging with both mCherry fluorescence and IFA. In the future, a strategy combining the utility of fluorescence in the

mosquito and *in vivo* imaging with luciferase in the vertebrate host will be ideal for conducting experiments involved with the initial transmission event. Shifting the genetic burden from virus to the host by engineering mosquito and mouse to express fluorescent and luminescent reporters in response to viral infection is one such approach. Using mosquitoes and mice engineered to express an ideal reporter in tandem with a virus that expresses an activator with a small insert size could also be used to investigate arbovirus transmission.

Chapter IV: Summary

Construction of double-subgenomic IMP181 and McMillan WEEV transducing systems allowed visualization of viral infection in both vertebrate and invertebrate hosts. Bioluminescence by 5'dsMcM-FLUC infected mice led to the first imaging of New World alphavirus infection over time in a single animal. Previous work described the action of neurovirulent SINV (Cook and Griffin, 2003). Introduction of FLUC into the genome of an alphavirus caused significant attenuation but still allowed for imaging the route of viral infection to CNS invasion (Cook and Griffin, 2003). In contrast to SINV, many strains of WEEV are naturally neurovirulent in mice without repeated passage and artificial selection affecting the validity of its use as a model. *In vivo* imaging pointed towards the direct invasion of the CNS by 5'dsMcM-FLUC after or during dissemination to lymph nodes, liver, and spleen following s.c. injection in accordance with previous work with McMillan (Logue et al, 2009). Neurovirulent SINV appears to enter the CNS subsequent to spinal cord involvement (Cook and Griffin, 2003). Intranasal inoculation of 5'dsMcM-FLUC resulted in imaging consistent with infection of the olfactory bulb and direct entry into the CNS without involvement of secondary organs. While internal truncation of the FLUC insert occurred in vitro and in vivo with 5'dsMcM-FLUC, it was sufficiently stable for *in vitro* experiments using a low passage and successful *in vivo* imaging in mice up to several days post infection.

Prior work (Logue et al, 2010) described the efficacy of CLDCs in preventing mortality from McMillan challenge in CD-1 mice. This study used 5'dsMcM-FLUC in a similar set of experiments highlighting the utility of *in vivo* imaging in rapidly screening for protection against

infection. At one day post infection, the prophylactic administration of CLRCs resulted in complete protection against 5'dsMcM-FLUC infection. This was reflected in a demarcation between groups as 5'dsMcM-FLUC infected, untreated animals expressed bioluminescence at the site of injection while CLRC treatment was associated with complete abrogation of bioluminescence. Images of 5'dsMcM-FLUC were consistent in presentation of luminescence at the site of injection in CLRC untreated animals one day post infection. CD-1 mice infected with 5'dsMcM-FLUC and treated with CLRCs were consistently absent bioluminescence throughout the 5 day period of imaging.

Epifluorescent imaging in mosquitoes of midgut infection, dissemination, and salivary gland infection using expression of mCherry indicated WEEV transmission barriers in *C. tarsalis*. Epifluorescent microscopy was used to investigate the hypothesis of a salivary gland infection barrier in *C. tarsalis* CA strain mosquitoes. Previous work (Kramer et al, 1998) showed a salivary gland infection and replication barrier in different strains of *C. tarsalis* after 14 days of infection. In that study, transmission was related to the rate of salivary gland infection. The CA strain used in this study showed no such barrier at either time (7 or 14 days). Intrathoracic injection resulted in 70-90% of mosquitoes having salivary gland infection. However, a significant salivary gland escape barrier was described in this study. *C. tarsalis* CA strain mosquitoes were refractory to IMP181 and McMillan release in saliva when measured by rates of expectoration. IMP181 was associated with higher virus titers in collected saliva. Concomitant with virus detection in the lining of the salivary duct, 1×10^3 $TCID_{50}$ of WEEV were released into the saliva. During dissection, virus present in the hemocoel or mosquito tissues can contaminate dissected organs and cause false positive results. The use of mCherry to identify

infected salivary glands avoids the issue of potential contamination with infectious alphaviral particles or RNA with plaque titration or RT-PCR as methods of detection.

This study demonstrated the power of the 5'dsWEEV ATS combined with *in vivo* fluorescent and bioluminescent imaging in investigating activity of IMP181 in the mosquito and McMillan in mosquitoes and mice. The salivary gland barriers to transmission of WEEV in *C. tarsalis* were described in greater detail than in previous work. Expression of fluorescence allowed rapid screening of dissected salivary glands compared to IFA. Imaging of 5'dsMcM-FLUC infection in CD-1 mice revealed disseminated bioluminescence 2 days after s.c. injection. Intranasal inoculation of CD-1 mice with 5'dsMcM-FLUC resulted in bioluminescence from the nares of infected animals and involvement of the CNS. The use of *in vivo* imaging showed promise in unveiling routes of virus dissemination and CNS invasion. *In vivo* imaging demonstrated great utility in screening potential antiviral compounds for efficacy during animal testing.

REFERENCES

Adamson, J.D. and Dubo, S. (1942). “Clinical Findings in Encephalitis (Western Equine).” *The Canadian Medical Association Journal.* 530-537.

Adelman, Z., Blair, C., Carlson, J., Beaty, B.J., and Olson, K.E. (2001). “Sindbis virus-induced silencing of dengue viruses in mosquitoes.” *Insect Molecular Biology.* 10: 265 - 273.

Agapov, E. V., Frolov, I., Lindenbach, B. D., Prágai, B. M., Schlesinger, S., and Rice, C. M. (1998). “Noncytopathic Sindbis virus RNA vectors for heterologous gene expression.” *Proceedings of the National Academy of Sciences of the United States of America, 95*(22), 12989-94.

Aguilar, M.J. (1970). **“**Pathological Changes in Brain and Other Target Organs of Infant and Weanling Mice After Infection with Non-Neuroadapted Western Equine Encephalitis Virus” *Infection and Immunity,* 2: 533-542.

Aguilar, P. V., Adams, A.P., Wang, E., Kang, W., Carrara, A., Anishchenko, M., Frolov, I., and Weaver, S.C. (2008). "Structural and nonstructural protein genome regions of eastern equine encephalitis virus are determinants of interferon sensitivity and murine virulence." *Journal of Virology*, 82(10): 4920-30.

Allison, A. B. and Stallknecht, D. E. (2009). “Genomic sequencing of Highlands J virus: a comparison to western and eastern equine encephalitis viruses.” *Virus research, 145*(2), 334-40.

Anderson, Brian A. (1984). “Focal Neurologic Signs in Western Equine Encephalitis.” *Canadian Medical Association Journal,* 130: 1019-1021.

Artsob, H. and Spence, L. (1979). Arctic and Tropical Arboviruses, pp. 39-65. New York: Academic Press.

Ayers, J. R., Lester, T.L., and Angulo, A-P.B. (1994). "An epizootic attributable to western equine encephalitis virus infection in emus in Texas." *Journal of the American Veterinary Medicine Association* 205(4): 600-1.

Barrett, A.D., and S. Higgs. (2007). “Yellow fever: a disease that has yet to be conquered.” *Annual Review of Entomology* 52: 209-29.

Beasley, D. W., Whiteman, M.C., Zhang S., Huang, C.Y.-H., Schneider, B.S., Smith, D.R., Gromowski, G.D., Higgs, S., Kinney, R.M., and Barrett, A.D. (2005). "Envelope protein glycosylation status influences mouse neuroinvasion phenotype of genetic lineage 1 West Nile virus strains." *Journal of Virology* 79(13): 8339-47.

Beaty, B. J. (2005). "Control of arbovirus diseases: is the vector the weak link?" *Archives of Virology Supplement* (19): 73-88.

Bellamy, R.E., Reeves W.C., and Scrivani, R.P. “Experimental cyclic transmission of Western equine encephalitis virus in chickens and Culex tarsalis through a year.” *American Journal of Epidemiology*, March 1967.

Bennett, K. E., Beaty, B.J., and Black, W.C. (2005). "Selection of D2S3, an Aedes aegypti (Diptera: Culicidae) strain with high oral susceptibility to Dengue 2 virus and D2MEB, a strain with a midgut barrier to Dengue 2 escape." *Journal of Medical Entomology* 42(2): 110-9.

Bianchi, T. I., Aviles, G., Monath, T.P., and Sabattini, M.S. (1993). "Western equine encephalomyelitis: virulence markers and their epidemiologic significance." *American Journal of Tropical Medicine and Hygiene* 49(3): 322-8.

Brault, A.C., Foy, B.D., Myles, K.M., Kelly, C.L.H., Higgs, S., Weaver, S.C., Olson, K.E., Miller, B.R., and Powers, A.M. (2004). “Infection patterns of o’nyong nyong virus in the malaria-transmitting mosquito, Anopheles gambiae.” *Insect Molecular Biology* 13(6): 625-35.

Brault, A. C., Powers, A.M., Ortiz, D., Estrada-Franco, J.G., Navarro-Lopez, R., Weaver, S.C., and Beaty, B.J. (2004). "Venezuelan equine encephalitis emergence: enhanced vector infection from a single amino acid substitution in the envelope glycoprotein." *Proceedings of the National Academy of Sciences of the United States of America* 101(31): 11344-9.

Burroughs, A. L. and R. N. Burroughs (1954). "A study of the ecology of western equine encephalomyelitis virus in the Upper Mississippi River Valley." *American Journal of Hygiene* 60(1): 27-36.

Burton, A. N., Connell, R., Rempel, J.G., and Gollop, J.B. (1961). "Studies on Western equine encephalitis associated with wild ducks in Saskatchewan." *Canadian Journal of Microbiology* 7: 295-302.

Burton, A. N., J. R. McLintock, and Rempel, J. (1966). "Western equine encephalitis in Saskatchewan birds and mammals 1962-1963." *Canadian Journal of Microbiology* 12(1): 133-41.

Burton, A. N. and J. McLintock (1970). "Further evidence of Western encephalitis infection in Saskatchewan mammals and birds and in reindeer in northern Canada." *Canadian Veterinary Journal* 11(11): 232-5.

Calisher, C.H. (1994). “Medically important arboviruses of the United States and Canada.” *Clinical Microbiology Reviews* 7(1): 89-116.

Calisher, C. H., Karabatsos, N., Lazuick, J.S., Monath, T.P., and Wolff, K.L. (1988). "Reevaluation of the western equine encephalitis antigenic complex of alphaviruses (family Togaviridae) as determined by neutralization tests." *American Journal of Tropical Medicine and Hygiene* 38(2): 447-52.

Calisher, C. H., Monath, T.P., Mitchell, C.J., Sabattini, M.S., Cropp, C.B., Kerschner J., Hunt, A.R., and Lazuick, J.S. (1985). "Arbovirus investigations in Argentina, 1977-1980. III. Identification and characterization of viruses isolated, including new subtypes of western and

Venezuelan equine encephalitis viruses and four new bunyaviruses (Las Maloyas, Resistencia, Barranqueras, and Antequera)." *American Journal of Tropical Medicine and Hygiene* 34(5): 956-65.

Campbell, C. L., Keene, K. M., Brackney, D. E., Olson, K. E., Blair, C. D., Wilusz, J., and Foy, B. D. (2008). "Aedes aegypti uses RNA interference in defense against Sindbis virus infection." *BMC Microbiology, 8*(47), 1471-2180.

Causey, O. R., Casals, J., Shope, R.E., and Udomsakdi, S. (1963). "Aura and Una, Two New Group a Arthropod-Borne Viruses." *American Journal of Tropical Medicine and Hygiene* 12: 777-81.

Centers for Disease Control and Prevention. "Epidemiologic Notes and Reports Western Equine Encephalitis -- United States and Canada, 1987." *MMWR* 36, 39 (1987): 655-659.

Centers for Disease Control and Prevention. "Summary of Notifiable Diseases, United States, 1995." *MMWR* 44, 53 (1996): 1-87.

Chamberlain, R.W. and Sudia, W.D. (1957). "Mechanism of Transmission of Viruses by Mosquitoes." *Annual Review of Entomology* 6, 371-390.

Chamberlain, R W, Sikes R.K., and Kissling, R.E. (1954) "Use of chicks in eastern and western equine encephalitis studies." *Journal of Immunology (Baltimore, Md.: 1950)* 73, 2: 106-14.

Chevillon, C., Briant, L., Renaud, F., and Devaux, C. (2008). "The Chikungunya threat: an ecological and evolutionary perspective." *Trends in Microbiology* 16(2): 80-8.

Cockburn, T. A., Sooter, C.A., and Langmuir, A.D. (1957). "Ecology of western equine and St. Louis encephalitis viruses; a summary of field investigations in Weld County, Colorado, 1949 to 1953." *American Journal of Hygiene* 65(2): 130-46.

Collins, W. E. (1963). "Studies on the transmission of Semliki Forest virus by anopheline mosquitoes." *American Journal of Hygiene* 77: 109-13.

Contag, C. H., Contag, P.R., Mullins, J.I., Spilman, S.D., Stevenson, D.K., and Benaron D.A., (1995). "Photonic detection of bacterial pathogens in living hosts." *Molecular Microbiology* 18: 593–603.

Contag, C. H., Spilman, S.D., Contag, P.R., Oshiro, M., Eames, B., Dennery, P., Stevenson, D.K., and Benaron, D.A. (1997). "Visualizing gene expression in living mammals using a bioluminescent reporter." *Photochemical Photobiology* 66: 523–531.

Contag, C. H., Jenkins, D., Contag, P.R., and Negrin, R.S. (2000). "Use of reporter genes for optical measurements of neoplastic disease in vivo." *Neoplasia* 2: 41–52.

Cook, S. H. and D. E. Griffin (2003). "Luciferase imaging of a neurotropic viral infection in intact animals." *Journal of Virology* **77**(9): 5333-8.

Cooper, L. A., Sina, B.J., Turell, M.J., and Scott, T.W. (2000). "Effects of initial dose on eastern equine encephalomyelitis virus dependent mortality in intrathoracically inoculated Culiseta melanura (Diptera: Culicidae)." *Journal of Medical Entomology* 37(6): 815-9.

Danes, L., Rychterová, V., Kufner J., and Hrusková, J. (1973). “The role of the olfactory route on infection of the respiratory tract with Venezuelan equine encephalomyelitis virus in normal and operated Macaca rhesus monkeys. II. Results of histological examination.” *Acta virologica*, .

Danes, L., Rychterová, V., Kliment, V., and Hrusková, J. (1973, March). “Penetration of Venezuelan equine encephalomyelitis virus into the brain of guinea pigs and rabbits after intranasal infection.” *Acta virologica*.

Davidson, R.O. (1942). *Canadian Public Health Journal* 33: 388-398.

Davis, N. L., Willis, L.V., Smith, J.F., and Johnston, R.E. (1989). "In vitro synthesis of infectious venezuelan equine encephalitis virus RNA from a cDNA clone: analysis of a viable deletion mutant." *Virology* 171(1): 189-204.

de Groot, R. J., Hardy, W.R., Shirako, Y., and Strauss, J.H. (1990). "Cleavage-site preferences of Sindbis virus polyproteins containing the non-structural proteinase. Evidence for temporal regulation of polyprotein processing in vivo." *EMBO Journal* 9(8): 2631-8.

de la Monte, S., Castro, F., Bonilla, N.J., de Urdaneta, A.G., and Hutchins, G.M. (1985). "The systemic pathology of Venezuelan equine encephalitis virus infection in humans." *American Journal of Tropical Medicine and Hygiene* 34(1): 194-202.

de Lara Capurro, M., Coleman, J., Beernsten, B.T., Myles, K.M., Olson, K.E., Rocha, E., Krettli, A.U., and James, A.A. (2000). "Virus-expressed, recombinant single-chain antibody blocks sporozoite infection of salivary glands in Plasmodium gallinaceum-infected Aedes aegypti." *American Journal of Tropical Medicine and Hygiene* 62(4): 427-33.

Deresiewicz, R. L., Thaler, S.J., Hsu, L., and Zamani, A.A. (1997). "Clinical and neuroradiographic manifestations of eastern equine encephalitis." *New England Journal of Medicine* 336(26): 1867-74.

Devine, T. L., Venard, C.E., and Myser, W.C. (1965). "Measurement of Salivation by Aedes Aegypti (L.) Feeding on a Living Host." *Journal of Insect Physiology* 11: 347-53.

Diebold, S. S., Kaisho, T., Hemmi, H., Akira, S., and Reis, E.S.C. (2004). "Innate antiviral responses by means of TLR7-mediated recognition of single-stranded RNA." *Science* 303(5663): 1529-31.

Donnelly, S. M., Sheahan, B.J., and Atkins, G.J. (1997). "Long-term effects of Semliki Forest virus infection in the mouse central nervous system." *Neuropathology and Applied Neurobiology* 23(3): 235-41.

Donovan, C.R. and Bowman, M. (1942). “Epidemiology of encephalitis: western equine type, Manitoba, 1941.” *Canadian Medical Association Journal* 46:6 525-530.

Earnest, M.P., Goolishian, H.A., Calverly, J.R., Hayes, R.O., and Hill, H.R. (1971). “Neurologic, intellectual, and psychologic sequelae following western encephalitis. A follow-up study of 39 cases.” *Neurology* 21, 969-974.

Fang, Y., Brault A.C., and Reisen, W.K. (2009) “Short Report: Comparative Thermostability of West Nile , St . Louis Encephalitis , and Western Equine Encephalomyelitis Viruses during Heat Inactivation for Serologic Diagnostics.” *Tropical Medicine* 80 (5): 862-863.

Fazakerley, J. K., Cotterill, C.L., Lee, G., and Graham, A. (2006). "Virus tropism, distribution, persistence and pathology in the corpus callosum of the Semliki Forest virus-infected mouse brain: a novel system to study virus-oligodendrocyte interactions." *Neuropathology and Applied Neurobiology* 32(4): 397-409.

Ferreira, D. (2003). “Morphological variants of sindbis virus produced by a mutation in the capsid protein.” *Virology* 307(1): 54-66.

Andrew F.E., Chung B.Y., Fleeton M.N., and Atkins, J.F. (2008). “Discovery of frameshifting in Alphavirus 6K resolves a 20-year enigma.” *Virology Journal* 5: 108.

Forrester, N. L., Kenney J.L., Deardorff, E., Wang, E., and Weaver, S.C. (2008). "Western Equine Encephalitis submergence: lack of evidence for a decline in virus virulence." *Virology* 380(2): 170-2.

Foti, M., Granucci, F., and Ricciardi-Castagnoli, P.A., (2004). "A central role for tissue-resident dendritic cells in innate responses." *Trends in Immunology* 25(12): 650-4.

Foy, B. D., Myles, K.M., Pierro, D.J., Sanchez-Vargas, I., Uhlirova, M., Jindra, M., Beaty, B.J., and Olson, K.E. (2004). "Development of a new Sindbis virus transducing system and its characterization in three Culicine mosquitoes and two Lepidopteran species." *Insect Molecular Biology* 13(1): 89-100.

Foy, B. D. and Olson, K.E. (2008). "Alphavirus transducing systems." *Advanced Experimental Medical Biology* 627:19-34.

Franz, A. W., Sanchez-Vargas, I., Adelman, Z.N., Blair, C.D., Beaty, B.J., James, A.A., and Olson, K.E. (2006). "Engineering RNA interference-based resistance to dengue virus type 2 in genetically modified Aedes aegypti." *Proceedings of the National Academy of Sciences of the United States of America* 103(11): 4198-203.

Frolov, I., Hoffman, T.A., Pragai, B.M., Dryga, S.A., Huang, H.V., Schlesinger, S., and Rice, C.M. (1996). "Alphavirus-based expression vectors: strategies and applications." *Proceedings of the National Academy of Sciences of the United States of America* 93(21): 11371-7.

Frolov, I., Hardy, R., and Rice, C.M. (2001). "Cis-acting RNA elements at the 5' end of Sindbis virus genome RNA regulate minus- and plus-strand RNA synthesis." *RNA* **7**(11): 1638-51.

Fulhorst, C. F., Hardy, J.L., Eldridge B.F., Presser S.B., and Reeves W.C. (1994). "Natural vertical transmission of western equine encephalomyelitis virus in mosquitoes." *Science* 263(5147): 676-8.

Fulton, J.S. and Burton, A.N. (1953) “After Effects of Western Equine Encephalomyelitis in Man.” *Canadian Medical Association Journal* 69: 268-272.

Gaines, P. J., Olson, K.E., Higgs, S., Powers, A.M., Beaty, B.J., and Blair, C.D. (1996). "Pathogen-derived resistance to dengue type 2 virus in mosquito cells by expression of the premembrane coding region of the viral genome." *Journal of Virology* 70(4): 2132-7.

Gardner, C. L., Burke, C.W., Tesfay, M.Z., Glass, P.J., Klimstra, W.B., and Ryman, K.D. (2008). "Eastern and Venezuelan equine encephalitis viruses differ in their ability to infect dendritic cells and macrophages: impact of altered cell tropism on pathogenesis." *Journal of Virology* 82(21): 10634-46.

Garmashova, N., Gorchakov, R., Frolova, E., and Frolov, I. (2006). "Sindbis virus nonstructural protein nsP2 is cytotoxic and inhibits cellular transcription." *Journal of Virology* 80(12): 5686-96.

Garmashova, N., Gorchakov, R., Vokova, E., Paessler, S., Frolova, E., and Frolov, I. (2007). "The Old World and New World alphaviruses use different virus-specific proteins for induction of transcriptional shutoff." *Journal of Virology* 81(5): 2472-84.

Gauzzi, M.C., Del Corno, M., and Gessani, S. (2010). “Dissecting TLR3 signalling in dendritic cells.” *Immunobiology* 215: 713–723.

Geigenmuller-Gnirke, U., Weiss, B., Wright, R., and Schlesinger, S. (1991). "Complementation between Sindbis viral RNAs produces infectious particles with a bipartite genome." *Proceedings of the National Academy of Sciences of the United States of America* 88(8): 3253-7.

Gerhardt, R. (2006). "West Nile virus in the United States (1999-2005)." *Journal of the American Animal Hospital Association* 42(3): 170-7.

Grieder, F. B. and H. T. Nguyen (1996). "Virulent and attenuated mutant Venezuelan equine encephalitis virus show marked differences in replication in infection in murine macrophages." *Microbial Pathogenesis* 21(2): 85-95.

Greene, I. P., Lee, E.-young, Prow, N., Ngwang, B., and Griffin, D. E. (2008). “Protection from fatal viral encephalomyelitis : AMPA receptor antagonists have a direct effect on the inflammatory response to infection.” *Proceedings of the National Academy of Sciences of the United States of America 105*(9), 3575-3580.

Giltner, L.T. and M.S. Shahan. (1933). “Transmission of Infectious Equine Encephalomyelitis in Mammals and Birds.” *Science* 78: 63-64.

Giltner, L. T. and M. S. Shahan. (1933). "The Immunological Relationship of Eastern and Western Strains of Equine Encephalomyelitis Virus." *Science* 78(2034): 587-588.

Griffin, D. E. (1989). "Molecular pathogenesis of Sindbis virus encephalitis in experimental animals." *Advanced Virus Research* 36: 255-71.

Griffin, D. E. (2005). "Neuronal cell death in alphavirus encephalomyelitis." Curr Top Microbiol *Immunology* 289: 57-77.

Hahn, C. S., Lustig S., Strauss, E.G., and Strauss, J.H. (1988). "Western equine encephalitis virus is a recombinant virus." *Proceedings of the National Academy of Sciences of the United States of America* 85(16): 5997-6001.

Hahn, C. S., Hahn, Y.S., Braciale, T.J., and Rice, C.M. (1992). "Infectious Sindbis virus transient expression vectors for studying antigen processing and presentation." *Proceedings of the National Academy of Sciences of the United States of America* 89(7): 2679-83.

Hammon, W. M., Reeves, W.C., Brookman, B., Izumi, E.M., and Gjullin, C.M. (1941). "Isolation of the Viruses of Western Equine and St. Louis Encephalitis from Culex Tarsalis Mosquitoes." *Science* 94(2440): 328-330.

Hammon, W.M. (1942). “Summary of case against Culex tarsalis Coquillett as a vector of the St Louis and western equine viruses.” *Journal of Infectious Diseases* 70: 278.

Hammon, W.M. and Howitt, B.F. (1942) “Epidemiological aspects of encephalitis in the Yakima Valley, Washington: mixed St Louis and western equine types.” *American Journal of Hygiene* 35: 163.

Hammon, W. M., Reeves, W.C., Benner, S.R., and Brookman, B. (1945). “Human encephalitis in the Yakima Valley, Washington, 1942 with 49 virus isolations (western equine and St. Louis types) from mosquitoes.” *Journal of the American Medical Association* 128(16): 1133-1139.

Hardy, J.L., Reeves, W.C., Bruien, J.P., and Presser, S.B. (1979). “Vector competence of Culex tarsalis and other mosquito species for western equine encephalitis virus.” *Arctic and Tropical Arboviruses*. Academic Press, New York. 157-171.

Hardy, J.L., Houk, E., and Kramer, L.D. (1983). “Intrinsic factors affecting vector competence of mosquitoes for arboviruses.” *Environmental Health* 28: 229-262.

Hardy, J. L. (1987). "The ecology of western equine encephalomyelitis virus in the Central Valley of California, 1945-1985." *American Journal of Tropical Medicine and Hygiene* 37(3 Suppl): 18S-32S.

Hayes, R. O., LaMotte, L.C., and Holden, P. (1967). "Ecology of arboviruses in Hale County, Texas, during 1965." *American Journal of Tropical Medicine and Hygiene* 16(5): 675-87.

Hayes, C. G. and R. C. Wallis (1977). "Ecology of Western equine encephalomyelitis in the eastern United States." *Advances in Virus Research* 21: 37-83.

Hayes, C. G. (1978). “Variations in biological properties of geographic strains of western equine encephalomyelitis virus before and after passage in Culex tarsalis and Culiseta melanura.” *Acta virologica*. 22(5):401-9.

Heil, F., Hemmi, H., Hochrein, H., Ampenberger, F., Kirschning, C., Akira, S., Lipford, G., Wagner, H., and Bauer, S. (2004). "Species-specific recognition of single-stranded RNA via toll-like receptor 7 and 8." *Science* 303(5663): 1526-9.

Heikkila¨ J.E., Va¨ha¨-Koskela M.J.V., Ruotsalainen J.J., Martikainen M.W., Stanford M.M., McCart, J.A., Bell, J.C., and Hinkkanen, A.E. (2010). “Intravenously Administered Alphavirus Vector VA7 Eradicates Orthotopic Human Glioma Xenografts in Nude Mice.” *PLoS ONE* 5(1): e8603.

Heise, M. T., Simpson, D.A., and Johnston, R.E. (2000). "Sindbis-group alphavirus replication in periosteum and endosteum of long bones in adult mice." *Journal of Virology* 74(19): 9294-9.

Hemingway, J., Field, L., and Vontas, J. (2002). “An overview of insecticide resistance.” *Science (New York, N.Y.), 298*(5591): 96-7.

Higgs, S., Olson, K.E., Klimowski, L., Powers, A.M., Carlson, J.O., Possee, R.D., and Beaty, B.J. (1995). "Mosquito sensitivity to a scorpion neurotoxin expressed using an infectious Sindbis virus vector." *Insect Molecular Biology* 4(2): 97-103.

Higgs, S., Rayner, J.O., Olson, K.E., Davis, B.S., Beaty, B.J., and Blair, C.D. (1998). "Engineered resistance in Aedes aegypti to a West African and a South American strain of yellow fever virus." *American Journal of Tropical Medicine and Hygiene* 58(5): 663-70.

Hoff, G. L., Yuill, T.M., Iversen, J.O., and Hanson, R.P. (1970). "Selected microbial agents in snowshoe hares and other vertebrates of Alberta." *Journal of Wildlife Disease* 6(4): 472-8.

Hollidge, B. S., González-Scarano, F., and Soldan, S. S. (2010). “Arboviral encephalitides: transmission, emergence, and pathogenesis.” *Journal of neuroimmune pharmacology : the official journal of the Society on NeuroImmune Pharmacology*, *5*(3), 428-42.

Houk, E.J., Kramer, L.D., Hardy, J.L., and Chiles, R.E. (1985). “Western equine encephalomyelitis virus: in vivo infection and morphogenesis in mosquito mesenteronal epithelial cells.” *Virus Research* 2(2): 123-38.

Howitt, B.F. (1932). “Equine encephalomyelitis.” *Journal of Infectious Diseases* 51**:** 493

Hurlbut, H. S. (1966). "Mosquito salivation and virus transmission." *American Journal Tropical Medicine and Hygiene* 15(6): 989-93.

Hurst, E.W. (1934). “The histology of equine encephalomyelitis” *Journal of Experimental Medicine* 59: 529-546.

Hurst, E. W. (1936). “Infection of the rhesus monkey (Macaca mulatta) and the guinea-pig with the virus of equine encephalomyelitis.” *The Journal of Pathology and Bacteriology*, *42*(1), 271-302.

Jackson, A.C., Moench, T.R., Griffin, D.E., and Johnson, R.T. (1988). "The pathogenesis of spinal cord involvement in the encephalomyelitis of mice caused by neuroadapted Sindbis virus infection." *Laboratory Investigations* 56(4): 418-23.

Jackson, F.W. (1942). *Canadian Medical Association Journal* 47: 364-365.

Jelinkova, A., Danes, L., and Novak, M. (1974). “Electron microscopic demonstration of venezuelan equine encephalomyelitis in the olfactory bulb and tract of experimentally infected monkeys.” *Acta virologica*, *18*(2), 154-157.

Johnson, B. W., Olson, K.E., Allen-Miura, T., Rayms-Keller, A., Carlson, J.O., Coates, C.J., Jasinskiene, N., James, A.A., Beaty, B.J., and Higgs, S. (1999). "Inhibition of luciferase expression in transgenic Aedes aegypti mosquitoes by Sindbis virus expression of antisense luciferase RNA." *Proceedings of the National Academy of Sciences of the United States of America* 96(23): 13399-403.

Julander, J.G., Siddharthan, V., Blatt, L.M., Schafer, K., Sidwell, R.W., and Morrey, J.D., (2007). “Effect of exogenous interferon and an interferon inducer on western equine encephalitis virus disease in a hamster model.” *Virology* 360, 454–460.

Kaariainen, L. and T. Ahola (2002). "Functions of alphavirus nonstructural proteins in RNA replication." *Progress in Nucleic Acid Research and Molecular Biology Journal* 71: 187-222.

Kamrud, K. I., Olson, K.E., Higgs, S., Powers, A.M., Carlson, J.O., and Beaty, B.J. (1997). "Detection of expressed chloramphenicol acetyltransferase in the saliva of Culex pipiens mosquitoes." *Insect Biochemistry and Molecular Biology* 27(5): 423-9.

Karpf, A. R. and Brown, D.T. (1998). "Comparison of Sindbis virus-induced pathology in mosquito and vertebrate cell cultures." *Virology* 240(2): 193-201

Kawai, T. and S. Akira (2006). "Role of IPS-1 in type I IFN induction." *Nippon Rinsho* 64(7): 1231-5.

Keene, K. M., Foy, B.D., Sanchez-Vargas, I., Beaty, B.J., Blair, C.D., and Olson, K.E. (2004). "RNA interference acts as a natural antiviral response to O'nyong-nyong virus (Alphavirus; Togaviridae) infection of Anopheles gambiae." *Proceedings of the National Academy of Sciences of the United States of America* 101(49): 17240-5.

Kenney, J.L., Adams, A.P., and Weaver, S.C., (2010). “Transmission Potential of Two Chimeric Western Equine Encephalitis Vaccine Candidates in *Culex tarsalis*.” *American Journal of Tropical Medicine and Hygiene* 82: 354-359.

Kerr, J. F., Wyllie, A.H., and Currie, A.R. (1972). “Apoptosis: a basic biological phenomenon with wide-ranging implications in tissue kinetics.” *British Journal of Cancer* 26(4): 239-57.

Kiiver, K., Merits, A., and Sarand, I. (2008). "Novel vectors expressing anti-apoptotic protein Bcl-2 to study cell death in Semliki Forest virus-infected cells." *Virus Research* 131(1): 54-64.

Kramer, L. D., Hardy, J. L., Presser, S. B., and Houk, E. J. (1981). "Dissemination barriers for western equine encephalomyelitis virus in Culex tarsalis infected after ingestion of low viral doses. *The American journal of tropical medicine and hygiene*." *30*(1), 190-7.

Kramer, L. D., Hardy, J. L., and Presser, S. B. (1998). "Characterization of modulation of western equine encephalomyelitis virus by Culex tarsalis (Diptera: Culicidae) maintained at 32 degrees C following parenteral infection." *Journal of medical entomology*, *35*(3), 289-95.

Kramer, L. D. and H. M. Fallah (1999). "Genetic variation among isolates of western equine encephalomyelitis virus from California." *American Journal of Tropical Medicine and Hygiene* 60(4): 708-13.

Krug, A., Luker, G.D., Barchet, W., Leib, D.A., Akira, S., and Colonna, M. (2004). "Herpes simplex virus type 1 activates murine natural interferon-producing cells through toll-like receptor 9." *Blood* 103(4): 1433-7.

Kuhn, R. J., Niesters, H.G., Hong, Z., and Strauss, J.H. (1991). "Infectious RNA transcripts from Ross River virus cDNA clones and the construction and characterization of defined chimeras with Sindbis virus." *Virology* 182(2): 430-41.

Lamotte, L. C., Jr. (1960). "Japanese B encephalitis virus in the organs of infected mosquitoes." *American Journal of Hygiene* 72: 73-87.

LaStarza, M.W., Lemm, J.A., and Rice, C.M. (1994). "Genetic analysis of the nsP3 region of Sindbis virus: evidence for roles in minus-strand and subgenomic RNA synthesis." *Journal of Virology* 68(9): 5781-91.

Lee, J. H., Rowley, W.A., and Platt, K.B. (2000). "Longevity and spontaneous flight activity of Culex tarsalis (Diptera: Culicidae) infected with western equine encephalomyelitis virus." *Journal of Medical Entomology* 37(1): 187-93.

Lehane, M. J. (1997). "Peritrophic matrix structure and function." *Annual Review of Entomology* 42: 525-50.

Lemm, J. A., Rumenapf, T., Strauss, E.G., Strauss, J.H., Rice, C.M. (1994). "Polypeptide requirements for assembly of functional Sindbis virus replication complexes: a model for the temporal regulation of minus- and plus-strand RNA synthesis." *EMBO Journal* 13(12): 2925-34.

Leung, M. K., Burton, A., Iversen, J., and McLintok, J. (1975). "Natural infections of Richardson's ground squirrels with western equine encephalomyelitis virus, Saskatchewan, Canada, 1964-1973." *Canadian Journal of Microbiology* 21(7): 954-8.

Levine, B. and D. E. Griffin (1992). "Persistence of viral RNA in mouse brains after recovery from acute alphavirus encephalitis." *Journal of Virology* 66(11): 6429-35.

Levis, R., Weiss, B.G., Tsiang, M., Huang, H., and Schlesinger, S. (1986). "Deletion mapping of Sindbis virus DI RNAs derived from cDNAs defines the sequences essential for replication and packaging." *Cell* 44(1): 137-45.

Levis, R., Huang, H., and Schlesinger, S. (1987). "Engineered defective interfering RNAs of Sindbis virus express bacterial chloramphenicol acetyltransferase in avian cells." *Proceedings of the National Academy of Sciences of the United States of America* 84(14): 4811-5.

Levis, R., Schlesinger, S., and Huang, H.V. (1990). "Promoter for Sindbis virus RNA-dependent subgenomic RNA transcription." *Journal of Virology* 64(4): 1726-33.

Long, L., Jose, J., Xiang, Y., Kuhn, R.J., and Rossmann, M.G. (2010). “Structural changes of envelope proteins during alphavirus fusion.” *Nature* 468(7324): 705-708.

Liang, X. H., Kleeman, L.K., Jiang, H.H., Gordon, G., Goldman, J.E., Berry, G., Herman, B., and Levine, B. (1998). "Protection against fatal Sindbis virus encephalitis by beclin, a novel Bcl-2-interacting protein." *Journal of Virology* 72(11): 8586-96.

Lidbury, B. A., Simeonovic, C., Maxwell, G.E., Marshall, I.D., and Hapel, A.J. (2000). "Macrophage-induced muscle pathology results in morbidity and mortality for Ross River virus-infected mice." *Journal of Infectious Disease* 181(1): 27-34.

Li, L., Jose, J., Xiang, Y., Kuhn, R. J., and Rossmann, M. G. (2010). “Structural changes of envelope proteins during alphavirus fusion.” *Nature*, *468*(7324), 705-708. Nature Publishing Group.

Liu, C., Voth, D.W., Rodina, P., Shauf, L.R., and Gonzalez, G. (1970). “A comparative study of the pathogenesis of western equine and eastern equine encephalomyelitis viral infections in mice by intracerebral and subcutaneous inoculations.” *Journal of Infectious Disease* 122: 53–63.

Logue, C. H., Sheahan, B.J., and Atkins, G.J. (2008). "The 5' untranslated region as a pathogenicity determinant of Semliki Forest virus in mice." *Virus Genes* 36(2): 313-21.

Logue, C.H., Bosio, C.F., Welte, T., Keene, K.M., Ledermann, J.P., Phillips, A., Sheahan, B.J., Pierro, D.J., Marlenee, N., Brault, A.C., Bosio, C.M., Singh, A.J., Powers, A.M., and Olson, K.E., (2009). “Virulence variation among isolates of western equine encephalitis virus in an outbred mouse model.” *Journal of General Virology* 90: 1848-1858.

Logue, C.H., Phillips, A.T., Mossel, E.C., Ledermann, J.P., Welte, T., Dow, S.W., Olson, K.E., and Powers, A.M. (2010). “Treatment with cationic liposome-DNA complexes (CLDCs) protects mice from lethal Western equine encephalitis virus (WEEV) challenge.” *Antiviral Research* 87, 195–203.

Luby, J.P., Sanders, C.V., and Sulkin, E. (1971). “Interferon Assays and Quantitative Virus Determinations in a Fatal Infection In Man with Western Equine Encephalomyelitis Virus*.” *In Vitro* 20(5): 765-769.

Luker, G.D., Bardill, J.P., Prior, J.L., Pica, C.M., Piwnica-Worms, D., and Leib, D.A. (2002). “Noninvasive bioluminescence imaging of herpes simplex virus type 1 infection and therapy in living mice.” *Journal of Virology* 76: 12149–12161.

Lustig, S., Jackson, A.C., Hahn, C.S., Griffin, D.E., Strauss, E.G., and Strauss, J.H. (1988). "Molecular basis of Sindbis virus neurovirulence in mice." *Journal of Virology* 62(7): 2329-36.

MacDonald, G. H. and Johnston, R.E. (2000). "Role of dendritic cell targeting in Venezuelan equine encephalitis virus pathogenesis." *Journal of Virology* 74(2): 914-22.

Marquardt, W.C., Black, W.C. IV, Freier, J.E., Hagedorn, H.H., Hemingway, J., Higgs, S., James, A.A., Kondratieff, B., and Moore, C. G. (2005). *Biology of Disease Vectors* (2nd ed., p. 785). Elsevier Inc.

Matsumoto, M. and Seya, T. (2008). “TLR3: interferon induction by double-stranded RNA including poly(I:C).” *Advanced Drug Delivery Reviews* 60: 805–812.

McGugan, A.C. (1942). *Canadian Public Health Journal* 33: 148-151

Meyer, K. F., Haring, C.M., and Howitt, B. (1931). "The Etiology of Epizootic Encephalomyelitis of Horses in the San Joaquin Valley, 1930." *Science* 74: 227-228.

Monroe, S. S., Ou, J.H., Rice, C.M., Schlesinger, S., Strauss, E.G., and Strauss, J.H. (1982). "Sequence analysis of cDNA's derived from the RNA of Sindbis virions and of defective interfering particles." *Journal of Virology* 41(1): 153-62.

Monroe, S. S. and Schlesinger, S. (1983). "RNAs from two independently isolated defective interfering particles of Sindbis virus contain a cellular tRNA sequence at their 5' ends." *Proceedings of the National Academy of Sciences of the United States of America* 80(11): 3279-83.

Moore, A. T., Edwards, E.A., Brown, M.B., Komar, N., and Brown, C.R. (2007). "Ecological correlates of buggy creek virus infection in Oeciacus vicarius, southwestern Nebraska, 2004." *Journal of Medical Entomology* 44(1): 42-9.

Morgante, O., Barager E.M., and Herbert F.A. (1968). “Central nervous system disease in humans due to simultaneous epidemics of echovirus type 9 and western encephalomyelitis virus infection in Alberta.” *Canadian Medical Association Journal* 98(25): 1170-5.

Murray, K. O., Walker, C., and Gould, E. (2011). The virology, epidemiology, and clinical impact of West Nile virus: a decade of advancements in research since its introduction into the Western Hemisphere. *Epidemiology and infection*, *139*(6), 807-17.

Nagata, L. P., Hu, W.G., Parker, M., Chau, D., Rayner, G.A., Schmaltz, F.L., and Wong, J.P. (2006). "Infectivity variation and genetic diversity among strains of Western equine encephalitis virus." *Journal of General Virology* 87(8): 2353-61.

Niklasson, B., Espmark, A., and Lundstrom, J. (1988). "Occurrence of arthralgia and specific IgM antibodies three to four years after Ockelbo disease." *Journal of Infectious Disease* 157(4): 832-5.

Olson, J.G., Reeves W.C., Emmons, R.W., and Milby, M.M. (1979). “Correlation of *Culex tarsalis* population indices with the incidence of St. Louis encephalitis and western equine encephalomyelitis in California.” *Medicine* 28(2): 335-343.

Olson, K. E., Higgs, S., Gaines, P.J., Powers, A.M., Davis, B.S., Kamrud, K.I., Carlson, J.O., Blair, C.D., and Beaty, B.J. (1996). "Genetically engineered resistance to dengue-2 virus transmission in mosquitoes." *Science* 272(5263): 884-6.

Olson, K. E., Myles, K.M., Seabaugh, R.C., Higgs, S., Carlson, J.O., and Beaty, B.J. (2000). "Development of a Sindbis virus expression system that efficiently expresses green fluorescent protein in midguts of Aedes aegypti following per os infection." *Insect Molecular Biology* 9(1): 57-65.

Orvedahl, A. and Levine, B. (2008). "Autophagy and viral neurovirulence." *Cellular Microbiology* 10(9): 1747-56.

Ou, J. H., Strauss, E.G., and Strauss, J.H. (1983). "The 5'-terminal sequences of the genomic RNAs of several alphaviruses." *Journal of Molecular Biology* 168(1): 1-15.

Parikh, G.R., Oliver, J.D., and Bartholomay, L.C. (2009). “A haemocyte tropism for an arbovirus.” *Journal of General Virology* 90: 292-296.

Paredes, A., Weaver, S.C., Watowich, S., and Chiu, W. (2005). "Structural biology of old world and new world alphaviruses." *Archives of Virology Supplemental* (19): 179-85.

Peranen, J., Rikkonen, M., Liljestrom, and Kaariainen, L. (1990). "Nuclear localization of Semliki Forest virus-specific nonstructural protein nsP2." *Journal of Virology* 64(5): 1888-96.

Paulson, S. L. and Grimstad, P.R. (1989). "Replication and dissemination of La Crosse virus in the competent vector Aedes triseriatus and the incompetent vector Aedes hendersoni and evidence for transovarial transmission by Aedes hendersoni (Diptera: Culicidae)." *Journal of Medical Entomology* 26(6): 602-9.

Petrakova, O., Volkova, E., Gorchakov, R., Paessler, S., Kinney, R.M., and Frolov, I. (2005). "Noncytopathic replication of Venezuelan equine encephalitis virus and eastern equine encephalitis virus replicons in mammalian cells." *Journal of Virology* 79(12): 7597-608.

Pialoux, G., Gauzere, B.A., Jaureguiberry, S., and Strobel, M. (2007). "Chikungunya, an epidemic arbovirosis." *Lancet Infectious Diseases* 7(5): 319-27.

Pierro, D. J., Myles, K.M., Foy, B.D., Beaty, B.J., and Olson, K.E. (2003). "Development of an orally infectious Sindbis virus transducing system that efficiently disseminates and expresses green fluorescent protein in Aedes aegypti." *Insect Molecular Biology* 12(2): 107-16.

Pohl, C., Shishkova, J., and Schneider-Schaulies, S.. (2007). "Viruses and dendritic cells: enemy mine." *Cellular Microbiology* 9(2): 279-89.

Potter, M.E, Currier, R.W., Pearson, J.E., Harris, J.C., and Parker, R.L. (1977). "Western equine encephalomyelitis in horses in the Northern Red River Valley, 1975." *Journal of the American Veterinary Medical Association* 170(12): 1396-9

Powers, A. M., Kamrud, K.I., Olson, K.E., Higgs, S., Carlson, J.O., and Beaty, B.J. (1996). "Molecularly engineered resistance to California serogroup virus replication in mosquito cells and mosquitoes." *Proceedings of the National Academy of Sciences of the United States of America* 93(9): 4187-91.

Powers, A. M., Brault, A.C., Shirako, Y., Strauss, E.G., Kang, W., Strauss, J.H., and Weaver, S.C. (2001). "Evolutionary relationships and systematics of the alphaviruses." *Journal of Virology* 75(21): 10118-31.

Pudney, M., Leake, C. J., and Varma, M.G.R. (1979). Arctic and Tropical Arboviruses, pp. 245-262. New York: Academic Press.

Racaniello, V. R. and Baltimore, D. (1981). "Cloned poliovirus complementary DNA is infectious in mammalian cells." *Science* 214(4523): 916-9.

Raju, R. and Huang, H.V. (1991). "Analysis of Sindbis virus promoter recognition in vivo, using novel vectors with two subgenomic mRNA promoters." *Journal of Virology* 65(5): 2501-10.

Rayms-Keller, A., Powers, A.M., Higgs, S., Olson, K.E., Kamrud, K.I., Carlson, J.O., and Beaty, B.J. (1995). "Replication and expression of a recombinant Sindbis virus in mosquitoes." *Insect Molecular Biology* 4(4): 245-51.

Reed, D.S., Larsen, T., Sullivan, L.J., Lind, C.M., Lackemeyer, M.G., Pratt, W.D., and Parker, M.D., (2005). "Aerosol exposure to western equine encephalitis virus causes fever and encephalitis in cynomolgus macaques." *Journal of Infectious Disease* 192, 73-82.

Reed, L.J. and Muench, H. (1938). "A simple method of estimating fifty per cent endpoints". *The American Journal of Hygiene*, 27(3): 493-497

Reeves, W. C., Bellamy, R.E., Geib, A.F., and Scrivani, R.P. (1964). "Analysis of the Circumstances Leading to Abortion of a Western Equine Encephalitis Epidemic." *American Journal of Hygiene* 80: 205-20.

Reichert, E., Clase, A., Bacerry, A., and Larsen, J. (2009). Alphavirus antiviral drug development: scientific gap analysis and prospective research areas. Biosecurity and Bioterrorism: Biodefense, Strategy, Practice, and Science. 7, 415-427.

Reisen, W. K., Hardy, J.L., and Lothrop, H.D. (1995). "Landscape ecology of arboviruses in southern California: patterns in the epizootic dissemination of western equine encephalomyelitis and St. Louis encephalitis viruses in Coachella Valley, 1991-1992." *Journal of Medical Entomology* 32(3): 267-75.

Reisen, W. K., Hardy, J.L., Chiles, R.E., Kramer, L.D., Martinez, V.M., and Presser, S.B. (1996). "Ecology of mosquitoes and lack of arbovirus activity at Morro Bay, San Luis Obispo County, California." *Journal of the American Mosquito Control Association* 12(4): 679-87.

Reisen, W.K., Chiles R.E., Kramer, L.D., Martinez, V.M., and Eldridge, B.F. (2000).“Method of infection does not alter response of chicks and house finches to western equine encephalomyelitis and St. Louis encephalitis viruses.” *Journal of Medical Entomology* 37(2): 250-8.

Reisen, W.K., Chiles, R.E., Martinez, V.M., Fang, Y., and Green, E.N. (2003). “Experimental infection of California birds with western equine encephalomyelitis and St. Louis encephalitis viruses.” *Journal of Medical Entomology* 40(6): 968-82.

Reisen, W.K., Chiles R., Martinez V., Fang, Y., Green, E., and Clark, S. (2004). “Effect of dose on house finch infection with western equine encephalomyelitis and St. Louis encephalitis viruses.” *Journal of Medical Entomology* 41(5): 978-81.

Reisen, W.K., Martinez, V.M., Fang, Y., Garcia, S., Ashtari, S., Wheeler, S.S., and Carrol, B.D. (2006). “Role of California (Callipepla californica) and Gambel’s (Callipepla gambelii) Quail in the Ecology of Mosquito-Borne Encephalitis Viruses in California, USA.” *Vector-Borne and Zoonotic Diseases* 6(3): 248-261.

Reisen, W.K., Fang, Y., and Brault, A.C. (2008). "Limited interdecadal variation in mosquito (Diptera: Culicidae) and avian host competence for Western equine encephalomyelitis virus (Togaviridae: Alphavirus)." *American Journal of Tropical Medicine and Hygiene* 78(4): 681-6.

Renault, P., Solet, J.L., Sissoko, D., Balleydier, E., Larrieu, S., Filleul, L., Lassalle, C., Thiria, J., Rachou, E., de Valk, H., Ilef, D., Ledrans, M., Quatresous, I., Quenel, P., and Pierre, V. (2007). "A major epidemic of chikungunya virus infection on Reunion Island, France, 2005-2006." *American Journal of Tropical Medicine and Hygiene* 77(4): 727-31.

Rice, C. M., Levis, R., Strauss, J.H., and Huang, H.V. (1987). "Production of infectious RNA transcripts from Sindbis virus cDNA clones: mapping of lethal mutations, rescue of a temperature-sensitive marker, and in vitro mutagenesis to generate defined mutants." *Journal of Virology* 61(12): 3809-19.

Rocchetta, H.L., Boylan, C.J., Foley, J.W., Iversen, P.W., Letourneau, D.L., McMillian, C.L., Contag, P.R., Jenkins, D.E., and Parr, T.R. (2001). “Validation of a noninvasive, real-time imaging technology using bioluminescent Escherichia coli in the neutropenic mouse thigh model of infection.” *Antimicrobial Agents and Chemotherapy* 48: 129–137.

Rozdilksy, B., Roberstons, H.E., and Chorney, J. (1968). “Western Encephalitis : Report of Eight Fatal Cases.” *Canadian Medical Association Journal* 98: 79-86.

Rulli, N. E., Melton, J., Wilmes, A., Ewart, G., and Mahalingam, S. (2007). "The molecular and cellular aspects of arthritis due to alphavirus infections: lesson learned from Ross River virus." *Annals of the New York Academy of Sciences* 1102: 96-108.

Rumenapf, T., Strauss, E.G, and Strauss, J.H. (1995). "Aura virus is a New World representative of Sindbis-like viruses." *Virology* 208(2): 621-33.

Ryman, K. D., Klimstra, W.B., Nguyen, K.B., Biron, C.A., and Johnston, R.E. (2000). "Alpha/beta interferon protects adult mice from fatal Sindbis virus infection and is an important determinant of cell and tissue tropism." *Journal of Virology* 74(7): 3366-78.

Ryman, K. D., Meier, K.C., Gardner, C.L., Adegboyega, P.A., and Klimstra, W.B. (2007). "Non-pathogenic Sindbis virus causes hemorrhagic fever in the absence of alpha/beta and gamma interferons." *Virology* 368(2): 273-85.

Ryman, K. D. and Klimstra, W.B. (2008). "Host responses to alphavirus infection." *Immunology Reviews* 225: 27-45.

Sagripanti, J-L., Rom, A.M., and Holland, L.E. (2010). “Persistence in darkness of virulent alphaviruses, Ebola virus, and Lassa virus deposited on solid surfaces.” *Archives of virology* 155: 2035-2039.

Sahai, E. (2007). “Illuminating the metastatic process.” *Nature Reviews Cancer*. 7(10): 737-49.

Sanchez-Vargas, I., Travanty, E.A., Keene, K.M., Franz, A.W.E., Beaty, B.J., Blair, C.D., and Olson, K.E. (2004). "RNA interference, arthropod-borne viruses, and mosquitoes." *Virus Research* 102(1): 65-74.

Schoepp, R. J., Smith, J.F., and Parker, M.D. (2002). "Recombinant chimeric western and eastern equine encephalitis viruses as potential vaccine candidates." *Virology* 302(2): 299-309.

Scott, T. W., Hildreth, S.W., and Beaty, B.J. (1984). "The distribution and development of eastern equine encephalitis virus in its enzootic mosquito vector, Culiseta melanura." *American Journal of Tropical Medicine and Hygiene* 33(2): 300-10.

Scott, T. W. and Burrage, T.G. (1984). "Rapid infection of salivary glands in Culiseta melanura with eastern equine encephalitis virus: an electron microscopic study." *American Journal of Tropical Medicine and Hygiene* 33(5): 961-4.

Seabaugh, R.C., Olson, K.E., Higgs, S., Carlson, J.O., and Beaty, B.J. (1998). "Development of a chimeric sindbis virus with enhanced per Os infection of Aedes aegypti." *Virology* 243(1): 99-112.

Searle, J., Kerr, J.F.R., and Bishop, C.J. (1982). "Necrosis and apoptosis: distinct modes of cell death with fundamentally different significance." *Pathology Annual* 17(2): 229-59.

Sellers, R .F. and Maarouf, A.R.. (1988). “Impact of climate on western equine encephalitis in Manitoba, Minnesota and North Dakota, 1980-1983.” *Epidemiology and Infection* 101(3): 511-35.

Shabman, R. S., Morrison, T.E., Moore, C., White, L., Suthar, M.S., Hueston, L., Rulli, N., Lidbury, B., Ting, J.P-Y., Mahalingam, S., and Heise, M.T. (2007). "Differential induction of

type I interferon responses in myeloid dendritic cells by mosquito and mammalian-cell-derived alphaviruses." *Journal of Virology* 81(1): 237-47.

Sherman, M.B., and Weaver, S.C. (2010). “Structure of the recombinant alphavirus Western equine encephalitis virus revealed by cryoelectron microscopy.” *Journal of Virology* 84(19): 9775-82.

Shirako, Y. and Yamaguchi, Y. (2000). "Genome structure of Sagiyama virus and its relatedness to other alphaviruses." *Journal of General Virology* 81(5): 1353-60.

Silhol, M., Huez, G., and Lebleu, B., (1986). “An Antiviral State Induced in HeLa Cells by Microinjected Poly(rI). Poly(rC).” *Journal of General Virology* 67: 1867-1873.

Simmons, D. T. and Strauss, J.H. (1972). "Replication of Sindbis virus. II. Multiple forms of double-stranded RNA isolated from infected cells." *Journal of Molecular Biology* 71(3): 615-31.

Simmons, D. T. and Strauss, J.H. (1972). "Replication of Sindbis virus. I. Relative size and genetic content of 26 s and 49 s RNA." *Journal of Molecular Biology* 71(3): 599-613.

Smith, D. R., Carrara, A.S., Aguilar, P.V., and Weaver, S.C. (2005). "Evaluation of methods to assess transmission potential of Venezuelan equine encephalitis virus by mosquitoes and estimation of mosquito saliva titers." *American Journal of Tropical Medicine and Hygiene* 73(1): 33-9.

Smith, D. R., Arrigo, N.C., Leal, G., Muehlberger, L.E., and Weaver, S.C. (2007). "Infection and dissemination of Venezuelan equine encephalitis virus in the epidemic mosquito vector, Aedes taeniorhynchus." *American Journal of Tropical Medicine and Hygiene* 77(1): 176-87.

Soden, M., Vasudevan, H., Roberts, B., Coelen, R., Hamlin, G., Vasudevan, S., and La Brooy, J. (2000). "Detection of viral ribonucleic acid and histologic analysis of inflamed synovium in Ross River virus infection." *Arthritis & Rheumatology* 43(2): 365-9.

Soldan, S. S. and Gonzalez-Scarano, F. (2005). "Emerging infectious diseases: the Bunyaviridae." *Journal of Neurovirology* 11(5): 412-23.

Sponseller, M. L., Binn, L.N., Wooding, W.L., and Yager, R.H. (1966). “Field strains of western encephalitis virus in ponies: virologic, clinical, and pathologic observations.” *American Journal of Veterinary Research* 27:1591-1598.

Strauss, E. G., Rice, C.M., and Strauss, J.H. (1983). "Sequence coding for the alphavirus nonstructural proteins is interrupted by an opal termination codon." *Proceedings of the National Academy of Sciences of the United States of America* 80(17): 5271-5.

Strauss, J. H. and Strauss, E.G. (1994). "The alphaviruses: gene expression, replication, and evolution." *Microbiology Reviews* 58(3): 491-562.

Styer, L. M., Kent, K.A., Albright, R.G., Bennett, C.J., Kramer, L.D., and Bernard, K.A. (2007). "Mosquitoes inoculate high doses of West Nile virus as they probe and feed on live hosts." *PLoS Pathogens* 3(9): 1262-70.

Sweeney, T. J., Mailander, V., Tucker, A.A., Olomu, A.B., Zhang, W., Cao, Y., Negrin, R.S., and Contag, C.H.. (1999). "Visualizing the kinetics of tumor-cell clearance in living animals." *Proceedings of the National Academy of Sciences of the United States of America* 96: 12044–12049.

Syverton, J.T., Cox, H.R., and Olitsky, P.K. (1933). "Relationship of the Viruses of Vesicular Stomatitis and of Equine Encephalomyelitis." *Advancement Of Science* 78(2019): 216-217.

Taniguchi, T. (1978). "Site-directed mutagenesis on bacteriophage Qbeta RNA (author's transl)." *Tanpakushitsu Kakusan Koso* 23(3): 159-69.

Taylor, R. M. and Hurlbut, H.S. (1953). "The isolation of Coxsackie-like viruses from mosquitoes." *Journal of the Egyptian Medical Association* 36(9): 489-94.

Taylor, R. M., Hurlbut, H.S., Work, T.H., Kingston, J.R., and Frothingham, T.E. (1955). "Sindbis virus: a newly recognized arthropod transmitted virus." *American Journal of Tropical Medicine and Hygiene* 4(5): 844-62.

Thal, M. A., Wasik, B.R., Posto, J., and Hardy, R.W. (2007). "Template requirements for recognition and copying by Sindbis virus RNA-dependent RNA polymerase." *Virology* 358(1): 221-32.

Thomas, L. A. (1963). "Distribution of the Virus of Western Equine Encephalomyelitis in the Mosquito Vector, Culex Tarsalis." *American Journal of Hygiene* 78: 150-65.

Thompson, J. F., Hayes, L. S., and Lloyd, D. B. (1991). "Modulation of firefly luciferase

stability and impact on studies of gene regulation." *Gene, 103*(2), 171-7.

Tomar, S., Hardy, R.W., Smith, J.L., and Kuhn, R.J. (2006). "Catalytic core of alphavirus nonstructural protein nsP4 possesses terminal adenylyltransferase activity." *Journal of Virology* 80(20): 9962-9.

Travanty, E. A., Adelman, Z.N., Franz, A.W.E., Keene, K.M., Beaty, B.J., Blair, C.D., James, A.A., and Olson, K.E. (2004). "Using RNA interference to develop dengue virus resistance in genetically modified Aedes aegypti." *Insect Biochemical Molecular Biology* 34(7): 607-13.

Trent, D.W. and Grant, J.A. (1980). "A comparison of New World alphaviruses in the western equine encephalomyelitis complex by immunochemical and oligonucleotide fingerprint techniques." *The Journal of General Virology* 47(2): 261-82.

Trgovcich, J., Aronson, J.F., and Johnston, R.E. (1996). "Fatal Sindbis virus infection of neonatal mice in the absence of encephalitis." *Virology* 224(1): 73-83.

Trgovcich, J., Ryman, K., Extrom, P., Eldridge, J.C., Aronson, J.F., and Johnston, R.E. (1997). "Sindbis virus infection of neonatal mice results in a severe stress response." *Virology* 227(1): 234-8.

Tsetsarkin, K., Higgs, S., McGee, C.E., De Lamballerie, X., Charrel, R.N., and Vanlandingham, D.L.. (2006). "Infectious clones of Chikungunya virus (La Reunion isolate) for vector competence studies." *Vector Borne Zoonotic Diseases* 6(4): 325-37.

Tsetsarkin, K. A., Vanlandingham, D.L., McGee, C.E., and Higgs, S. (2007). "A single mutation in chikungunya virus affects vector specificity and epidemic potential." *PLoS Pathogens* 3(12): e201.

Tsiang, M., Monroe, S.S, and Schlesinger, S. (1985). "Studies of defective interfering RNAs of Sindbis virus with and without tRNA Asp sequences at their 5' termini." *Journal of Virology* 54(1): 38-44.

Tsiang, M., Weiss, B.G., and Schlesinger, S. (1988). "Effects of 5'-terminal modifications on the biological activity of defective interfering RNAs of Sindbis virus." *Journal of Virology* 62(1): 47-53.

Tucker, P. C., Strauss, E.G., Kuhn, R.J., Strauss, J.H., and Griffin, D.E. (1993). "Viral determinants of age-dependent virulence of Sindbis virus for mice." *Journal of Virology* 67(8): 4605-10.

Turell, M. J. and Spielman, A. (1992). "Nonvascular delivery of Rift Valley fever virus by infected mosquitoes." *American Journal of Tropical Medicine and Hygiene* 47(2): 190-4.

Turell, M. J., Tammariello, R.F., and Spielman, A. (1995). "Nonvascular delivery of St. Louis encephalitis and Venezuelan equine encephalitis viruses by infected mosquitoes (Diptera: Culicidae) feeding on a vertebrate host." *Journal of Medical Entomology* 32(4): 563-8.

Vanlandingham, D. L., Hong, C., Klingler, K., Tsetsarkin, K., McElroy, K.L., Powers, A.M., Lehane, M.J., and Higgs, S. (2005). "Differential infectivities of o'nyong-nyong and chikungunya virus isolates in Anopheles gambiae and Aedes aegypti mosquitoes." *American Journal of Tropical Medicine and Hygiene* 72(5): 616-21.

Vogel, P., Kell, W.M., Fritz, D.L., Parker, M.D., and Schoepp, R.J. (2005). "Early events in the pathogenesis of eastern equine encephalitis virus in mice." *American Journal of Pathology* 166(1): 159-71.

Wang, C. Y., Dominguez, G., and Frey, T.K. (1994). "Construction of rubella virus genome-length cDNA clones and synthesis of infectious RNA transcripts." *Journal of Virology* 68(6): 3550-7.

Wang, H., Blair, C.D., Olson, K.E., and Clem, R.J. (2008). "Effects of inducing or inhibiting apoptosis on Sindbis virus replication in mosquito cells." Journal of General Virology 89(11): 2651-61.

Weaver, S. C., Scherer, W.F., Cupp, E.W., and Castello, D.A. (1984). "Barriers to dissemination of Venezuelan encephalitis viruses in the Middle American enzootic vector mosquito, Culex (Melanoconion) taeniopus." *American Journal of Tropical Medicine and Hygiene* 33(5): 953-60.

Weaver, S. C., Scott, T.W., Lorenz, L.H., Lerdthusnee, K., and Romoser, W.S. (1988). "Togavirus-associated pathologic changes in the midgut of a natural mosquito vector." *Journal of Virology* 62(6): 2083-90.

Weaver, S. C., Scott, T.W., Lorenz, L.H., and Repik, P.M. (1991). "Detection of eastern equine encephalomyelitis virus deposition in Culiseta melanura following ingestion of radiolabeled virus in blood meals." American Journal of Tropical Medicine and Hygiene 44(3): 250-9.

Weaver, S. C., Lorenz, L.H., and Scott, T.W. (1992). "Pathologic changes in the midgut of Culex tarsalis following infection with Western equine encephalomyelitis virus." *American Journal of Tropical Medicine and Hygiene* 47(5): 691-701.

Weaver, S. C., Lorenz, L.H., and Scott, T.W. (1993). "Distribution of western equine encephalomyelitis virus in the alimentary tract of Culex tarsalis (Diptera: Culicidae) following natural and artificial blood meals." *Journal of Medical Entomology* 30(2): 391-7.

Weaver, S. C., Hagenbaugh, A., Bellew, L. A., Netesov, S. V., Volchkov, V. E., Chang, G. J., Clarke, D. K., Gousset, L., Scott, T. W., Trent, D. W., and Holland, J.J. (1993). "A comparison of the nucleotide sequences of eastern and western equine encephalomyelitis viruses with those of other alphaviruses and related RNA viruses." *Virology* 197(1): 375-90.

Weaver, S. C., Kang, W., Shirako, Y., Rumenapf, T., Strauss, E.G., and Strauss, J.H. (1997). "Recombinational history and molecular evolution of western equine encephalomyelitis complex alphaviruses." *Journal of Virology* 71(1): 613-23.

Weaver, S. C. and Barrett A.D. (2004). "Transmission cycles, host range, evolution and emergence of arboviral disease." *Nature Reviews Microbiology* 2(10): 789-801.

Weaver, S. C. (2006). "Evolutionary influences in arboviral disease." *Current Topics in Microbiology and Immunology* 299: 285-314.

White, L. J., Wang, J.G., Davis, N.L., and Johnston, R.E. (2001). "Role of alpha/beta interferon in Venezuelan equine encephalitis virus pathogenesis: effect of an attenuating mutation in the 5' untranslated region." *Journal of Virology* 75(8): 3706-18.

Wielgosz, M.M., Raju, R. and Huang, H.V. (2001). “Sequence requirements for Sindbis virus subgenomic mRNA promoter function in cultured cells.” *Journal of Virology* 75: 3509–3519.

Wyckoff, R.W.G. and Tesar W.C., (1939). “Equine encephalitis in monkeys.” *Journal of Immunology* 37: 329-343.

Xiong, C., Levis, R., Ping, S., Schlesinger, S., Rice, C.M., and Huang, H.V. (1989). "Sindbis virus: an efficient, broad host range vector for gene expression in animal cells." *Science* 243(4895): 1188-91.

Zacks, M.A. and Paessler, S. (2010). “Encephalitic alphaviruses.” *Veterinary Microbiology* 140(3-4): 281-286.

Zaitseva, M., Kapnick, S.M., Scott, J., King, L.R., Manischewitz, J., Sirota, L., Kodihalli, S., and Golding, H., (2009). “Application of bioluminescence imaging to the prediction of lethality in vaccinia virus-infected mice.” *Journal of Virology* 83: 10437-10447.

Zaks, K., Jordan, M., Guth, A., Sellins, K., Kedl, R., Izzo, A., Bosio, C., and Dow, S. (2006). “Efficient immunization and cross-priming by vaccine adjuvants containing TLR3 or TLR9 agonists complexed to cationic liposomes.” *Journal of Immunology* 176: 7335–7345.

Zhang, M., Fang, Y., Brault, A. C., and Reisen, W. K. (2011). “Variation in Western equine encephalomyelitis viral strain growth in Mammalian, avian, and mosquito cells fails to explain temporal changes in enzootic and epidemic activity in California.” *Vector borne and zoonotic diseases (Larchmont, N.Y.)*, *11*(3), 269-75.

Zlotnik, I., Peacock, S., Grant, D.P., and Batter-Hatton, D. (1972). "The pathogenesis of western equine encephalitis virus (W.E.E.) in adult hamsters with special reference to the long and short term effects on the C.N.S. of the attenuated clone 15 variant." *British Journal of Experimental Pathology* 53(1): 59-77